

# MODELLING THE RESPONSE OF LIZARDS TO THERMAL LANDSCAPE

Teng Fei

Examining committee:

Prof. dr. V.G. Jetten  
Prof. dr. A. Veldkamp  
Prof. dr. W. Bouten  
Prof. dr. R.R. Giménez

University of Twente  
University of Twente  
University of Amsterdam  
University of Malaga

ITC dissertation number 231  
ITC, P.O. Box 6, 7500 AA Enschede, The Netherlands

ISBN 978-90-6164-359-3  
Cover designed by Benno Masselink  
Printed by ITC Printing Department  
Copyright © 2013 by Teng Fei



**UNIVERSITY OF TWENTE.**

**ITC**

FACULTY OF GEO-INFORMATION SCIENCE AND EARTH OBSERVATION

# MODELLING THE RESPONSE OF LIZARDS TO THERMAL LANDSCAPE

DISSERTATION

to obtain  
the degree of doctor at the University of Twente,  
on the authority of the rector magnificus,  
prof.dr. H. Brinksma,  
on account of the decision of the graduation committee,  
to be publicly defended  
on Wednesday July 10, 2013 at 14:45 hrs

by  
Teng Fei  
born on 2 August 1981  
in Shanghai, China

This thesis is approved by

**Prof. dr. Andrew K. Skidmore,**  
**Dr. Albertus G. Toxopeus,**  
**Dr. Tiejun Wang,**

Promotor  
Assistant promotor  
Assistant promotor

## ACKNOWLEDGEMENTS

This PhD thesis is the outcome of years of study at the department of natural resources of the Faculty of Geo-information Science and Earth Observation, University of Twente. This PhD journey for me was a highly valuable period of professional and human growth in a friendly international atmosphere.

My first thoughts go to my promoter, Prof. Andrew K. Skidmore, without whom this thesis would not have existed. He was and continues to be an ideal mentor. He was always there to put me back on my feet and provided direction with his wisdom. I will always remember the first day I was in his office, he encouraged me to think more about the ‘why questions’ at the beginning of a scientific research project. This suggestion echoed in my ears as the years passed and as time and hard work slowly turned me from an engineer into a scientific worker. It is my good fortune and honour that his wisdom infuses every part of my research: from proposal preparation to experimental design, from trouble shooting to article writing. I will also cherish the fantastic memories of the annual PhD student BBQs hosted by the friendly Skidmore family.

I am greatly indebted to my co-supervisors, Dr. Albertus G. Toxopeus, Dr. Valentijn Venus and Dr. Tiejun Wang, for their strong, valuable, and patient advice on this journey. I am grateful for their guidance on mathematical modelling and reptilian physiology, for their strong support on the design and implementation of the animal experiments, and for helping guide my research through areas of thick fog.

To the many researchers who gave me valuable comments and meaningful discussion on this journey, I want to express my gratitude and respect to these people, at ITC of Twente: Martin Schlerf, David Rossiter, Jan de Leeuw; at Wageningen University: Prof. Herbert Prins, Jingsong Li, Yuan Zeng and, at Wuhan University: Guofeng Wu, Wenxiu Gao, Yaolin Liu, Yanfang Liu, Qinyun Du and Lin Li.

Thanks to Dierenpark De Oliemeulen my cooperation partner on site where an animal experiment was carried out. Special thanks go to Mr. Sjef van Overdijk who assisted setting up the experiment and maintained the servers placed in the

zoo. I was much impressed by his deep knowledge of biology and his enthusiasm for animals.

To my friends, I cannot stop smiling when thinking of you. Thanks go to my colleagues in ITC, in particular Mohammad Abouali, Wei Ouyang, Paco Ferri, Roshanak Darvishzadeh, Sabrina Carvalho, Anas Fauzi, Atkilt Girma, Aidin Niamir, Claudia Pittiglio, Ullah Saleem, Ben Wielstra, Ha Nguyen, Tyas Basuki, Moses Cho, Jelle Ferwerda, Mhosisi Masocha, Nicky Knox, Filiz Bektas Balcik, Ajay Bhakta Mathema, and to the warm Chinese group at ITC, especially Xiang Zhang, Yali Si, Xi Zhao, Pu Hao, Fangfang Chen, Xia Li and Dongpo Deng. They gave me lots of invaluable suggestions not only on my research but also on every aspect of my PhD life – from the selection of the presentation template to the selection of beer.

My deep gratitude goes to Ms. Eva Skidmore whose excellent English editing helped me to publish my first paper. I also appreciate Esther Hondebrink who offered her generous help on the translation of the abstract of this thesis into the Dutch language. Many thanks go to Mr. Stephen C. McClure and Dr. Stephan Anguesser who helped proofreading several thesis chapters.

Special thanks go to my friends Mr. Ding Zheng and Ms. Lichun Wang in Enschede, the Netherlands. They treated me like if I were their own son. I do, however, expect for one more badminton game.

Most of all I would like to thank all my family who, as always, has given me endless love and support throughout my PhD journey. In particular I would like to thank my wife Meng Bian and my son Alan for their love and understanding. I thank my mother-in-law who spent a tremendous amount of time caring for my son. Without your support, I could do nothing.

I am sincerely grateful to the review committee for their supportive and rich comments on this PhD thesis. Their careful comments gave me strong guidance on how to improve the work and provided extremely valuable insights to guide the future progress of my research.

# TABLE OF CONTENTS

<b>Acknowledgements .....</b>	<b>i</b>
<b>Chapter 1 General Introduction.....</b>	<b>1</b>
1.1 Background.....	2
1.2 Research Problem Statement.....	6
1.3 Research Objectives and Questions.....	9
1.4 The Target Species.....	9
1.5 Outline of the Thesis .....	11
<b>Chapter 2 A Body Temperature Model for Lizards as Estimated from the Thermal Environment.....</b>	<b>15</b>
2.1 Introduction .....	17
2.2 Model Description.....	19
2.2.1 Heat Exchange Terms .....	19
2.2.2 Body Temperature Simulation.....	22
2.3 Model Evaluation.....	23
2.3.1 Experimental Design.....	23
2.3.2 Calibration of the Body Temperature Model.....	25
2.3.3 Validation of the Body Temperature Model .....	26
2.3.4 Sensitivity Analysis of the Body Temperature Model.....	27
2.4 Results .....	27
2.4.1 Absorbance of the Lizard's Skin.....	27
2.4.2 Calibration of the Body Temperature Model.....	28
2.4.3 Validation of the Body Temperature Model .....	29
2.4.4 Sensitivity Tests of the Body Temperature Model.....	30
2.5 Discussion .....	33
2.6 Conclusion.....	36
<b>Chapter 3 Predicting Micro Thermal Habitat of Lizards in a Dynamic Thermal Environment.....</b>	<b>37</b>
3.1 Introduction .....	39
3.2 Method.....	41
3.2.1 Target Animal and Experimental Setup.....	41
3.2.2 Data Collection.....	43
3.2.3 Model Building.....	44
3.2.4 Model Validation .....	47
3.3 Results and Discussion .....	48
3.3.1 Model Parameterization.....	48
3.3.2 Thermal Habitat Use .....	49
3.4 Conclusion.....	53

<b>Chapter 4</b>	<b>Model the Natural Terrain Elevation of Lizard Micro</b>	
<b>habitat</b>		<b>55</b>
4.1	Introduction .....	57
4.2	Methods.....	58
4.2.1	<i>Study Site</i> .....	58
4.2.2	<i>The Rangefinder</i> .....	59
4.2.3	<i>Data Collection</i> .....	60
4.2.4	<i>Accuracy Assessment</i> .....	62
4.3	Results .....	63
4.3.1	<i>DEM Generated with One Scan</i> .....	63
4.3.2	<i>DEM Generated with Two Scans</i> .....	65
4.4	Discussion and Conclusions.....	68
<b>Chapter 5</b>	<b>Model the Land Surface Temperature of Lizard</b>	
<b>Microhabitat Using Microclimate Data</b>		<b>71</b>
5.1	Introduction .....	73
5.2	Methods.....	74
5.2.1	<i>Study Area</i> .....	74
5.2.2	<i>Data Collection</i> .....	75
5.2.3	<i>Input Data Selection</i> .....	76
5.2.4	<i>Optimizing Neural Network</i> .....	79
5.2.5	<i>Model Validation</i> .....	80
5.3	Results .....	80
5.3.1	<i>Input Data Selection</i> .....	80
5.3.2	<i>Optimizing Neural Network Setting</i> .....	84
5.3.3	<i>Prediction Accuracy</i> .....	84
5.4	Discussion and Conclusion.....	85
<b>Chapter 6</b>	<b>Predicting the Spatial Use of Local Habitat of a Lizard</b>	
<b>using Thermal Roughness Index</b>		<b>89</b>
6.1	Introduction .....	91
6.2	Materials and Methods .....	94
6.2.1	<i>Thermal Landscape Simulation</i> .....	94
6.2.2	<i>Calculation of Thermal Roughness Index</i> .....	95
6.2.3	<i>Habitat Occupancy Simulation of a Lizard</i> .....	96
6.2.4	<i>Comparing the Thermal Roughness Index with Simulated</i> <i>Habitat Occupancy</i> .....	97
6.2.5	<i>Test the Thermal Roughness using Field Observation</i> .....	98
6.3	Results .....	100
6.3.1	<i>Simulated Thermal Habitat</i> .....	100
6.3.2	<i>Thermal Roughness Map</i> .....	101
6.3.3	<i>Habitat Occupancies Simulated by Animal Movement Models</i> <i>with Different Sized Lizards</i> .....	102

6.3.4	<i>Comparing the Thermal Roughness Index and Habitat Occupancies</i> .....	102
6.3.5	<i>Thermal Roughness Maps versus Actual Habitat Occupancy of Lizards</i> .....	103
6.4	Discussion .....	104
6.5	Conclusion.....	106
<b>Chapter 7</b>	<b>Synthesis</b> .....	<b>107</b>
7.1	Introduction .....	109
7.2	Species Distribution models.....	112
7.3	Model Animal Responses to the Thermal Environment in a Laboratory .....	113
7.4	Modelling the Key Factors of the Thermal Landscape in the Animal's Natural Habitat.....	116
7.5	Thermal Roughness Index as a Proxy to Indicate Habitat Occupancy by Lizards.....	117
7.6	Implications.....	118
7.7	General Conclusion.....	119
	<b>Bibliography</b> .....	<b>121</b>
	<b>Author's Biography</b> .....	<b>139</b>
	<b>Summary</b> .....	<b>141</b>
	<b>Samenvatting</b> .....	<b>143</b>
	<b>ITC Dissertation List</b> .....	<b>145</b>



# **CHAPTER 1**

## **GENERAL INTRODUCTION**

## **1.1 Background**

With the exponential growth of the human population over the past century, the world is being transformed from a large natural system into a man-made ecosystem (Vitousek et al., 1997). Consequently, many wildlife species have suffered reduction in abundance or range (Skidmore, 2002). To halt the loss of biodiversity and restore ecosystems, wildlife management requires reliable and consistent information on the abundance and distribution of species as well as their habitats (Skidmore, 2002; Roy et al., 2004).

Mapping the distribution of species does not only benefit wildlife conservation planning, but also helps improve our understanding of species-habitat relationships in highly modified landscapes (Brady and Flather, 2003). Why some species are present in some places and absent in others forms a crucial question in ecology (Krebs, 1978). To answer this question, various species distribution models (SDMs) have been developed and applied widely at many different scales over the last three decades (Elith and Leathwick, 2009).

Species distribution models are models that relate species distribution data to the environmental and/or spatial characteristics of those locations (Elith and Leathwick, 2009). These models can contribute to the understanding and/or prediction of species' distribution across a landscape (Sinclair et al., 2010). In general, species distribution models can be classified by their modelling approach, dividing them into two groups: inductive/statistical models and deductive/mechanistic models.

An inductive model combines known species occurrence records with layers of environmental variables (Corsi et al., 2000). In such a model (Figure 1-1), it is assumed that a species has a preferred range of values for environmental variables such as elevation, temperature, and vegetation cover. These preferred ranges are firstly assessed; then the relationships between species and environmental variables are analysed; and finally the probability of the species' presence may be correlated to the environmental variables (Guisan and Zimmermann, 2000). As a result, the species' distribution can be predicted and mapped. Such models are static and probabilistic in nature, since they statistically link the geographical distribution of species or communities to their present environment (Guisan and Zimmermann, 2000). As it is a key

assumption of the inductive approach that species are in equilibrium with their environment, applying these models under non-equilibrium conditions, such as climate change or species invasion, needs to be carefully assessed (Elith and Leathwick, 2009).

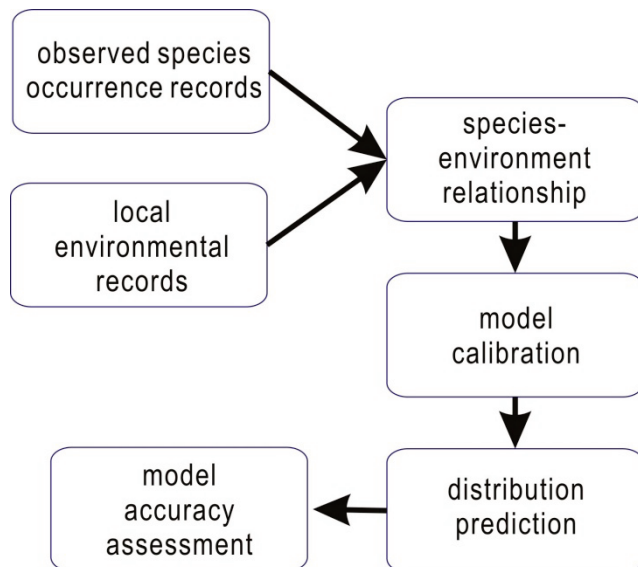


Figure 1-1 Inductive species distribution models

The deductive model is an alternative strategy, explicitly incorporating the mechanistic links between the functional traits of organisms and their environments in the modelling of species distribution (Kearney and Porter, 2009) (Figure 1-2). Unlike inductive models, which rely on a substantial number of reliable species occurrence records, deductive models use logical reasoning – a logical method for identifying specific consequences stemming from a known set of facts, usually biological or physiological facts (Morin et al., 2007). Buckley et al. (2010) have further classified the deductive models into three categories: models that translate environmental conditions into biologically relevant metrics; models that capture environmental sensitivities of survivorship and fecundity; and models that use energy to link environmental conditions and demography. All of these deductive models describe relatively important processes potentially constraining the distribution of a species (such as biological/biophysical processes that underlie movement, survival, and reproduction) to predict its spatial range. Theoretically, therefore, deductive models should be better at predicting species' range dynamics than inductive

models (Kearney and Porter, 2009). However, the deductive approach requires an accurate understanding of how a species relates to the environment, as well as an accurate estimation of many bio-physical parameters under a wide range of environmental conditions (Buckley et al., 2010).

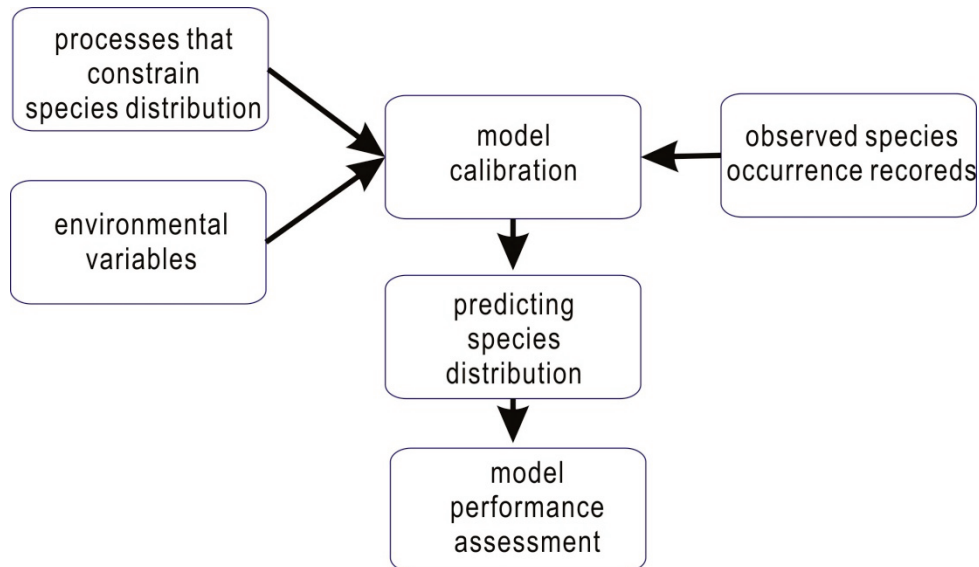


Figure 1-2 Deductive species distribution models

In various species distribution modelling studies the thermal environment has formed an important predictor, especially in the context of global climate change (Mysen, 1990; Gottfried et al., 1999, Kearney et al., 2010). To link the thermal environment to a species, many species distribution models have employed indirect predictors such as elevation in terrestrial studies (Porter, 1989; Gottfried et al., 1999; Fischer and Lindenmayer, 2005), or water depth in marine studies (Block et al., 2001; Garza-Pérez et al., 2004). These, however, rarely directly affect species distribution (Elith and Leathwick, 2009). Instead, these proxy predictors are correlated with more functionally relevant predictors such as temperature and radiation (Elith and Leathwick, 2009). Some models include proxy predictors such as air temperature or solar radiation (Fischer et al., 2002), or both (Zeng et al., 2010). However, any proxy predictor is a simplification (sometimes an oversimplification) of the actual thermal environment.

According to the energy transfer theory, the heat from a thermal environment can influence the body temperature of a terrestrial animal in several ways, namely through radiation (short wave and long wave), convection, and conduction (Porter and Gates, 1969). A change in body temperature may lead to physiological responses (Dawson and Bartholomew, 1958; Waldschmidt and Tracy, 1983; Medina et al., 2009) and spatial responses of the animal (Row and Blouin-Demers, 2006; Angilletta et al., 2009b). The energy exchange process within the animal-environment system has been successfully modelled by several bio-physical models of varying complexity (Porter, 1967; Porter and Gates, 1969; Beckman et al., 1973; Porter et al., 1973; Bakken and Gates, 1975; Tracy, 1982). However, when modelling a specific species from an energy exchange point of view, it is difficult to determine which model should be employed and what the proper parameters for the model should be. Moreover, most of these energy exchange models calculate how the body temperature of animals responds to the thermal environment, while few of them integrate energy exchange into species distribution models or predict the spatial response of the animals (Porter et al., 2002; Angilletta et al., 2009a). If we define the “thermal landscape” as the landscape pattern of the thermal environment that combines the effects of all thermal sources on an animal, then theoretically, the interaction between an animal and its thermal environment can be extended to a spatial context.

The thermal environment is crucial to the behaviour of ectotherms as it directly impacts on their body temperature (Waldschmidt and Tracy, 1983). By altering its location continuously, an ectotherm is able to maintain a crude form of body temperature control (Raymond and Montgomery, 1976). Figure 1-3 illustrates the body temperature changes of a 4200g lace monitor (*Varanus varius*) during a single day, recorded by radio telemetry (temperature signalling radio transmitter implanted). As can be seen, the lizard has near perfect thermoregulation when active, and the correlation between its body temperature and the air temperature is not significantly different from 0 (Cowles and Bogert, 1944; Porter et al., 1973; Huey and Slatkin, 1976).

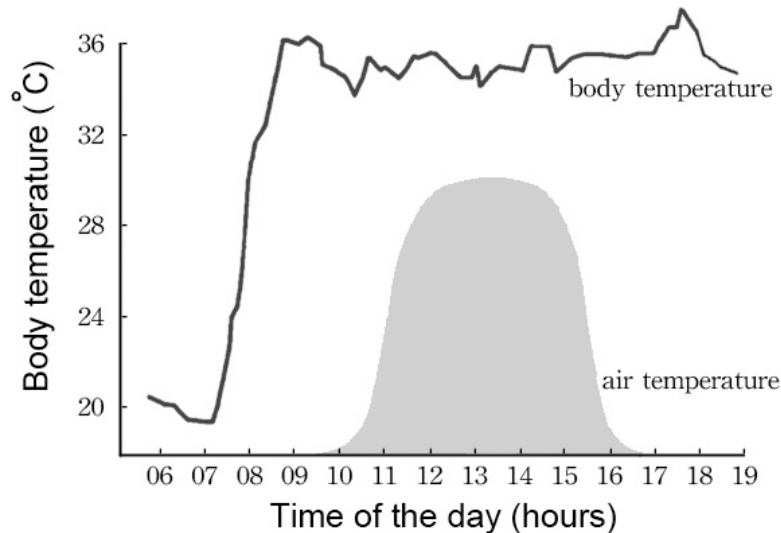


Figure 1-3 Body temperature of a lace monitor (*Varanus varius*) during a single day, recorded by means of radio telemetry (redraw after Huey & Slatkin, 1976)

Although many studies have focused on the impact of the thermal environment on the growth and development of ectotherm embryos (Angilletta et al., 2009b), the metabolic processes (Harwood, 1979), the behavioural processes (Stephen and Porter, 1993; Nicholson et al., 2005; Sears, 2005; Rouag et al., 2006), and the ability of locomotion (Waldschmidt and Tracy, 1983), less were explored with respect to how the thermal landscape shapes the use of the local habitat by ectotherms (Deitschman, 1973; Wicker et al., 1980; Rosenzweig, 1981; Waldschmidt and Tracy, 1983). As Huey (1991) has pointed out: “it is time to reintroduce the thermal physiology of ectotherms into ecology.”

## 1.2 Research Problem Statement

### ➤ Challenges in parameterizing a bio-physical model to accurately predict transient body temperatures of ectotherms

Many researchers have set up models of varied complexity to quantify environment-animal energy exchange based on the physics of heat transfer and the known physiological properties of animals (Beckman et al., 1973; Porter et al., 1973; Tracy, 1976; 1982; Blouin-Demers and Nadeau, 2005). These deductive models usually need experimental data for calibration (O'Connor and Spotila, 1992; Skidmore, 2002). However, such experimental data may be

lacking or difficult to measure directly (Conroy et al., 1995). In our case, for example, directly measuring heat capacity of the animals without changing their behaviour is difficult. How to fine-tune a bio-physical model to accurately predict transient temperatures of target animals is one of the research problems that need to be addressed.

➤ **Lack of understanding in the mechanism of behavioral thermoregulation of ectotherms translated into habitat use at a local scale**

Thermal physiology of animals and animal distribution are two subjects that have been developed almost independently, despite widespread acknowledgement that they must be related (Claireaux et al., 1995). Although there is extensive literature on reptile thermoregulation (Cowles and Bogert, 1944; Huey, 1974; Huey and Slatkin, 1976; Avery, 1978; Cowgell and Underwood, 1979; Lee, 1980; De Long et al., 1986; Huey and Bennett, 1987; Huey et al., 1989; Hertz et al., 1993; Arnold et al., 1995; Autumn and Nardo, 1995; Bauwens et al., 1996; Downes and Shine, 1998; Luiselli and Akani, 2002; Fitzgerald et al., 2003; Bennett, 2004), there are surprisingly few studies that relate thermoregulation to the utilization of space by ectotherms. Statistical approaches have established the relation between the distribution of organisms and their thermal environment (Heikkinen et al., 2006), however, these approaches are highly site-based and cannot easily be extrapolated beyond their calibration range or applied to a novel situation (e.g., climate change). Ideally, we should be able to model this relationship based on a physical understanding of the process of behavioural thermoregulation. Therefore, a process-based model, rather than a statistical model of the process, should proffer insight in how behavioural thermoregulation can be translated into habitat use by ectotherms, with the aim of achieving optimal predictive power (Kearney and Porter, 2004).

➤ **Lack of methods to model the thermal landscape at an animal's natural habitat**

A thermal landscape is the landscape pattern of a thermal environment that combines effects from all thermal sources. While at the scale of animal's micro-habitat often a homogeneous distribution of air temperature is assumed, solar radiation reaching the ground and substrate temperatures are both difficult to map at this fine scale. This is caused by topography affecting solar radiation

received and thus affecting surface temperature, as well as by radiation and surface temperature both being highly dynamic and heterogeneously distributed. Mapping topography at a lizard's micro-habitat scale is challenging. The spatial resolution of digital terrain models (DTMs) derived from satellite/airborne remote sensing data is often too coarse (Kelly et al., 1977; Toutin, 2002; Nikolakopoulos et al., 2006). GPS derived points are usually too widely spaced in complex terrain to satisfy accuracy requirements. Stereo-photogrammetry suffers from shaded relief (Linder, 2009). DTMs derived from ground based LiDAR (Light Detection And Ranging) are accurate, but less cost-effective for a small project at micro-habitat scale (Leberl et al., 2010). Therefore, a flexible, inexpensive yet accurate method to measure the topography of a microhabitat needs to be developed and tested.

Land surface temperature (LST) is another important thermal characteristic in microhabitats of animals. The spatial resolution of satellite/airborne based LST products fails to meet the requirements of microhabitat studies (Leyequien et al., 2007; Huang et al., 2008). Additionally, the accessibility of thermal infrared remote sensing data is strongly influenced by weather conditions, such as cloud cover, further limiting the use of remote sensing data for land surface temperature retrieval at small scales. Instead of through direct observation, land surface temperature may also be obtained by modelling. A surface energy balance model uses knowledge of underlying physical principles to provide a complete description of the process of energy exchange of the land-atmospheric interface, however, the data and skill required to solve the various terms in the model are prohibitive for operational applications (Sobrino et al., 2004). A simple yet accurate model is needed to compute the dynamics of land surface temperature at micro-habitat scale.

➤ **Inductive models based on environmental factors are ill-suited while dynamic models for animal movement or dispersal are computationally intensive**

The animal-environment variable based inductive models do not form suitable tools to model the effect of thermal habitat on ectotherms for two reasons: 1. compared with other environmental factors, the thermal environment is highly dynamic at different temporal scales, which makes it difficult to describe as a static environmental factor (Fei et al., 2012a). 2. The ectotherms use behavioural thermoregulation as a way to control body temperature, which

means they can temporally take advantage of places with very different thermal properties to perform thermoregulation (Raymond and Montgomery, 1976). As inductive models simply correlate the animals' occurrences with the thermal environment in which they were observed (both in hot and cold thermal environments), this results in a low correlation between thermal conditions and occurrences, leading to a very limited predictability of the model.

The deductive approach, as an alternative modelling strategy, is process based. Therefore, it has the ability to cope with the highly dynamic process of energy exchange. However, deductive models usually have a much heavier computational load (Morale, 2001). Compared with inductive models, deductive models normally also require more prior knowledge, which is often unavailable.

### **1.3 Research Objectives and Questions**

The following broad research question forms the main focus of this thesis:

Does the pattern of habitat occupancy of lizards respond to the pattern of the thermal landscape?

To tackle this question the following specific research questions have been posed:

1. How can the body temperature of an ectotherm be accurately modelled in a changing thermal environment?
2. How does the behavioural thermoregulation of ectotherms affect the spatial utilization of their micro-habitat?
3. What are the key factors affecting the thermal landscape of ectotherms; and what are the applicable methods to measure/model these factors in the animal's natural (micro-) habitat?
4. Does a thermal index that indicates the habitat preference of ectotherms exist?

### **1.4 The Target Species**

The *Timon lepidus* (Ocellated lizard, see Figure 1-4) is a ground-dwelling lizard, widely distributed in Spain, Portugal, southern France and northwestern Italy. It is a characteristic species of the western Mediterranean climate (Salvador, 1998). The *Timon lepidus* is found in open and dry areas of woodland, scrubland, olive groves, vineyards, meadows, arable areas, and sandy or rocky sites. This lizard is generally present in areas containing refuges, such

as bushes, stone walls, rabbit burrows, and other hollows. This species is the largest European lizard and can reach a body length of up to 90 cm and a weight of more than 500 g. The skin color of an adult has a camouflaging effect comprising mottled blue, green and brown patches interspersed with brighter spots. In the wild, this lizard feeds on insects, snails, newly hatched birds, and fruits (Pleguezuelos et al., 2008). It is an oviparous species, laying between 7 and 25 eggs per year depending on the weight of the female. This species usually lays one clutch per year, at the beginning of June (depending on the latitude), although two clutches per year have been reported in some populations. Four subspecies have been described in the Iberian Peninsula varying in size, coloration and dentition; these are *T.l.lepidus*, *T.l.ibericus*, *T.l.nevadensis*, and *T.l.oteroi* (Mateo, 2006).

*Timon lepidus* was chosen as the target animal of this study for several reasons. Firstly, it is a widely studied species, resulting in the availability of abundant data and pre-knowledge (Mateo, 2004; Rouag et al., 2006). Secondly, this species is found in Portugal and Spain and is listed as near threatened (Pleguezuelos et al., 2008), therefore, it is relatively easy to obtain individuals for laboratory experiments or to find them in their natural habitat. Finally, this species actively and carefully regulates its body temperature by means of behavioral thermoregulation.



Figure 1-4 The target species: *Timon lepidus* (photo by A.G. Toxopeus, using under permission)

## 1.5 Outline of the Thesis

This thesis consists of several research papers which, combined, fulfil the objectives of the study: to model the response of lizards to a dynamic thermal landscape. Each paper is presented as a thesis chapter.

Chapter 1 places this study in an ecological context, defines the thermal landscape, presents the significance of this research, states the research problems and research objectives, describes the target species, and outlines the structure of the thesis.

Chapter 2 aims to predict the body temperature of lizards from the thermal environment using a bio-physical model. A parameterization technique is applied to increase the accuracy of the predictions. The hypothesis tested is that the response of a lizard's body temperature to the thermal environment can be accurately modelled and predicted by the bio-physical model.

Chapter 3 investigates the behavioural thermoregulation pattern of the target species under laboratory conditions, and simulates the spatial movement pattern by integrating the bio-physical model developed in Chapter 2 with a spatially explicit, cellular automaton based model. Through simulation, the microhabitat occupancy is predicted and mapped. The hypothesis tested is that the utilization of space by lizards under laboratory conditions is a response to the thermal landscape. Chapter 2 and Chapter 3 focus on the modelling of the animal's responses (based on temperature and on spatial utilization, respectively) to a dynamic thermal environment. To make predictions about the animal's response, these models require input from the thermal landscape. In laboratory conditions, such input is easy to obtain as the thermal conditions are manipulated and every significant thermal variable is recorded. However, in order to test the models in the natural (field) area where the animal resides, the thermal landscape of that site needs to be measured.

Chapter 4 explores the possibility of developing a flexible, economical, yet accurate method to construct a fine scale DEM. One such method is illustrated and tested.

Chapter 5 models land surface temperature using microclimate data, sun position, time information, and terrain information (aspect and slope) as input, based on artificial neural networks. The terrain information is extracted from the fine scale DEM developed in Chapter 4. This chapter systematically examines the effectiveness of the predictors used to estimate land surface temperature. The question whether microclimate data can be used to predict land surface temperature at a fine scale is answered. Chapter 4 and Chapter 5 thus explore applicable methods for modelling key factors of thermal landscapes in the field. With these methods, the thermal environment of a microhabitat can be modelled outside the laboratory.

Chapter 6 proposes a habitat index called 'thermal roughness' for ectotherms. Based on this index habitat usage by ectotherms can be predicted in a spatially explicit way. The predictions are compared with both computer simulations (developed in Chapter 2 and Chapter 3) and field observations. The results show that natural microhabitat usage in response to the thermal environment by an ectotherm can be approximated by this thermal roughness index.

Finally, Chapter 7 discusses the interrelationships between the Chapters (as seen in an overview in Figure 1-5), and suggests direction for possible future study.

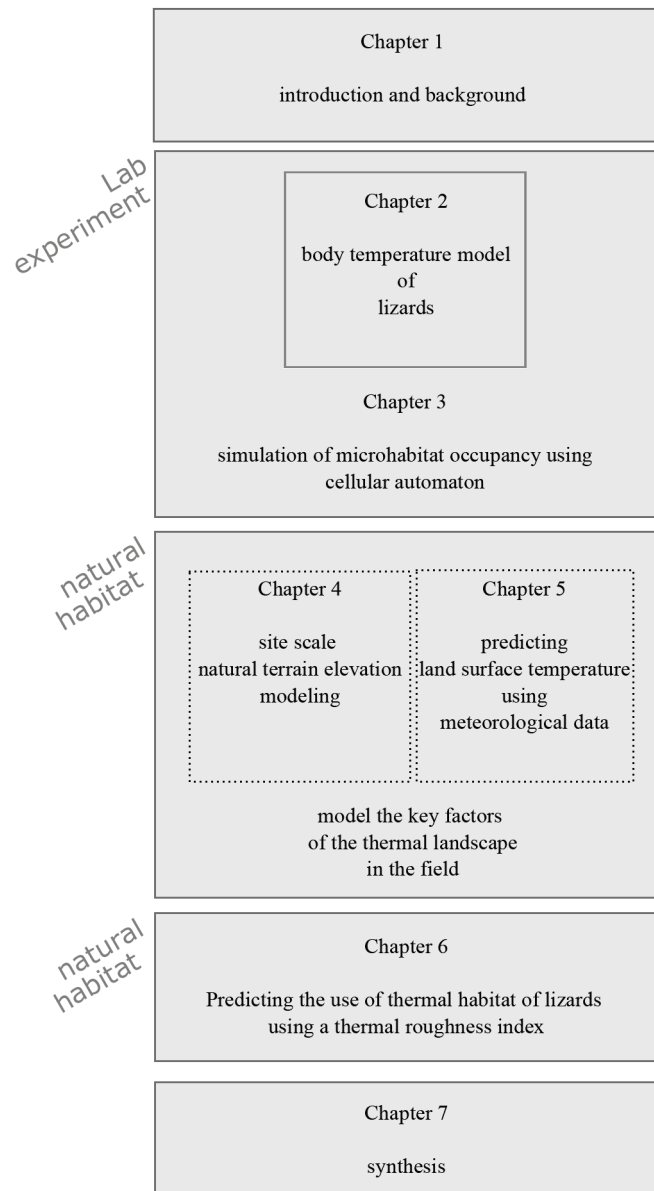


Figure 1-5 The connections between core chapters



## **CHAPTER 2**

### **A BODY TEMPERATURE MODEL FOR LIZARDS AS ESTIMATED FROM THE THERMAL ENVIRONMENT**

---

This chapter is based on: Fei, T., Skidmore, A.K., Venus, V., Wang, T., Schlerf, M., Toxopeus, A.G., van Overjijk, S., Bian, M., Liu, Y., 2012. A body temperature model for lizards as estimated from the thermal environment. *Journal of Thermal Biology* 37, 56 - 64.

## **Abstract**

A physically based model was built to predict the transient body temperature of lizards in a thermally heterogeneous environment. Six heat transfer terms were taken into account in this model: solar radiation, convective heat flow, longwave radiation, conductive heat flow, metabolic heat gain and respiratory energy loss. In order to enhance the model predictive power, a Monte Carlo simulation was employed to calibrate the bio-physical parameters of the target animal. Animal experiments were conducted to evaluate the calibrated body temperature model in a terrarium under a controlled thermal environment. To avoid disturbances of the animal, thermal infrared imagers were used to measure the land surface temperature and the body temperature. The results showed that the prediction accuracy of lizard's transient temperature was substantially increased by the use of Monte Carlo techniques (RMSE=0.59°C) compared to standard model parameterization (RMSE=1.35°C). Because the model calibration technique presented here is based on physical principles, it should be also useful in more complex, field situations.

## 2.1 Introduction

The climate change debate (Parmesan and Yohe, 2003) has generated widespread interest in the response of organisms to the thermal environment (Sinclair et al., 2003). The thermal environment is especially important for ectotherms in order to control their internal body temperature and physiological functions (Sabo, 2003; Row and Blouin-Demers, 2006). Thermal conditions influence ectotherms on: (1) growth, development and survival of embryos (Angilletta et al., 2009); (2) metabolic processes such as digestion (Harwood, 1979); (3) behavioral processes such as activity (Stephen and Porter, 1993; Nicholson et al., 2005; Sears, 2005; Rouag et al., 2006), locomotion (Waldschmidt and Tracy, 1983), microhabitat selection (Porter and James, 1979; Angilletta et al., 2009; Schofield et al., 2009); and (4) spatial distribution and life history traits of populations (Porter and Tracy, 1983; Kearney and Porter, 2004; Medina et al., 2009).

Ectotherms are organisms that control their body temperature through external means (Avila, 1995). An ectotherm controls its temperature by adjusting its behaviour like re-positioning its body within a thermal environment (Bartholomew, 1966; Hammel et al., 1967). By responding to changes in the thermal landscape, the animals maintain a thermodynamic balance over an extended period of time (Barlett and Gates, 1967). For example, lizards regulate their body temperature by many activities such as climbing to the top of the bushes to bask or orienting to the direction of the sun in order to receive more radiative energy (Bennett, 2004); flattening their body on hot rocks to conduct more heat to the body (Sabo, 2003); making postural adjustments to control the area of body surface exposed to the sun or to the cool winds (Bartholomew, 1966); keeping their mouth wide open (gaping) to cool down when the body temperature might become too high (Spellerberg, 1972; Raymond and Montgomery, 1976), as well as retiring to cool locations underground or in the shade (Barlett and Gates, 1967). To quantify these thermal transfer processes, heat transfer models have been used to calculate the energy exchange between an ectotherm and the environment (Beckman et al., 1973; Porter et al., 1973; Tracy, 1976; 1982; Blouin-Demers and Nadeau, 2005).

Many researchers have set up different models with various complexities to quantify environment-animal energy exchange based on the physics of heat

transfer and the known physiological properties of animals (Porter, 1967; Beckman et al., 1973; Porter et al., 1973; Tracy, 1976; 1982; Waldschmidt and Tracy, 1983; O'Connor and Spotila, 1992; O'Connor, 1999). For animals in general, a thermodynamic equilibrium model was developed (Porter and Gates, 1969), by considering the thermal consequence of metabolic rate, absorbed radiation, convection, conduction, long wave radiation, water loss and work done. Using desert lizards as a target species, simplified energy balance models were proposed: Porter et al. (1973b) considered solar radiation, long wave radiation and convection as key independent variables, while using a two-layer concentric cylinder model to simulate the thermal properties of the target species. Later, a similar model (Waldschmidt and Tracy, 1983) considered the effects of solar radiation, outgoing longwave radiation, convection and conduction for the body temperature of a one-noded (unibody) lizard. Some biophysical models that describe transient temperature incorporated the thermal environment, thermal capacity and physiological control of heat exchange to provide context to the incremental body temperature attained by the animals (Beckman et al., 1973; Christian et al., 2006; Schofield et al., 2009). As the nature of ectotherms' behavioural thermoregulation, when moving in a complex thermal environment, the current body temperature of an ectothermic animal depends not only on the instantaneous thermal environment, but also on the body temperatures that the animal had in the recent past and its thermal capacity (Tracy, 1982). Therefore in this study, a model was developed that takes into account the transient temperatures of lizards moving in a thermally heterogeneous environment.

As Levins (1968) pointed out, a predictive model may have generality or accuracy, but not both. On the one hand, inductive empirical models tend to be simple and ignore some complexities of the specific animals in specific environments (O'Connor and Spotila, 1992). Inductive empirical models are easy to construct and need fewer parameters, but may have a lower accuracy. They work best when used with individuals of smaller body size or simple body shape. Conversely, more complex, deductive models that aim for higher accuracy usually need more information for calibration (O'Connor and Spotila, 1992; Skidmore, 2002). But such information may be missing from the literature or difficult to estimate through measurement. For example, one can neither measure the skin depth of target animals without capturing them in the

field, nor measure the conductivity coefficient outside the laboratory. Alternatively, retrieving parameters through observable data may be a method to obtain the parameters of a bio-physical model (Christian and Roger, 2001; Marsili-Libelli et al., 2003). The hard-to-measure parameters can be estimated by several search algorithms such as trying possible parameter-combinations using a look-up table to obtain a final model that delivers outputs which fit the observed data best. These algorithms have been used to parameterize ecological models such as predator-prey models (Cao et al., 2008), algal growth models (Marsili-Libelli et al., 2003) and animal population models (Conroy et al., 1995), though not for parameter estimation of body temperature.

The objective of this study was to fine-tune a bio-physical model to predict transient temperatures of lizards. More specifically, our study aimed to predict accurately the body temperature dynamics of a lizard in any given thermal environment with a physically based model through a rigorous calibration procedure based on Monte Carlo simulation techniques. The results of the temperature prediction were validated and evaluated by an independent dataset of animal observation conducted in a controlled environment.

## 2.2 Model Description

### 2.2.1 Heat Exchange Terms

From a physical perspective, the energy exchange between a lizard and its environment has been described by Porter's models (Porter and Gates, 1969; Porter et al., 1973). According to his models, the body temperature depends on the balance of the general energy flow, which is the sum of the solar radiation absorbed by the lizard ( $Q_{solar,rad}$ ), the convective heat flow ( $Q_{conv}$ ) and the infrared radiation (long wave radiative heat) ( $Q_{longwave}$ ). In addition, conductive heat flow ( $Q_{cond}$ ) between a lizard and the land surface, energy gain ( $Q_{meta}$ ) by food intake (metabolism) and energy loss through respiration and water evaporation ( $Q_{waterloss}$ ) were also included in his subsequent studies (Porter, 1989) as they were found to have noticeable influence on the body temperature of the animal (Templeton, 1970; Porter, 1989; Clark et al., 2006; Tracy et al., 2010). In summary, the total energy intake of a lizard in a fixed time interval ( $\Delta Q_e$ ) may be written as:

$$\Delta Q_e = \Delta Q_{solar,rad} + \Delta Q_{conv} + \Delta Q_{longwave} + \Delta Q_{cond} + \Delta Q_{meta} - \Delta Q_{waterloss} \quad (\text{Eq. 1-1})$$

### *Solar Radiation*

The direct solar energy incident on the lizard provides heat which is especially important for the animal when the ambient temperature is low (Porter, 1967). The incremental energy received from solar radiation  $\Delta Q_{solar,rad}$  may be written as:

$$\Delta Q_{solar,rad} = \alpha_L A_p Q_{solar} \quad (\text{Eq. 1-2})$$

where  $\alpha_L$  is the absorbance of lizard skin, representing the fraction of the radiative energy absorbed by the lizard.  $Q_{solar}$  is the radiation intensity in units of  $Wm^{-2}$ , and  $A_p$  is the projected lizard area for direct and scattered solar radiation. We assumed this projected area equals the vertical projected area, which is about 0.4 times of the total surface area ( $m^2$ ) of the lizard  $A_L$  (Porter et al., 1973). The surface area can be estimated from the body mass of the lizard in unit of kilogram ( $M_{lizard}$ ), as described in the formula deduced from (O'Connor, 1999), with empirical coefficient  $a = 0.0314$ :

$$A_L = a\pi(M_{lizard})^{2/3} \quad (\text{Eq. 1-3})$$

### *Convection*

The convective heat transfer is one of the major modes of heat transfer between the environment and the lizard. The incremental energy from convection between the air and lizard's body ( $\Delta Q_{conv}$ ) can be expressed as:

$$\Delta Q_{conv} = h_L A_{air} (T_{air} - T_{skin}) \quad (\text{Eq. 1-4})$$

where  $h_L$  stands for the convective heat transfer coefficient of lizard, in units of  $Wm^{-2}K^{-1}$ . We assume an arbitrary value of convective heat transfer coefficient for a wind speed less than 0.5 m/s environment as follows:  $h_L=10.45 Wm^{-2}K^{-1}$  (Porter et al., 1973).  $A_{air}$  is the skin area that exposed in the air, which is assumed that  $A_{air} = 0.9A_L$ .  $T_{air} - T_{skin}$  is the difference between the surrounding air temperature  $T_{air}$  and lizard skin temperature  $T_{skin}$ .

### *Net Longwave Radiation*

The net longwave radiation ( $Q_{longwave}$ ) is the sum of the net infrared radiation exchange to the lizard from surrounding objects. It can be derived from the Stefan–Boltzmann law:

$$\Delta Q_{longwave} = \varepsilon_{lizard} A_{down} \sigma (T_{earth}^4 - T_{skin}^4) + \varepsilon_{lizard} A_{up} \sigma (T_{glass}^4 - T_{skin}^4) \quad (\text{Eq. 1-5})$$

where the lizards' infrared energy income is separated into two parts: radiation from the underlying surface with a temperature of  $T_{earth}$ , as well as from the

surrounding glass walls and cover of the terrarium with a temperature of  $T_{glass}$ .  $T_{glass}$  is assumed to be the same as the air temperature  $T_{air}$ . The emissivity of lizard's skin ( $\epsilon_{lizard}$ ), was set to 0.95 according to (Campbell and Norman, 1977; Turner and Tracy, 1986). As a fraction of the total lizard area  $A_L$ ,  $A_{down}$  and  $A_{up}$  are the areas of skin "facing toward" (but not contacting with) the ground surface and the sky, respectively. In this study,  $A_{down} = 0.3A_L$  (when standing upright) or  $A_{down} = 0$  (when lies down), and  $A_{up} = 0.6A_L$  were considered appropriate estimations (Barlett and Gates, 1967).  $\sigma$  is the Stefan–Boltzmann constant, which is  $5.67 \times 10^{-8} (Wm^{-2}K^{-4})$ .

### Conduction

Thermal conduction may be substantial for lizard's thermoregulation (Bujes and Verrastro, 2006). Following Fourier's law the heat conducted from the underlying surface to the body  $Q_{cond}$  can be represented as:

$$\Delta Q_{cond} = \frac{A_{contact} K_{lizard} (T_{earth} - T_{skin})}{\delta / 2} \quad (\text{Eq. 1-6})$$

where  $A_{contact}$  is the area lizard contacts with the ground. It depends on the posture of lizard:  $A_{contact}$  was set to  $0.1A_L$  when standing and  $A_{contact}=0.4A_L$  when lying.  $K_{lizard}$  is the thermal conductivity and was set to  $0.50 \text{ WK}^{-1}\text{m}^{-1}$  according to (Porter et al., 1973).  $\delta$  is the measured average diameter of the lizard body.

### Metabolism

Although the daily metabolism level of lizards is not as high as that of birds or mammals of equal size, a noticeable contribution of metabolism to lizards' body temperature has been observed (Dawson and Bartholomew, 1958; Bennett and Nagy, 1977). The effect of metabolism on body temperature was considered in some studies for lizards, as an increase of metabolic rate may lead to a small but significant increase of body temperature (Brown and Au, 2009). If we assume 20.9 Joules of heat is produced for each cubic centimetre of oxygen consumed (Porter et al., 1973), the metabolic rate ( $\Delta Q_{meta}$ ) can be expressed as a function of body mass ( $M_{lizard}$ ) and body temperature in degrees Celsius ( $T_{lizard\_inC}$ ) (Clark et al., 2006):

$$\Delta Q_{meta} = 0.348 \exp(0.022T_{lizard\_inC} - 0.132) M_{lizard} \quad (\text{Eq. 1-7})$$

where  $M_{lizard}$  is the mass of the lizard in kilograms.  $T_{lizard\_inC}$  is the core lizard body temperature in Celsius, which is assumed to be the same as the lizard's skin temperature. Because the ratio of internal to external resistance (Biot number) is very small for a lizard in a typical environment (Porter et al., 1973), the skin temperature yields a good approximation of the core body temperature (Barlett and Gates, 1967; Waldschmidt and Tracy, 1983). This equation shows that the rate of metabolic heat increases proportionally to the body temperature.

### *Respiratory Loss*

The lizard's body temperature also has an impact on its respiratory water loss which removes the latent heat of body water during vaporization. At low air temperature, energy is lost through respiration at a constant rate that is independent of the body temperature. As the temperature rises, the speed of respiratory loss increases (Templeton, 1970). It has been suggested that the energy loss corresponding to water loss for *desert iguanas* (*Dipsosaurus dorsalis*) could be written as :

$$\begin{aligned} \Delta Q_{resp} &= 0.272m_{lizard} && (T_{lizard\_inC} < 20^{\circ}\text{C}) \\ \Delta Q_{resp} &= 0.0836m_{lizard}e^{0.0586T_{lizard\_inC}} && (20^{\circ}\text{C} \leq T_{lizard\_inC} < 36^{\circ}\text{C}) \\ \Delta Q_{resp} &= 0.003m_{lizard}e^{0.1516T_{lizard\_inC}} && (T_{lizard\_inC} \geq 36^{\circ}\text{C}) \end{aligned} \quad (\text{Eq. 1-8})$$

As hardly any useful data are available on the energy loss by water vaporization for *Timon lepidus* (Ocellated lizard), this study uses the above formulas derived from desert iguanas, since the two lizards have similar body size and live in relatively similar environments.

### **2.2.2 Body Temperature Simulation**

With the quantification of the lizard's energy budget, the dynamic changes of body temperature under changing thermal conditions can be modelled by:

$$\Delta T = \frac{\Delta Q_e}{M_{lizard}c_{lizard}} \quad (\text{Eq. 1-9})$$

Where  $\Delta T$  is the body temperature changes in a certain period of time,  $\Delta Q_e$  is the net energy received within that time,  $M_{lizard}$  stands for the mass of the lizard in unit of kg, and  $c_{lizard}$  represents the specific heat capacity of the animal.

An estimation of the specific heat capacity of  $3762\text{Jkg}^{-1}$  of a lizard ( $c_{lizard}$ ) was made by Porter (1973b). This value was adopted to calculate the body

temperature change in a fixed time interval. The numerical model was implemented with Simulink® (Mathwork, 2008), iterating by a 10-second fixed time step. Figure 2-1 details the model as a diagram, and specifically shows how parameters and heat transfer terms are connected and how the energy exchange leads to the dynamic balancing of the body temperature of lizard.

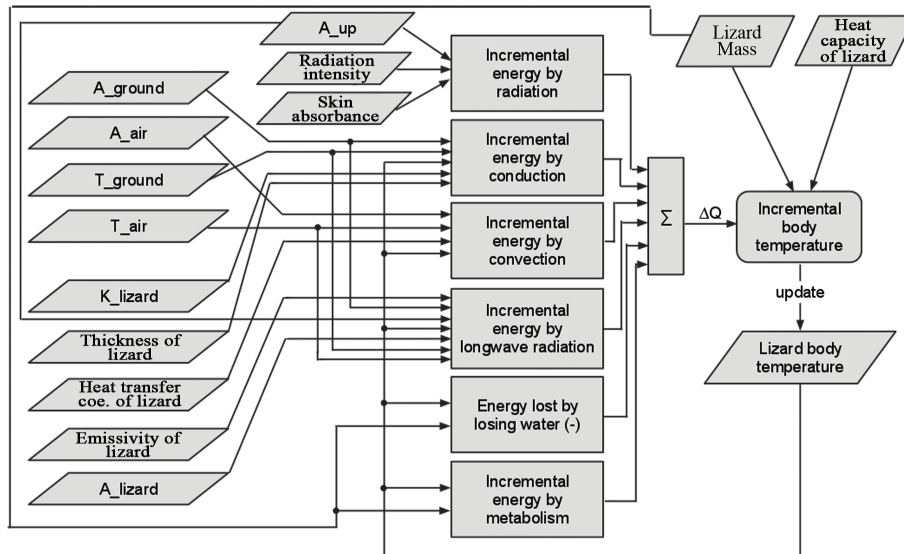


Figure 2-1 Lizard's body temperature dynamics, decided by thermal environment and physiological parameters. A\_lizard, A\_ground, A\_air, and A\_up stand for the total area of the target lizard, the area that the lizard contacts with the ground, the area the lizard exposes in the air and the projection area of the lizard, respectively; T\_ground, T\_air represents the ground temperature and the air temperature of the thermal environment in Celsius.

## 2.3 Model Evaluation

### 2.3.1 Experimental Design

*Timon lepidus* (Ocellated lizard) was chosen as the target animal for developing the model as it is widely studied and the model may be parameterized. It is a ground-dwelling lizard that is widely distributed in Spain, Portugal, southern France and north-western Italy. The skin colour of an adult has a camouflaged effect comprising mottled blue, green and brown patches interspersed with brighter spots. In the wild, it feeds on insects, snails, newly hatched birds and fruits (Pleguezuelos et al., 2008).

### *Terrarium Configuration*

An experiment was carried out at a reptile zoo “Dierenpark De Oliemeulen” during September, 2008 in Tilburg, the Netherlands. A glass terrarium of size 245cm x 120cm x 115cm was constructed. At the bottom of the terrarium, at least 10 cm of gravel and sand were mixed to form a flat substrate surface. Photoperiod was maintained at 14L:10D with a 100-Watt heat lamp. An infrared heat lamp of 100W provided additional heat input for 5 h during the middle of the photophase. A 4-year-old male *Timon lepidus* was kept in the terrarium for 10 days before the experiment started, in order that the lizard could acclimatize to the new environment. The lizard was fed on vegetables, crickets, newly born mice, and some fruits such as apple and banana.

Traditionally, the body temperature of lizards is measured by a contact thermometer that reads the cloacal temperature, or by an inbuilt data logger and radio transmittance device implanted inside the lizard’s body (Kerr et al., 2008). In this study, however, thermal infrared imagers were used that read the body temperature remotely. This approach has three main advantages: Firstly, it measures the body temperature without physical contact with the lizard, so the measurements were not affected by the changing metabolic rate as a response of struggling. Second, the thermal imagers measured also the surface temperature of the substrate, based on which the conductive energy exchange between animal and the ground could be calculated. Thirdly, the animal was not handled or stressed in any way by the measurement process. Three IRISYS® 1011 thermal imagers were mounted in a row at 2m above the bottom of the terrarium, pointing down with their field-of-views (FOVs) covering a continuous rectangular area of the bottom (33 cm x 100 cm).

### *Data Collection*

During the experiment, the brightness temperature (i.e., the temperature of a black body when emitting an equivalent amount of radiation) of both the lizard and the land surface were measured by the IRISYS 1011 thermal imagers. The land surface temperature just beneath the lizard was interpolated from the measurements of the surrounding 8 pixels. The air temperature was recorded by “Hobo™ Temperature Smart Sensors” placed at the height of the lizard; and the full spectrum radiation within the terrarium was mapped by “Hobo™ Silicon Pyranometer Smart Sensors”. Some researchers argued that the skin absorbance

( $\alpha_L$ ) of some lizards co-varied with the body temperature, especially when the body temperature is higher than 38°C (Norris, 1965; Porter, 1967), while other studies consider it constant (Waldschmidt and Tracy, 1983). Therefore, to determine whether the reflectance of the lizard skin varied with the body temperature, we used a FieldSpec-3 spectrometer (ASD, Boulder, USA) to measure the spectral reflectance of the target lizard under two different body temperatures. 20 spectra were measured at body temperatures of 36°C and 40°C respectively, followed by a t-test to determine whether there was a significant difference on the skin reflectance of target species at different body temperatures (Table 2-1).

Table 2-1 Details of the data collection of the experiment

Variable	Unit	Spatial Resolution	Recording Interval	Device	Accuracy *specified by the manufacturer
Lizard Surface Temperature	°C	4.4cm <sup>2</sup>	10 s	IRISYS 1011 thermal imager	±0.3K
Ground Surface Temperature	°C	4.4cm <sup>2</sup>	10 s	IRISYS 1011 thermal imager	±0.3K
Air Temperature	°C	--	10 min	Temperature and RH Smart Sensor	±0.7K
Full Spectrum Radiation	W <sup>2</sup> /m <sup>2</sup>	Interpolated to 4.4cm <sup>2</sup>	--	Hobo™ Silicon Pyranometer Smart Sensor	±15 W <sup>2</sup> /m <sup>2</sup>
Skin Spectral Reflectance	--	--	Spectral resolution : 3.5 nm at 700 nm	ASD FieldSpec® 3 spectrometer	--

### 2.3.2 Calibration of the Body Temperature Model

The lizard body temperature model has 6 input variables and 9 parameters (Table 2-2). The input variables were directly measured while the parameters were received from the literature (standard parameterization). To further improve the performance of the model and generate realistic parameters (improved parameterization), we re-estimated the model parameters using a Monte Carlo simulation. In a preliminary step, the 9-dimensional parameter space was sampled over an equally distributed grid. Across each parameter's range, which was assumed to be ±10% of its reference value, the body temperature model was run at each sample point using the input of the actual thermal environment of the animal experiment, thereby predicting the range in

body temperature over time. Meanwhile, the observed lizard body temperature dynamics were recorded, and later compared with the predicted values.

Specifically, the calibration used the root mean square error (RMSE) to compute the deviation between the observed body temperatures and predicted temperatures. The parameter combination by which the prediction had the lowest RMSE was selected, allowing the bio-physical parameters of the lizard to be determined from the body temperature observations.

Table 2-2 Input parameters ranges setting for the look-up table

Parameters	Measured / Estimated	Symbol / Unit	Ranges setting for parameter adjustment
Lizard mass	M	$m_{lizard}$ (kg)	0.19
Land surface temperature	M	$T_{earth}$ (K)	297.15
Air temperature	M	$T_{air}$ (K)	297.65
Initial lizard skin temperature	M	$T_{skin}$ (K)	303.15
Radiation intensity	M	$Q_{solar}$ ( $Wm^{-2}$ ,)	300
Skin absorbance	M	--	0.936
Lizard specific heat capacity	E	$C_{lizard}$ ( $JK^{-1}g^{-1}$ )	3.762±0.37
Lizard thickness	E	$\delta$ (m)	0.015±0.0015
thermal conductivity	E	$K_{lizard}$ ( $W K^{-1}m^{-1}$ )	0.502±0.050
convection coefficient	E	$h_L$ ( $Wm^{-2}K^{-1}$ )	10.450±1.045
Lizard Area	E	$A_L$ ( $m^2$ )	0.032±0.003
Contacting area with the earth	E	$A_{down}$ ( $m^2$ )	0.003±0.0003 *
Projected lizard area	E	$A_p$ ( $m^2$ )	0.013±0.001
Emissivity of lizard skin	E	--	0.950±0.1
Emissivity of land surface	E	--	0.950±0.1

\* The  $A_{down}$  is centered on 0.4  $A_L$ , as the lizard kept lying flattened when measuring

### 2.3.3 Validation of the Body Temperature Model

Independent observations (N=31) of lizard's body temperature were collected to validate the body temperature model. These data were chosen based on two criteria: (1) continuous body temperature records when the lizard was moving within the field of view of the thermal imagers; and (2) while within the field of view, both heating and cooling phases were experienced by the lizard. The observations were compared with model simulations and the root mean square error (RMSE) of the temperature prediction was calculated.

### 2.3.4 Sensitivity Analysis of the Body Temperature Model

As a method to test the robustness of the model, sensitivity analysis is necessary as it examines how different values of independent variables will impact the result (Chinneck, 2004), which is the body temperature of the lizard in this case. We analysed how a change in each input variable affects the body temperature prediction after 1 and 10 minutes. The sensitivity of the model was estimated by increasing and decreasing each input parameter by 10% from its typical value, while leaving the other input variables constant. The testing thermal environment was: ground temperature of 24°C, air temperature of 24.5°C, radiation intensity of 300W<sup>2</sup>/m<sup>2</sup>, and the initial lizard body temperature of 20°C.

## 2.4 Results

### 2.4.1 Absorbance of the Lizard's Skin

In the 40 measurements, the skin absorption varied little and did not show significant difference at different body temperatures. Figure 2-2 shows the spectral absorption curve of the lizard's skin. The spectral reflectance showed that there was no significant effect of lizard body temperature on absorbance (t-test, n=40, p=0.139,  $\alpha=0.05$ ). Therefore, we consider  $\alpha_L$  to be a constant value of 0.936.

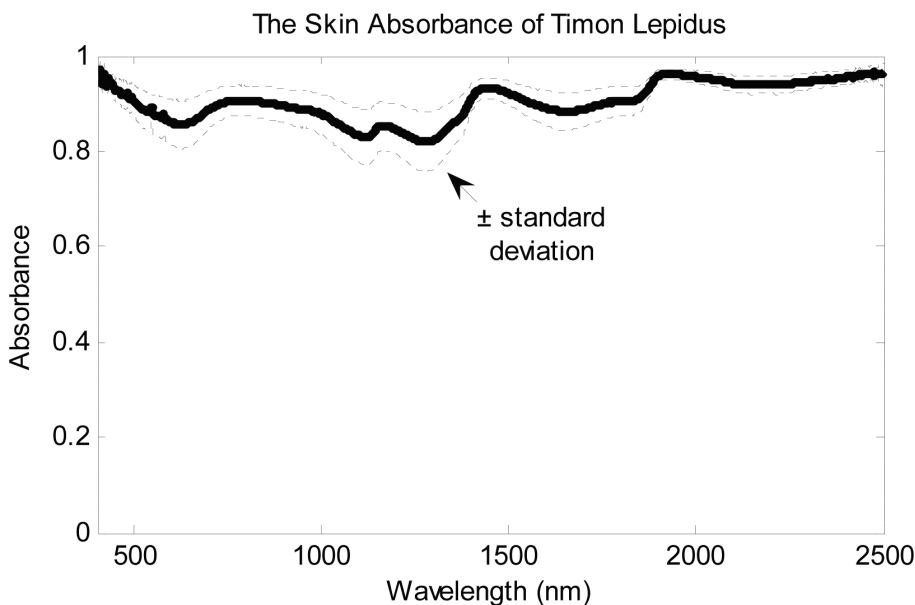


Figure 2-2 The spectral absorbance of the *Timon lepidus*' skin in 40 spectral measurements, showing mean value (solid line) and standard deviation (dotted lines).

### 2.4.2 Calibration of the Body Temperature Model

After improved parameterization, the root mean square error (RMSE) of the predicted body temperature was 0.44°C, when the body temperature rose from 26.40°C to 31.40°C degree (Figure 2-3), while the RMSE was 0.24°C when the body temperature dropped from 33.9 to 32.0 degree (Figure 2-4). With the standard parameters received from the literature, however, the RMSE values of the predicted body temperature were 4.19 °C (rising temperature) and 0.79 °C (temperature drop), respectively.

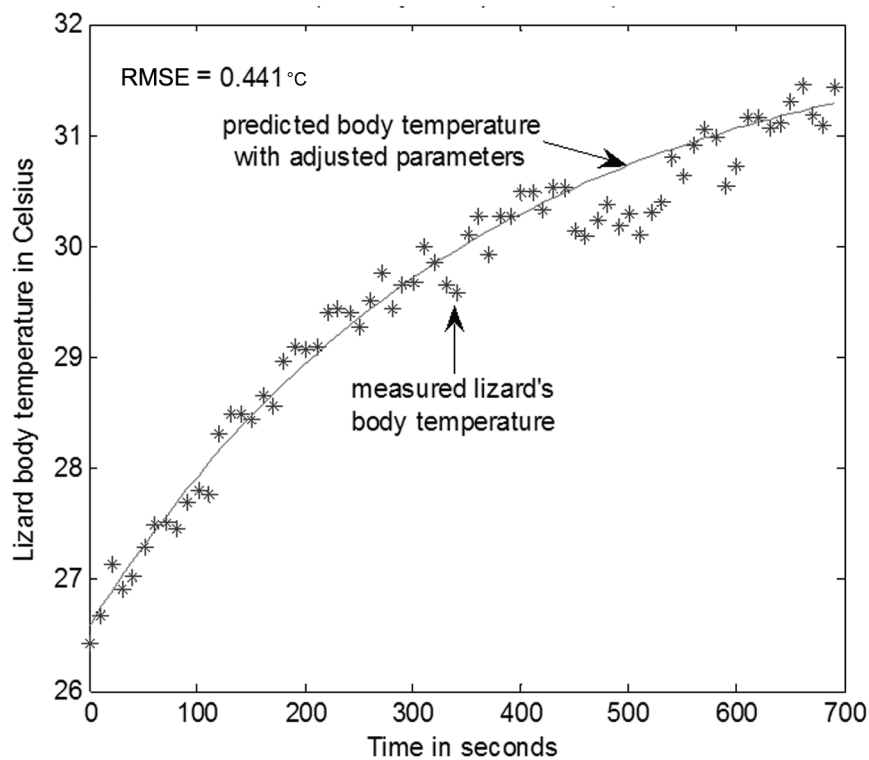


Figure 2-3 Model parameterization: the predictions made by the body temperature model with the best parameters fitting training data of a basking lizard

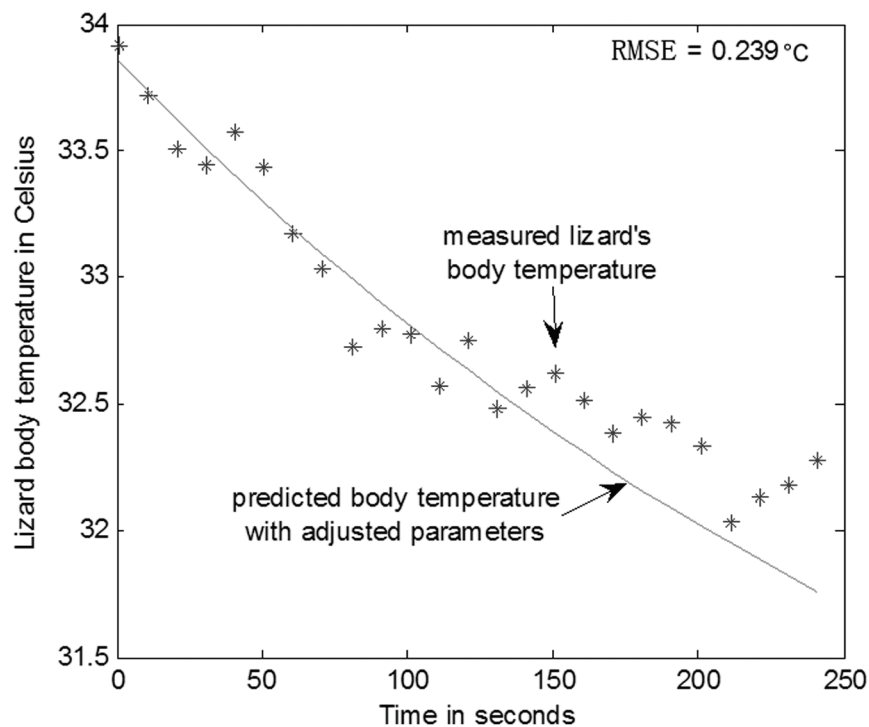


Figure 2-4 Model parameterization: the predictions made by the body temperature model with the best parameters fitting training data of a cooling lizard

### 2.4.3 Validation of the Body Temperature Model

The independent dataset (N=31) of the measured lizard body temperatures was used to validate the calibrated model. To avoid biased results, a period in which the lizard experienced both heating and cooling phases was chosen. The model performance may be visually compared in Figure 2-5 before and after the parameterization when using the independent validation dataset. Figure 2-6 illustrates the model performance with the improved parameters in term of RMSE: after the calibration, the RMSE of temperature prediction decreased from 1.35°C to 0.59°C.

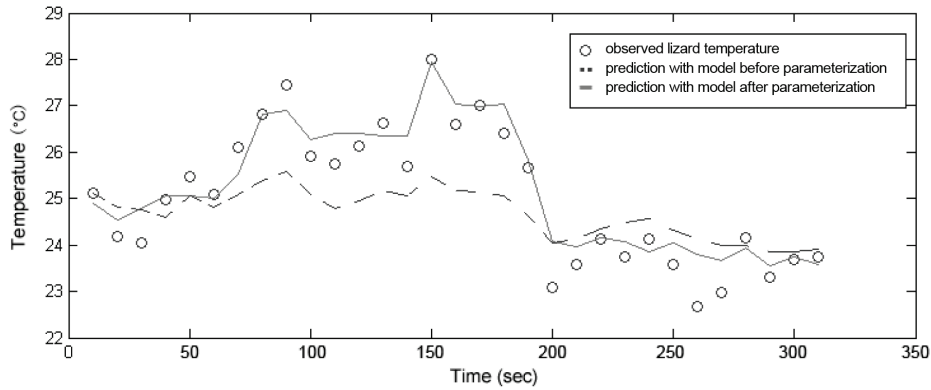


Figure 2-5 The comparison between the prediction errors of the body temperature model before (dotted line) and after (solid line) parameterization

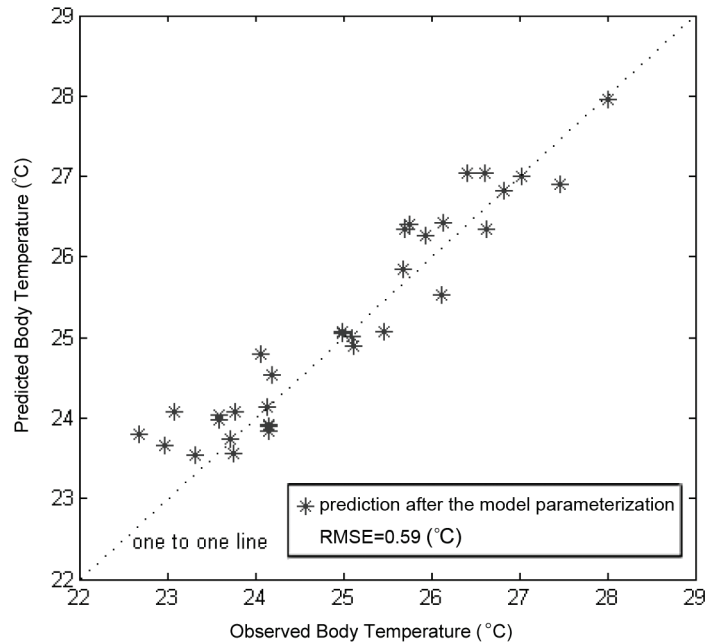


Figure 2-6 The observed body temperature vs. the predictions of the calibrated model, model validation using independent dataset

#### **2.4.4 Sensitivity Tests of the Body Temperature Model**

Sensitivity tests were performed to determine how responsive the body temperature change is to each of the parameters we estimated for the representative lizard we've chosen. Figure 2-7 shows how each input variable affects the body temperature prediction during the following one minute. In addition to the initial body temperature, the air temperature and ground surface

temperature had important influences on the body temperature of the lizard. Direct radiation intensity was relatively less sensitive compared with the above two thermal parameters.

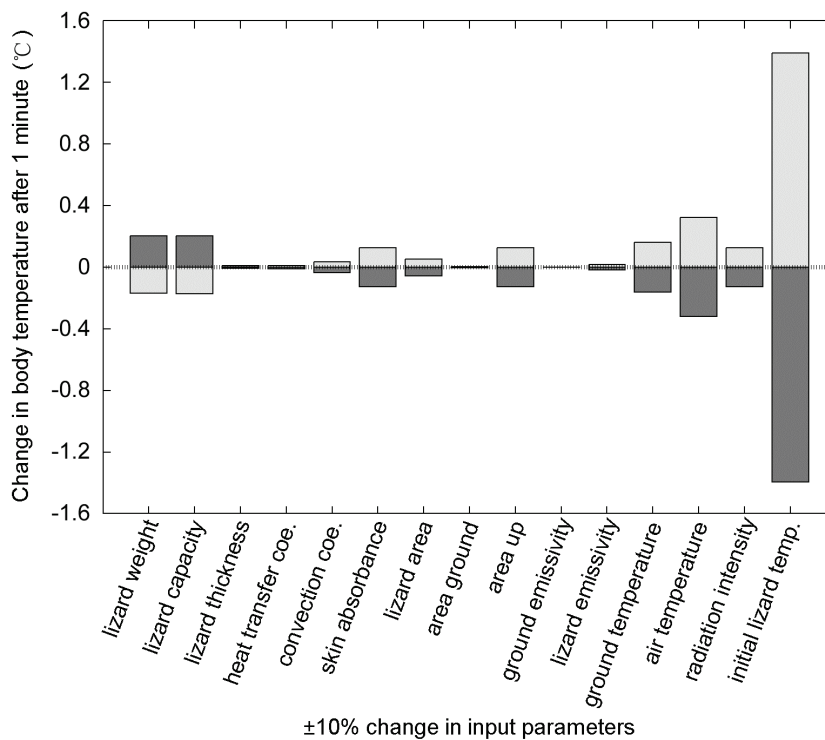


Figure 2-7 The sensitivity of lizard body temperature responding to input parameters: one-min test. Each parameter is increased and decreased by 10% from its estimated value, while leaving the other inputs constant. Lighter coloured bars illustrate the results of increasing the parameters; darker coloured bars represent the results of decreasing the parameters.

Figure 2-8 shows how each input variable affects the body temperature prediction for the following 10 minutes. This time, the ground surface temperature and air temperature dominate the final body temperature of lizards, while the initial body temperature has no effect. In addition, a 10% increase in radiation intensity or skin absorbance can raise the body temperature by 2% within 10 minutes, which means the final body temperature is also sensitive to the radiation received.

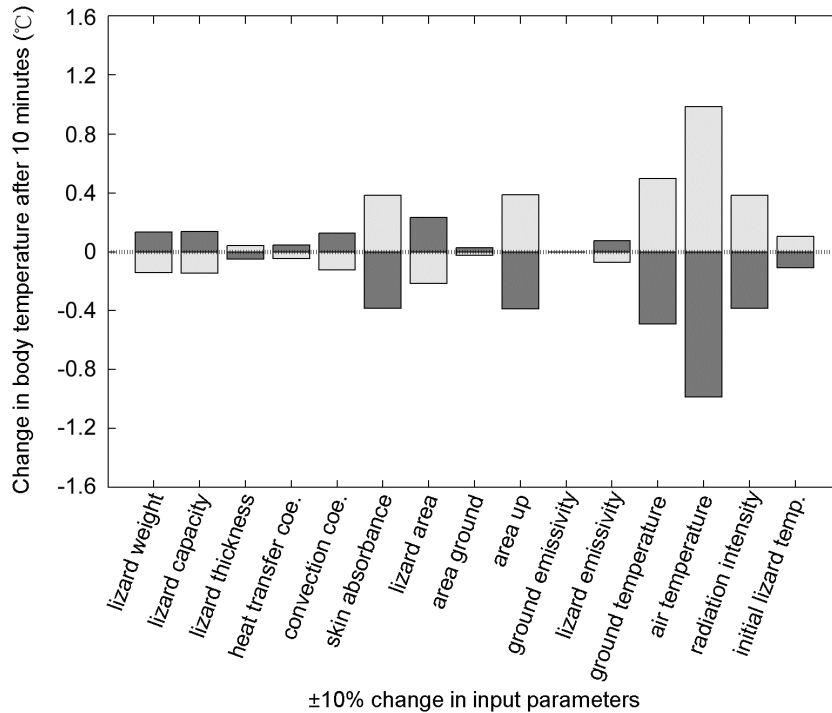


Figure 2-8 The sensitivity of lizard body temperature responding to input parameters: ten-min test. Each parameter is increased and decreased by 10% from its estimated value, while leaving the other inputs constant. Lighter coloured bars illustrate the results of increasing the parameters; darker coloured bars represent the results of decreasing the parameters.

It can be noted that the response of three variables (convection coefficient, lizard area and lizard emissivity) change direction between the 1-min test and the 10-min test. It's because in the most of the time within the 1-min test, the lizard was colder than the environment. As a result, energy transferred from the environment to the animal through conduction, convection and long-wave radiation had a positive impact on the temperature of the lizard, so higher values of these variables (meaning faster exchange rate of energy) led to a higher final body temperature; while in the 10-min test, as the lizard soon got warmer than the environment, so the energy transferred from the animal to the environment had a negative impact on the body temperature of the lizard. As a result, a higher value of these variables led to a lower final body temperature.

## 2.5 Discussion

With a bio-physical model, we predicted the transient body temperature of a lizard, *Timon lepidus*, in response to the thermal environment. In this model, six heat transfer terms were taken into account: solar radiation, convective heat flow, longwave radiation, conductive heat flow, metabolic heat gain and respiratory energy loss. The instantaneous values of these terms were calculated from the thermal environment and the parameters of the target animal, namely, body mass, size, skin absorbance, specific heat capacity, conductive heat transfer coefficient, convection coefficient and surface area. We estimated some heat related bio-physical parameters that were difficult to measure in-situ by using a Monte Carlo simulation on the basis of reference values obtained from literature. As a result, the accuracy of the body temperature prediction was improved. Before the parameter estimation, the RMSE of the body temperature prediction was 1.35°C; while after, it dropped to 0.59°C. The results of the study showed that the body temperature model with the Monte Carlo parameterization technique presented here can accurately reflect the body temperature dynamics of lizards confined in a laboratory condition.

The ground surface temperature and air temperature are the two environmental factors to which the body temperature of a lizard appears to be most sensitive. Although many bio-physical models have accounted for the heat exchange between an animal and the substrate (Tracy, 1976; O'Connor and Spotila, 1992), in practical terms, the thermal characteristics of the ground surface often vary substantially and are difficult to measure in the field (O'Connor and Spotila, 1992). In this study, the successful application of the thermal infrared imagers with considerate spatial interpolation offered a new approach to monitor the thermal landscape accurately and remotely. According to the observation of the study, the heat transfer term of the metabolic energy gain did not entirely offset the evaporative energy loss, as some studies suggested (Bartholomew, 1982; Tracy, 1982). Therefore, ignoring or inaccurately measuring them may have a negative impact on the prediction accuracy of the model. For example, if the three terms of conduction, metabolic gain and evaporative loss are ignored, the model RMSE increases from 0.59 °C to 0.85°C.

It can be noted in Figure 2-3, that at around 500 seconds, the model slightly overestimated the lizard's temperature. To explain this phenomenon, the

experimental records were checked. We found that the lizard was curled up during this period, so the temperature of the body and the cooler tail was possibly mixed in one thermal infrared pixel. It is reasonable that the value of the mixed pixel is therefore lower than the actual body temperature. We also noted that the lizard cools at a slightly slower rate than predicted (Figure 2-4 after 150 sec.), though this phenomenon has been previously noted (Bartholomew and Lasiewski, 1965; Bartholomew, 1982). A possible reason may be attributed to circulatory shutdown in the appendages (Porter et al., 1973). When cooling, a lizard may slow down the blood flow rate in the appendages by vasoconstriction to conserve energy (Dzialowski and O'Connor, 1999; 2004).

For the independent dataset, the model gave an unbiased body temperature prediction with RMSE of 0.59 °C (Figure 2-8). It was suspected that there were three possible sources causing this error, i.e., the inaccurate measurement of the environment, the simplification of the model, and the parameterization of the model. For the measurement of the environment, the convection is difficult to characterize accurately, especially due to the turbulent flows from environment (Vogel, 1981). The contact area between land surface and the lizard was also difficult to measure and could only be assumed in this study. The radiation was not always perpendicular to the land surface, but also from the side, which may have an impact on the amount of radiation received by lizards. This possible source of error was not considered in this study. Regarding the model structure, the model description of the heat transfer processes was simplified, but the heat fluxes are complex. We assumed that all heat transfer coefficients were static, such as the convection heat transfer coefficient, while in reality, coefficients are simple empirical approximations for complex heat exchange processes. Determining the coefficients under one set of conditions and applying them under another may be a source of error (O'Connor and Spotila, 1992). Assumptions about the target animal also allowed a simplification of the model: The body shape of the animal was assumed to consist of a series of cylinders - one for the main body and six for the appendages, as O'Connor (1999) proposed. However, the diversity in the shape of lizards may introduce error when estimating surface area as well as to the heat transfer terms, thereby weakens the predictive ability of the model. The energy loss attributed to the passing of faeces and urine, the rapid temperature rise after food intake (Clark et

al., 2006), and the energy consumption through activity were not considered in our model, but could be added. In addition, a thermally homogeneous object was used to represent the target species, while the heat transfer inside the body is far more complex (Georges, 1979; Dorcas and Peterson, 1997), even the surface temperature distribution of the lizard is not always homogeneous. Some multi-layered models considered the different conductivities and positions of the animal components, such as flesh, bones, fat, blood and skin (Porter and Gates, 1969; Porter et al., 1973; Tracy, 1976). However, such models require more detailed data about the animal than that is normally available (O'Connor and Spotila, 1992). As for the parameterization process, previous studies have shown that parameter optimization may lead to equifinality, i.e., models with different parameters all lead to acceptable results when the information content in calibration data is not in balance with the model complicity (Mitchell et al., 2009). This is the inborn limitation of this parameter retrieval method. To reduce this effect, we firstly made use of prior knowledge from literature to determine the rough values of the parameters, and then validated the model using data from both heating and cooling phases of the lizard. With these efforts we expected to pinpoint parameters and to diminish the possibility of error-posting. Despite all of these errors, because the experiment was carried out in a terrarium, many environmental factors such as wind speed, air temperature, substratal surface temperature and radiation were constant or controlled or have been carefully recorded, leading to a satisfactory accuracy of body temperature prediction.

However, to test the performance of the body temperature model in the field, by up-scaling the experiment to a natural lizard's microhabitat, challenges emerge through variation in environmental factors, as well as measurement limitations imposed by the instrumentation. At field scale, topography and vegetation cover may not be homogenous, and radiative energy received by the animal consists of direct and indirect radiation in the open area. As a result, additional field data such as the slope and aspect of the habitat, the vegetation cover, the canopy density, and the diffuse sunlight has to be considered to calculate the actual radiative energy received. Because different land covers have different emissivity, an emissivity map of substrate has to be estimated for a correct retrieval of ground surface temperature, to get ipso facto an accurate calculation of conduction. The wind speed at the height of a lizard has to be measured in-

situ because in the field wind will dramatically affect the convection. Also the feeding activities need to be noted because the body temperature is significantly lower when fasting than after feeding (Wang et al., 2002) (contrary to in our laboratory conditions where food was always available). In addition, as there is no hard boundary of lizard's home range, it is expected that the animal will live across a much larger territory. In order to record the ground surface temperature dynamics for a much wider area, the thermal infrared imager should have a much higher spatial resolution to ensure that pure pixels of 'lizard' can be recorded so the body temperature of the animal can be retrieved accurately. Despite all the difficulties, the model used in this study is physically based and therefore has the ability to cope with field situations when parameterized by the Monte Carlo method presented in this paper.

## **2.6 Conclusion**

This paper described a bio-physical model for body temperature simulations and the use of a Monte Carlo technique to refine model parameters based on reference values from the literature. In conclusion, the transient body temperature of an ectotherm was modelled accurately from its thermal environment in a laboratory setting. The model inversion technique for the retrieval of thermal characteristics of the animal from continuous body temperature observation clearly enhanced the accuracy of temperature prediction. Although it was not the scope to test the body temperature model and the calibration techniques in a field environment, the model due to its physical nature has the potential to work under field condition, proper model parameterization provided. Up-scaling the model to a real lizard habitat under natural conditions will be the scope of following research activities that will build on the presented work.

# CHAPTER 3

## PREDICTING MICRO THERMAL HABITAT OF LIZARDS IN A DYNAMIC THERMAL ENVIRONMENT

---

This chapter is based on: Fei, T., Skidmore, A.K., Venus, V., Wang, T., Toxopeus, A. G., Bian, M., Liu, Y., 2012. Predicting micro thermal habitat of lizards in a dynamic thermal environment. *Ecological Modelling* 231, 126-133.

## **Abstract**

Understanding behavioural thermoregulation and its consequences is a central topic in ecology. In this study, a spatial explicit model was developed to simulate the movement and thermal habitat use of lizards in a controlled environment. The model incorporates a lizard's transient body temperatures with a cellular automaton (CA) algorithm and links the physiology knowledge of the animal with the spatial utilization of its microhabitat. The model assumed that a lizard tries to maintain its preferred body temperature in a dynamic thermal environment by continuously selecting positions with different thermal conditions. The sequence of chosen positions formed a chain defining the individual's path, to be later aggregated into a map of thermal habitat use. An experiment was designed to test the model. An ocellated lizard (*Timon lepidus*) was kept in a terrarium with controlled dynamic thermal environment, and the thermal environment as well as the movement of the lizard were recorded by a variety of sensors. The model was tested to predict the spatial utilization of a lizard's thermal habitat in the terrarium based on three categories: high, moderate and low occupancy. The simulated results were compared with observations from the animal experiment. The predicted overall pattern of the micro-habitat occupancy of the lizard within 4 days matched the observation, at an overall accuracy of 75.7%. The results suggest that thermal habitat use by lizards in a controlled environment may be predicted by the integrated model of the lizard's body temperature and the CA algorithm.

### 3.1 Introduction

Wildlife conservation and management requires reliable information on the abundance and spatial distribution of species and their habitats (Skidmore, 2002; Broitman et al., 2009). Many studies conclude that the spatial distribution of species or communities is statistically related to their present environment (Guisan and Zimmermann, 2000). Climate in combination with other environmental factors has been used to explain vegetation distribution (Neilson, 1995; Jobbágy and Jackson, 2000; Bachelet et al., 2001) and animal distribution (Edgar, 1983; Fischer et al., 2001; Pearson and Dawson, 2003; Skidmore et al., 2011). Among environmental factors, thermal properties have been considered important for both terrestrial (Poole and Heard, 2003; Row and Blouin-Demers, 2006; Wang et al., 2010; Zeng et al., 2010) and aquatic animals (Block et al., 2001; Schofield et al., 2009). The thermal environment is of particular importance to ectotherms since their body temperature is in equilibrium with their environment. Thermal conditions play an important role in various aspects of the physiology, biology and ecology of ectothermic species. For instance, growth, development and survival of embryos (Angilletta et al., 2009), metabolic processes such as digestion (Harwood, 1979), behavioural processes such as activity (Stephen and Porter, 1993; Nicholson et al., 2005; Sears, 2005; Rouag et al., 2006), locomotion (Waldschmidt and Tracy, 1983), microhabitat selection (Porter and James, 1979; Angilletta et al., 2009; Schofield et al., 2009) and spatial distribution and life history traits of populations (Porter and Tracy, 1983; Kearney and Porter, 2004; Medina et al., 2009) of ectotherms may all be affected. In recent years, with the global warming debate receiving much attention, it inspired wide discussion on how ectotherms respond to environmental changes at different scales. Models that predict environmental change as well as depict ectothermic responses have been developed (Cramer et al., 2001; Walther et al., 2002; Kearney and Porter, 2004; Araújo et al., 2006; Deutsch et al., 2008; Pierce et al., 2009; Seo et al., 2009; Wiens et al., 2009). However, in most studies the thermal environment was considered as a one dimensional environmental factor. Although at regional or global scale it is acceptable that the thermal environment stands for ambient temperature, it is an oversimplification at a microhabitat scale (Fei et al., 2011b).

Since the temperature of land objects varies in space and time, the thermal environment within a habitat is extremely heterogeneous (Sabo, 2003). To cope

with the wide diversity of habitat thermal qualities, ectotherms are able to maintain a crude form of body temperature by continuously shifting their location (Raymond and Montgomery, 1976). This is called behavioural thermoregulation. Most studies on behavioural thermoregulation have focused on the activity patterns of animals (Porter et al., 1973; Eifler et al., 2008). Some studies have linked the thermal environment to habitat use by ectotherms (Spellerberg, 1972; Schlesinger and Shine, 1994; Vitt et al., 1997; Kerr et al., 2003; Row and Blouin-Demers, 2006). However, relatively little is known about how behavioural thermoregulation of ectotherms translates into their spatial distribution at micro-habitat level (Blouin-Demers and Nadeau, 2005).

Statistical models are popular in ecology and are often used to link environmental properties with species distribution (Woodward and Cramer, 1996). Methods such as generalized linear models (Vincent and Haworth, 1983), artificial neural networks (Gutiérrez-Estrada et al., 2008) and co-kriging spatial interpolation (Georgakarakos and Kitsiou, 2008) have been successfully applied to the mapping of thermal habitats of animals. However, as a result of the lack of underlying ecological/biological functions and mechanisms in such a model, the generality of the model has to be sacrificed. Moreover, most statistical predictive models are built based on a dataset collected in the field, and automatically assume equilibrium between the environment and observed species distributions (Guisan and Zimmermann, 2000). These factors limit applications of statistical models in a fast-changing environment. Unfortunately, the movement and thermal habitat use of ectotherms are often highly complex and dynamic, as they frequently shuttle between spots with different thermal conditions. An alternative to the statistically based static modelling is the dynamic approach. Only a few species have been studied in terms of their response to dynamic environmental change, though such models have been successfully applied in ecology, including in simulating a forest pattern (Urban et al., 1991), vegetation distribution dynamics (Moore and Noble, 1993), the movement of ants on a trail (Kunwar et al., 2004), and the movement of birds during a breeding season (Betts et al., 2008).

One of the dynamic modelling approaches is called cellular automaton (CA). CA is a discrete rule-based model that constitutes a mathematical system in which simple components (rules) act together to recreate complicated patterns

of behaviour (Wolfram, 1984; Mynett and Chen, 2004). CA offers the possibility to infer movements from given transition rules built on physiological simulation of the target species, and has two main advantages over other methods. Firstly, it provides a clear arranged spatial structure which is binding on landscape and movement modelling; second, the fixed neighbourhood relationships between cells make possible the description of local interactions by transition rules (Lutz, 1997). The potential of CA to predict animal distribution was explored in the famous CA “game of life” (Conway, 1970), where the population dynamics of a simplified ecosystem was simulated in a spatially explicit manner. Examples such as modelling the foraging movements of kittiwakes (Ford et al., 2007) and the dispersal of plateau pika on the Qinghai-Xizang plateau (Liu and Zhou, 2007) illustrate the successful application of cellular automata in ecology. However, a spatially explicit CA model simulating how animals, especially ectotherms, use their thermal habitat related to their physiology has rarely been seen. Animal physiology and animal distribution dynamics are two subjects that have been developing almost in parallel, despite widespread acceptance that they must be somehow related (Claireaux et al., 1995). Therefore, filling the gap between physiological knowledge of ectotherms and observed animal distribution patterns forms an important issue in ecological modelling.

This study aimed to develop an integrated model that incorporates the lizard body temperature into a cellular automaton algorithm to simulate movement and predict the micro thermal habitat use by lizards in a controlled but dynamic environment.

## **3.2 Method**

### **3.2.1 Target Animal and Experimental Setup**

An experiment was carried out in reptile park “Dierenpark de Oliemeulen” during 22 to 29 September 2008 in Tilburg, the Netherlands. Ocellated lizard (*Timon Lepidus* (Daudin, 1802)) was chosen as target animal in this study. This lizard is a ground-dwelling species widely distributed in Spain, Portugal, southern France, and north-western Italy. It is one of the largest lizard species in Europe with a typical adult body length of 30 - 70 cm (Mateo, 2004). The skin colour of an adult is a mixture of blue, green, and brown, with brighter spots. In the wild the species feeds on insects, snails, newly hatched birds, and fruits. The

body parameters of an adult *Timon lepidus* from the reptile park, including gender, age, snout-vent-length (SVL), tail length and weight, were measured before it was placed in a terrarium. Other thermal-related parameters (detailed in Table 3-1) of the lizard were also estimated based on measurements according to (Chato, 1966; Barlett and Gates, 1967; Beckman et al., 1973; Porter et al., 1973).

Table 3-1 Measured and estimated body parameters of a *Timon lepidus* used in this study

Parameters	Measured / Estimated	Value	Unit
Gender	M	Male	--
SLV	M	19.5	(cm)
Tail length	M	14.5	(cm)
Body mass	M	190.0	(g)
Skin absorbance	M	$9.36 \times 10^{-2}$	--
Specific heat capacity	E	3.76	(JK <sup>-1</sup> g <sup>-1</sup> )
Lizard thickness	E	1.50	(cm)
Heat transfer coefficient. (conduction)	E	0.50	(Wm <sup>-1</sup> K <sup>-1</sup> )
convection coefficient	E	10.45	(Wm <sup>-2</sup> K <sup>-1</sup> )
Lizard area	E	$1.87 \times 10^{-2}$	(m <sup>2</sup> )
Contact area with the earth when moving	E	$1.87 \times 10^{-3}$	(m <sup>2</sup> )
Contact area with the earth when basking	E	$7.48 \times 10^{-3}$	(m <sup>2</sup> )
Projected lizard area	E	$7.70 \times 10^{-3}$	(m <sup>2</sup> )
Emissivity of lizard skin	E	0.95	--

The glass terrarium set up for the lizard was 245 x 120 x 115 cm. On the bottom of the terrarium, gravel and sand were mixed to form a flat substrate of at least 10 cm. Rocks, burrows, UV-lamps, heating devices, and a fog generator were placed and adjusted in the terrarium to simulate the geography and micro-climate of the lizard's natural habitat (Figure 3-1). To simulate the daily variation in temperature and radiation, the photoperiod was maintained at a constant 11.5 hours of light and 12.5 hours of darkness per day using 100 W heating lamps. An infrared heat lamp provided additional heat for five hours

during the middle of the photophase. The light period started at 8:30 and ended at 19:00 each day. The lizard was kept in the terrarium for 15 days before starting the experiment, to allow the lizard to acclimatize to the new environment. The lizard was fed on crickets, newly born mice, vegetables, and fruits such as apple and banana.

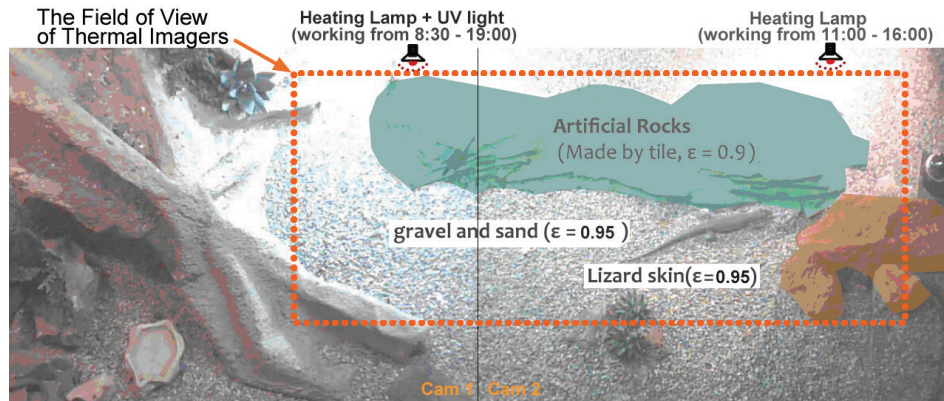


Figure 3-1 The top view of the terrarium, the FOV of the thermal imagers, and the materials and emissivities of the bottom surface

Three IRISYS 1011 thermal imagers (each with a resolution of 16 x 16 pixels) were mounted in a row at 2m above the ground surface of the terrarium, pointing down with a field-of-view (FOV) covering a continuous rectangular area of the base of 33 x 100 cm. Two webcams (Logitech communication STX with an optical resolution of 640 x 480 pixels) were mounted at the same height, with a FOV covering the whole base. Temperature sensors (Hobo™ temperature and relative humidity smart sensors, Onset Computer Co.) were placed at a height of 10 cm above the ground surface to record the air temperature inside the terrarium.

### 3.2.2 Data Collection

During the experiment the brightness temperature (the temperature a black body emitting the same amount of radiation would have) of both the lizard and the ground surface of the terrarium were measured by three IRISYS 1011 thermal imagers. The air temperature was recorded by the Hobo™ temperature sensors, while the full spectrum radiation within the terrarium was mapped by a 'Hobo™ silicon pyranometer smart sensor'. The motion of the lizard was detected using the software 'ZoneMinder V1.3', the lizard's activity triggering the optical recordings by the two webcams. The recorded video made it possible

to track the centroid position of the lizard at all times. The details of the collected data are given in Table 3-2.

Table 3-2. Details on the data collection for the experiment.

Variable	Unit	Spatial Resolution	Recording Interval	Device	Accuracy *
Lizard Surface Temperature	°C	4.4cm <sup>2</sup>	30 s	IRISYS 1011 thermal imager	±0.3K
Ground Surface Temperature	°C	4.4cm <sup>2</sup>	30 s	IRISYS 1011 thermal imager	±0.3K
Lizard's Location	--	0.25 cm <sup>2</sup>	When Motion Detected	Logitech Webcams (communication. STX)	--
Air Temperature	°C	--	10 min	Temperature and RH Smart Sensor	±0.7K
Radiation	W <sup>2</sup> /m <sup>2</sup>	Interpolated to 4.4cm <sup>2</sup>	--	Hobo™ Silicon Pyranometer Smart Sensors	±15 W <sup>2</sup> /m <sup>2</sup>

\* inferred from manufacturer

### 3.2.3 Model Building

#### *Framework of the Cellular Automaton*

To coincide with the resolution of the ground surface temperature observations within the terrarium, a two-dimensional artificial microhabitat of 48 by 16 grid cells was defined. For each cell covering an area of 4.4 cm<sup>2</sup> two properties were measured: the surface temperature showing the current averaged land surface temperature of the cell, and the radiation intensity representing the intensity of emitted energy received by the cell. A simulated “lizard” was located in a random initial cell within the artificial microhabitat. Following a set of transition rules, the lizard was able to move to one of the eight neighbouring cells in one time step, as a response to thermal environmental changes. Lizard movement was controlled by the transition rules with a time interval of 30 seconds (the time resolution of the ground surface temperature recording). During the simulation the locations of the simulated lizard were recorded at every step. The sequence of chosen positions formed a chain defining the individual's path, to be translated to the map of thermal habitat use later. To prevent the simulation from being trapped in a local optimization, random

moves were added in the algorithm to reposition the lizard. To eliminate the sensitivity of the result to the initial position of the virtual lizard, and to enhance the robustness of the algorithm, the final result of the spatial utilization of the microhabitat was obtained by averaging 100 runs of the model, which had all used random initial positions for the lizard.

### *Transition rules*

Transition rules form the core of a CA algorithm (Chen et al., 2002). These rules depend on the behavioural traits of the modelled species, their response to thermal landscape dynamics, and their ability to perceive their environment. The assumption made here is that during the day time (from 8:30 to 19:00) the lizard will try to maintain its preferred body temperature ( $T_p$ ) for as long as possible. When its body temperature falls below (or increases above)  $T_p$ , it will sense the ambient temperature within a certain distance (one cell in our model) and with a chance  $P$  it will move to the warmest (or coldest) cell in its vicinity. The probability  $P$  is assumed to be positively related to the difference between the lizard's actual body temperature ( $T_b$ ) and its preferred body temperature ( $T_p$ ), which means the greater the difference between the two temperatures, the more likely it is the lizard will move. At night (from 19:00 to 8:30), the simulated lizard is assumed to retreat to its burrow.

### *Body Temperature Model for Lizards*

As the behavioural response of lizards depends on body temperature, a bio-physical body temperature model was applied to simulate the lizard's body temperature in response to thermal environmental changes. The model included parameters of the thermal environment of the lizard such as conductive, convective, and radiative heat transfer terms and gave predictions on changes in body temperature. With the body temperature model, the real-time incremental body temperature  $Q_e$  could be calculated from the air temperature, the land surface temperature, the amount of shortwave and longwave radiation received, the metabolic heat, and the evaporative heat loss, by expressing it as:

$$\Delta Q_e = \Delta Q_{solar,rad} + \Delta Q_{conv} + \Delta Q_{longwave} + \Delta Q_{cond} + \Delta Q_{meta} - \Delta Q_{waterloss} \quad (\text{Eq. 2-1})$$

with  $Q_{solar,rad}$  and  $Q_{longwave}$  representing the solar radiation and the environmental longwave radiation, respectively, absorbed by the lizard;  $Q_{conv}$  representing the convective heat flow, and  $Q_{cond}$  the conductive heat flow between a lizard and

the land surface;  $Q_{meta}$  representing the energy gain by metabolic process (Clark et al., 2006) and  $Q_{waterloss}$  the energy loss through respiration and water evaporation (Templeton, 1970). The details of the model are to be found in Porter et al. (1973), and the model was parameterized with measurements and estimations illustrated in Table 3-1. The values of the parameters listed in the table were fixed by an earlier study, and the detail of the parameterization process can be found at (Fei et al., 2012a).

### Model Integration

To simulate the interaction between individual lizards and the thermal landscape, the measured thermal landscape dynamics were coupled with the integrated model of the body temperature model and the cellular automaton algorithm, which was programmed and visualized within Matlab 7.1. The flow chart (Figure 3-2) illustrates the process of the integrated model simulating the thermal habitat use by the lizard.

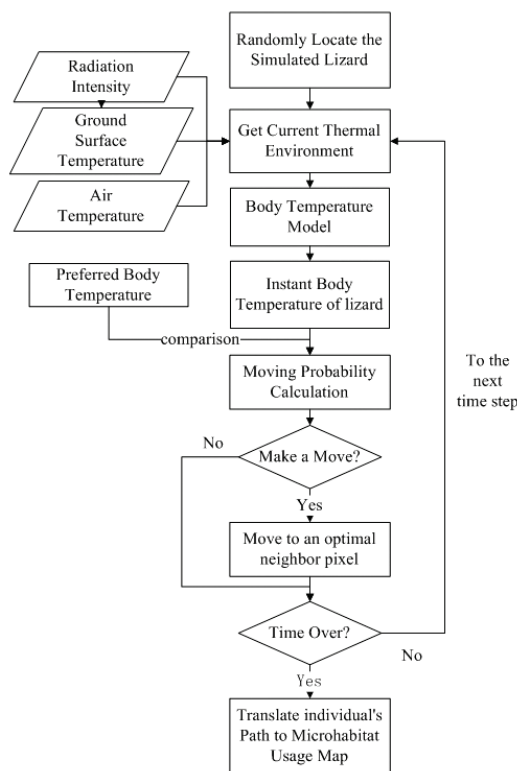


Figure 3-2 Flow chart of the integrated model which simulate the dynamic process of thermal habitat use by the lizard

### Model Parameterization

The range of preferred body temperatures ( $T_p$ ) was measured along a photo-thermal gradient, according to the method provided by Ladyman and Bradshaw (2003). The floor of the terrarium was covered with gravel, enabling the lizard to move freely, and producing a land surface temperature gradient of 18 to 48 °C. The lizard was able to adapt its body temperature by selecting a position at an appropriate distance from the heat source. During the lizard's active time over nine days, 80 random samples of its measured body temperature were taken and averaged to be used as preferred body temperature  $T_p$  of the species. The probability  $P$  that the lizard moved to a neighbouring pixel in one time step was the only parameter that needed to be determined. It was assumed to be positively related to the difference between its current body temperature  $T_b$  and its preferred body temperature  $T_p$ . The relationship was assumed to be linear with a slope of  $k$  where  $P$  was smaller than 1. The probability  $P$  can be written as:

$$P = k(|T_b - T_p|), \quad \text{when } (|T_b - T_p| < \frac{1}{k})$$

$$P = 1, \quad \text{when } (|T_b - T_p| \geq \frac{1}{k}) \quad (\text{Eq. 2-2})$$

The goal was to estimate coefficient  $k$  with the aim to achieve the most realistic result. The slope  $k$  is positive by definition. A simulation with one hundred runs was executed with  $k$  ranging from 0.1 to 10 at intervals of 0.1. The model used different values of  $k$  to simulate 4 days of animal behaviour. The results were compared with the observed (recorded) microhabitat occupancy, and the agreement between the two was calculated using the correlation coefficient of all pixels. As a result, a  $k$  value with the highest  $r$  was determined. The tracking data collected from 22 to 25 September 2008 were used for model parameterization.

### 3.2.4 Model Validation

The CA algorithm was validated by comparing the simulated spatial utilization of the microhabitat with the actual spatial utilization of the microhabitat derived from independently observed data collected from 26 to 29 September 2008. The simulated thermal environment used the observed air temperature dynamics, radiation dynamics and land surface temperature dynamics as input. Therefore

the simulated thermal environment aims to theoretically replicate the (real) animal experiment. To assess the performance of the simulation, the predicted and observed spatial utilization maps were compared. The attribute occupancy was amalgamated into three categories as such a spatial attribute is inherently uncertain and should only be validated qualitatively. The three categories were: high occupancy (>20 minutes per day on average), moderate occupancy (10 to 20 minutes per day) and low occupancy (<10 minutes per day). Afterwards, the overall accuracy of the model was calculated by means of a classification error matrix derived from the two maps.

### **3.3 Results and Discussion**

#### **3.3.1 Model Parameterization**

Preferred body temperature ( $T_p$ ), the temperature an animal chooses when exposed to a photo-thermal gradient, was measured for the *Timon lepidus*. Table 3-3 shows that 35.3 °C was the average preferred body temperature  $T_p$  for this lizard when active.

Table 3-3. Measurements of the preferred body temperature of *Timon lepidus*

	<b>Min</b>	<b>Max</b>	<b>Std</b>	<b>Mean (N=80)</b>
Temperature (°C)	26.5	41.6	4.1	35.3

Figure 3-3 details the determination of parameter  $k$  by the CA algorithm. As shown in the figure, the X-axis represents the  $k$  value as tested from 0.1 to 10, with step intervals of 0.1. The Y-axis represents the overall accuracy of the predicted spatial utilisation. The result shows that the model performed best when  $k = 0.3$ .

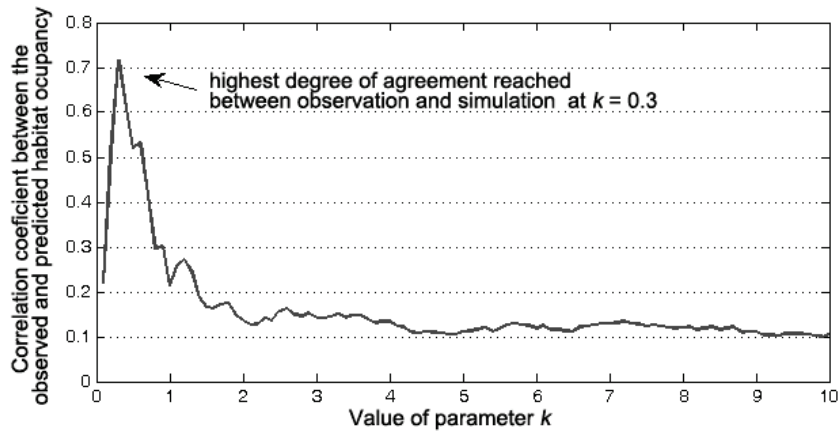


Figure 3-3 The determination of parameter k in the cellular automata algorithm. At  $k=0.3$  the model yielded a best match between prediction and observation.

### 3.3.2 Thermal Habitat Use

Figure 3-4 forms an example of how the movement pattern of a simulated lizard translates into spatial utilization. The simulated lizard started at a random position located on the left side of the image. After 10 minutes (20 steps), the lizard moved to the right side of the image. During this period, it stayed in the upper-left corner for the longest time (i.e. indicated by a more reddish colour). It was clear that after 60 minutes the lizard made most frequent use of the upper-left part of its microhabitat, where a heat source was available. After 24 hours in simulation, the lizard had visited almost every spot in the simulated microhabitat, with several locations having been visited more often than others: the pattern of thermal habitat utilization had emerged.

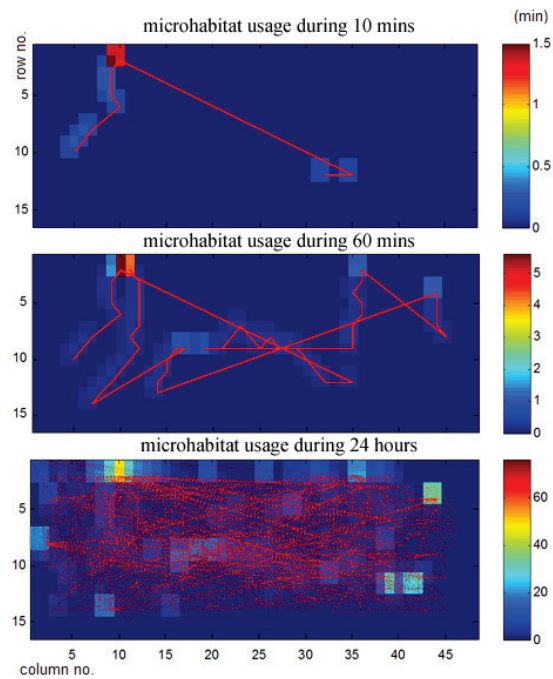


Figure 3-4 Movement and thermal habitat use by a simulated lizard during 10 minutes, 1 hour, and 1 day, respectively.

The integrated model was run to simulate the thermal habitat use by a lizard during a 96-hour experiment. The results of this simulation are illustrated in Figure 3-5 in a spatially explicit way. The cell colour on the map represents the total time the lizard spent in a particular cell.

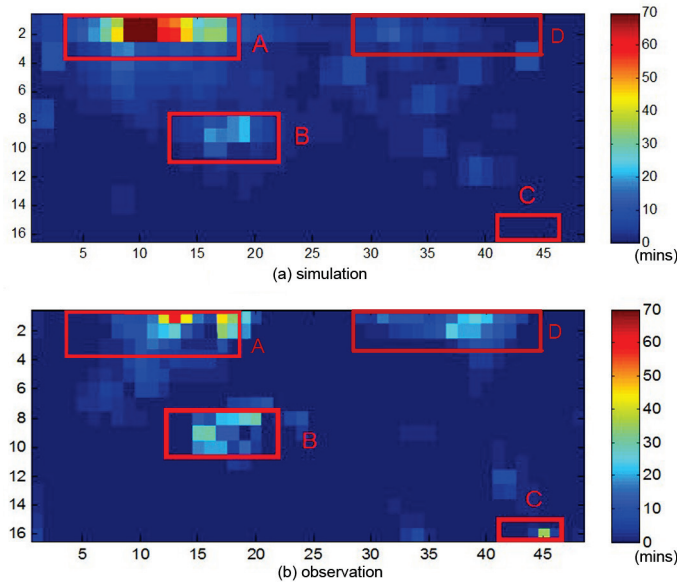


Figure 3-5 (a) simulated lizard's habitat occupancy vs. (b) observed lizard's habitat occupancy. The colour represents microhabitat occupation in terms of time the centroid of the lizard spent at each cell (in minutes) within 4 days. Each grid cell represents an area of 4.4cm<sup>2</sup>.

For validation, the observatory lizard tracking data was aggregated, classified and compared with the simulation. The accuracy of the simulated thermal habitat use was calculated using a confusion matrix, in which the different levels of occupancy between simulation and actual observation were summarised. The result showed an overall accuracy of 75.7% (Table 3-4). It also showed the simulation slightly over-estimated the activity of the lizard.

Table 3-4. Confusion matrix of the simulated vs. observed microhabitat occupancy (unit: pixel)

Simulation \ Observation	high occupancy	Moderate occupancy	low occupancy	Row total
	high occupancy	<b>28</b>	16	4
Moderate occupancy	9	<b>29</b>	32	70
low occupancy	47	78	<b>525</b>	650
Column total	84	123	561	overall accuracy: <b>75.7%</b>

This result revealed that the thermal environment and the behavioural thermoregulation can be mapped to explain the lizard's microhabitat use.

Furthermore, using a cellular automaton algorithm, the spatial pattern of microhabitat occupancy can be simulated solely based on an energy point of view.

The upper-left area (marked: 'A' in Figure 3-5) was mapped as the most frequently used area, accounting for about 49% of total active time of the lizard. It was the most frequently occupied area because it provided a constant source of heat and radiation, which a lizard needs to stay active. The lizard tended to use this area to maintain its body temperature, especially in the morning and in the late afternoon when no other heat source was available. Area B in Figure 3-5 was a colder place not only because it was further away from the heat source than area A, but also because it was located in the shade of an artificial rock (Figure 3-6). Area A and B provided highly contrasting thermal conditions enabling the animal to regulate its body temperature by shuttling between the two areas.

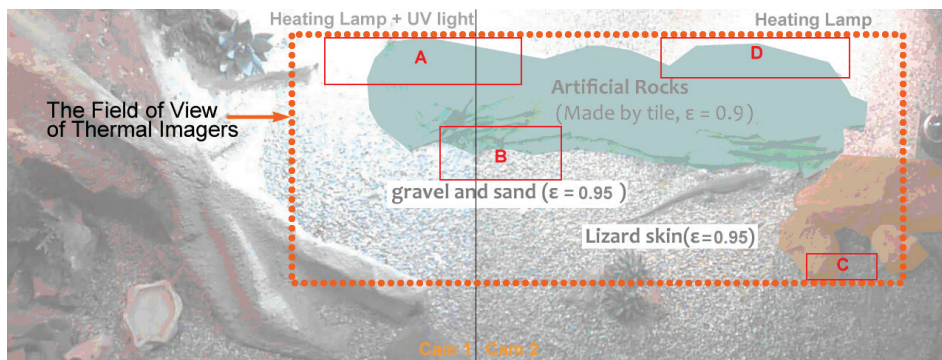


Figure 3-6 The most frequently used microhabitat by a real lizard in the terrarium in the field view of thermal imaging cameras.

In reality, the real lizard spent less time in area A than predicted, and more time in area D (Figure 3-5). It is possible that the memory ability of the lizard was underestimated. It was assumed the simulated lizard sensed the optimal thermal environment with a fixed radius at each step. The simulated lizard would then not notice the additional heating lamp in area D, as it was turned on at every 11:00, unless it was near D. However, it seemed that memory effect enabled the real lizard to wait in area D even before the new heat/light source was switched on, increasing the time spent in that area.

Although the CA model predicted the way a lizard would use its microhabitat, not all movements can be explained by behavioural thermoregulation alone.

Food, water, as well as other important environmental factors and environment-animal interactions may cause a lizard to move and could account for the 24.3% of error (Table 3-4) between the simulated and observed habitat use by the lizard. Consider area C in Figure 3-5, for example, where the real lizard spent more than 30 minutes in four days, without any obvious relation with the thermal preferences of lizards being found. Perhaps some small rocks placed in area C provided shelter (Figure 3-6) for the lizard to hide behind when disturbed by zoo visitors near the terrarium.

The next phase of our work is to validate the performance of the model to a natural lizard's microhabitat by up-scaling the experiment. As the scale changes, additional factors should be considered to model the thermal environment of the animal, In order to represent inherent landscape complexities. Also, animals may respond differently in the field because of the additional environmental factors, so the transition rules of the model have to be modified accordingly, such as introducing animal territory, defensive behaviour and community interactions. In addition, when working at a landscape scale, the individual based model needs to be upgraded to a multi-agent based model, so the interactions between individuals could be modelled as well.

### **3.4 Conclusion**

Simulating the behavioural thermoregulation of lizards based on an integrated model of the lizard body temperature and a cellular automaton algorithm may to a large degree predict the thermal habitat use by a lizard in a controlled environment. Nevertheless, nature is complex and heterogeneous and therefore challenging to model (Levins, 1966). In order to gain the full picture of a lizard's microhabitat selection, especially in an open field, other factors besides thermal environment, such as food, water and defence mechanisms of lizards, which surely also play an important role will need to be considered in future studies.



# CHAPTER 4

## MODEL THE NATURAL TERRAIN ELEVATION OF LIZARD MICRO HABITAT

---

This chapter is based on: Fei, T., Ferri, P., Venus, V., Toxopeus, A.G., Skidmore, A.K., Bian, M., 2012. Natural terrain elevation modelling from a laser rangefinder point cloud, *Journal of Applied Remote Sensing*. (in review).

## **Abstract**

A low-budget alternative for building fine-scale natural terrain elevation for small areas (<1000 m<sup>2</sup>) has been developed. A lightweight handheld infrared laser rangefinder was utilized to measure the topography of the land surface. By wirelessly communicating with the rangefinder from a portable computer, the relative spatial locations of the target formed a point cloud which were displayed and recorded on the fly. Supplementary data collected from different observation points can be merged together to minimize shadow zones and increase the local accuracy of the DEM product, depending on the importance of features in the terrain. Quantitative evaluations were performed with independent check-points (ICPs) measured by a level. Results showed that the vertical accuracy of the DEM achieved was around 20 cm. The method offers a low cost and flexible approach for building fine-scale DEMs.

## 4.1 Introduction

A digital elevation model (DEM) is an ordered array of points that represents the spatial distribution of (relative) elevations in a landscape (Moore et al., 1991). Terrain attributes derived from DEMs, such as gradient, aspect and topographic position, have been widely used as important spatial variables in various scientific research projects, including ecological studies (Turner et al., 2003; Estes et al., 2010; Skidmore et al., 2011), hydrological studies (Sharma et al., 2011; Yamazaki et al., 2012), soil mapping (Mueller and Pierce, 2003; Pei et al., 2010) and archaeology (Vogel and Märker, 2010). As a result, many geographic information systems and resource inventory systems are being developed for storing topographic information as primary data for spatial analysis (Moore et al., 1991).

A wide variety of DEMs collected from space-borne platforms can be obtained from government agencies. For example, the Advanced Space-borne Thermal Emission and Reflection Radiometer (ASTER) launched on board NASA's Terra spacecraft represents elevation at a 15 m horizontal resolution and a 9 – 92 m vertical accuracy, depending on the topography and vegetation cover (Toutin, 2002; Nikolakopoulos et al., 2006); SPOT-5 (Satellite Pour l'Observation de la Terre 5) is capable of producing DEMs with a 15 m horizontal resolution, with a vertical error of 10 m in the best conditions (SPOT-IMAGE-Co., 2005); the Gestalt Photomapping System, which can be mounted on airborne platforms, has a vertical accuracy of 0.022–0.03% of the aircraft flying height and is therefore capable of producing a DEM of 10 m resolution (Kelly et al., 1977). The Shuttle Radar Topography Mission (SRTM) is expected to provide DEMs at a resolution of 30 m for the United States and 90 m for outside areas, with a vertical RMSE of 16 m (Nikolakopoulos et al., 2006). However, these space-borne sensors typically produce DEMs that average information over tens of square meters or more (Turner et al., 2003), which is too coarse for some applications, such as animal microhabitat studies in ecology, which require much more detailed and accurate elevation information over often a small terrain area. The collection of topographic data for such a small terrain area can be accomplished by using field survey methods, such as levelling, differential GPS, stereo photogrammetry or Lidar (light detection and ranging); however, these methods have obvious limitations. For instance, levelling is flexible but inefficient, and labour consuming for

DEM mapping. Differential GPS does not achieve a high accuracy on elevation measurements. In most cases it requires a ground-based reference station. With close-range stereo photogrammetry, it is possible to produce a highly accurate elevation model over complex ground surfaces (Butler et al., 1998). However, this method requires two semimetric cameras, multiple vantage points and careful planning of the light sources and camera positions. Ground based LIDAR, as a fast-developing 3D mapping technology, has the great advantages of scanning speed and accuracy, but the high cost limits its application. Moreover, all the methods mentioned above have a common drawback: the portability of the devices needed for the measurement is a problem for field work, especially in remote areas.

One other possibility is offered by low-cost and lightweight near-infrared laser rangefinders (NIR-LRF), despite the fact that they are designed for measuring distance. A laser rangefinder is based on time-of-flight measurement, where a short emitting laser pulse is transmitted and its time of travel is accurately measured with respect to the received signal from a target. The emitted laser energy is in the near-infrared wavelength region, hence the name. Nowadays, more and more rangefinders feature an integrated compass and a tilt-meter, which allow users to accurately measure the angle of azimuth and the inclination of a target, as well as the distance to the observer. Therefore, if measured from the same location, by knowing the distance and the inclination and azimuth of the target points, the position of the target points can be fixed in a 3D space. After having collected enough points, the point cloud of the target surface can be interpolated to a DEM.

This paper illustrates a method of efficiently constructing a DEM with a lightweight, low-cost laser rangefinder. The accuracy of the digital elevations generated was evaluated with independent check points.

## **4.2 Methods**

### **4.2.1 Study Site**

The study area was located at El Torcal de Antequera National Park, Málaga, Spain (latitude  $+36^{\circ}59'5''$ , longitude  $-4^{\circ}31'38''$ ). The 30 x 30 m site was situated at the northern foot of the limestone mountain of El Torcal. The region is characterized by a Mediterranean semiarid landscape: dry and firm soil,

sparse herbaceous plants and thinly scattered woody plants (mostly *Retama sphaerocarpa* and some scattered European fan palms [*Chamaerops humilis*]). The topography of the study site was complex, with rocks and dried herbaceous plants. The site is one of the microhabitats for the ocellated lizard (*Timon lepidus*).

#### 4.2.2 The Rangefinder

The TruPulse 360B (Laser Technology, Inc., USA, Figure 4-1) is a lightweight, low-cost laser rangefinder that measures slope distance (straight-line distance between the rangefinder and the point measured), inclination and azimuth. It can calculate horizontal distance, vertical distance, height, and missing line values between two measured points. It is equipped with 7x optics, in-scope data display, a serial port and an integrated Bluetooth® wireless communication module. The technique specifications for the device is detailed in Table 4-1.



Figure 4-1 TruPulse 360B – the laser rangefinder

Table 4-1 Specifications for the TruPulse 360B laser rangefinder

Dimensions	15.2 x 6.4 x 12.7 cm
Weight	0.2 kg
Maximum range	1575 m
Accuracy	3–5 cm
Inclinometer range	± 90°
Inclinometer accuracy	± 0.1°

### **4.2.3 Data Collection**

#### *Scanning Preparation*

The experimental setup was performed at the study area on a cloudy day at a temperature of 25°C. The rangefinder was mounted on a 1.7 m high tripod to keep a stable position, and standing 2 m outside the site of interest, to have a wide view. A laptop was programmed to connect with the rangefinder wirelessly by Bluetooth®, using Matlab® 2008a. First, the program checked the status of the rangefinder and, if connected, set the communication port and baud rate. When ready, it sent commands ordering the remote device to take a measurement, and waiting until the device sent back data on slope distance, azimuth, and inclination value of the target point. These data were stored in a text file after an accuracy check. Depending on the observation conditions, the rangefinder may send back data in one of two modes: high-accuracy mode, with 0.1 m accuracy, and low-accuracy mode, with 1 m accuracy. The accuracy information (high or low) was also stored with the above numeric data as metadata. Low-accuracy results were likely caused by one of the following conditions, according to our experience: 1. More than one target, with different distances, fell in the center area of the crosshairs of the lens. 2. The rangefinder was not kept stable, or 3. The target was moving when measuring. All low-quality data were filtered and removed later.

#### *Scanning Strategy*

Before scanning the terrain surface, we specified one main observation position and one supplementary position next to the study area to ensure that any surface point in the area could be seen from at least one of the two positions. To ensure the success of the subsequent merging of the two scans to minimize shadow (no-data) zones in the DEM, 12 distinguishable reference points (painted iron nails) were positioned in the study area beforehand, spread equally over the site. Before scanning from each observation position, the positions of the reference points were first measured by the rangefinder in a certain sequence.

It took the rangefinder about 1–3 seconds to measure the distance, azimuth and inclination of each target point. After transmitting the data to the computer, it waited for 1 second for us to move the direction slightly, aiming at a new point nearby. At this speed, about 1000 land surface points could be collected in one hour. The study area was scanned column by column. For the first 1000

measurements collected at the main observation position, the measured points were equally distributed over the study area. For the second 1000 measurements at the same observation position, densely distributed points were assigned to measure complex topographic features such as rocks, shrubs and salient relief. As a consequence, higher concentrations of points were collected in order to capture more complex topographic features, and lower concentrations of points were collected in the more featureless parts of the survey area.

As we moved to the second observation position, about 1500 supplemental points from the position were collected. Half of these points were focused on shadow (no-data) areas from the first observation position, as well as to portray complex topographic features; the other half of these points were randomly distributed over the study area.

#### *DEM Generation*

First, the records of distance, azimuth and inclination from the first scan were mapped to points plotted in X, Y, Z space by transforming the spherical coordinates to Cartesian coordinates (Figure 4-2):

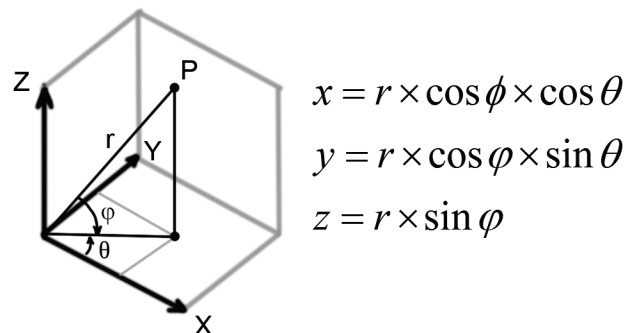


Figure 4-2 Transfer of the records from spherical coordinates to Cartesian coordinates

Where  $r$  is the slope distance between the rangefinder and the target point,  $\phi$  is the inclination angle, and  $\theta$  is the azimuth angle relative to the north. The two scans from different viewing points into one point cloud were then merged. By registering the relative locations of the reference points together (Bonnaffe et al., 2007), data collected from the second viewing point were aligned to the coordinates of the first scan. The alignment process was stopped when resulting in the least square error between the reference pairs.

It is impossible to get comprehensive values of data points at every position of the terrain, because of practical constraints. Thus, interpolation is important and fundamental for the graphing and analysis of DEM data. A variety of methods for interpolating a surface from a set of points have been proposed. Among them, linear interpolation, spline interpolation (Wahba, 1981) and kriging (Goovaerts, 2000) were applied in this study to define the most suitable method of interpolating a point cloud to a grid DEM. Due to the relatively small volume of data (3500 points) to be analyzed, segmentation of the grid was not necessary (Agarwal et al., 2006).

#### **4.2.4 Accuracy Assessment**

Quantitative evaluations were performed with independent check points (N=30) for the DEMs generated: The relative elevations of the 30 random independent check points were measured by levelling, with an accuracy of 5 mm. These points were used to check the quality of the DEM generated. First, we compared the elevations at check points between the DEM's derived from only the first scan and the independent observations; then, the relationship between the elevation error and the distance from the observing points were tested. Finally, the DEM derived from the merged point clouds from the two scans was tested in terms of elevation accuracy.

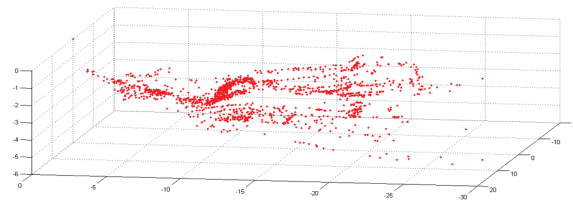
Merging the point clouds measured from two observing points allowed us to avoid no-data areas and increase the accuracy of the DEM. Reference points were set to calibrate the relative coordination between the two scans. As the number of the reference points needed for this method remains unknown, therefore, as many as 12 reference points were set. To test the optimal number of reference points needed, other independent test points (N=30) in the study area were measured twice from two observation positions for their positions. The two results were aligned using an increasing number of reference points (from 1 to 12), and the horizontal errors between the same test points in the two scans were computed.

## **4.3 Results**

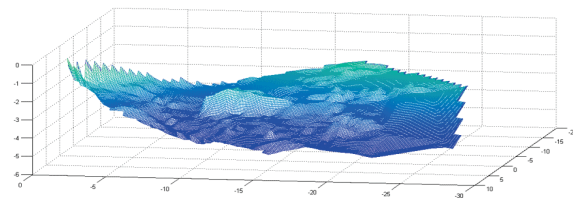
### **4.3.1 DEM Generated with One Scan**

DEMs, with a 0.1 m sampling resolution, were created from the point cloud collected from the first scan. Three interpolation methods were compared: linear, nearest-neighbours, and kriging interpolation, in terms of the appearance, as well as the mean square error at the independent check points.

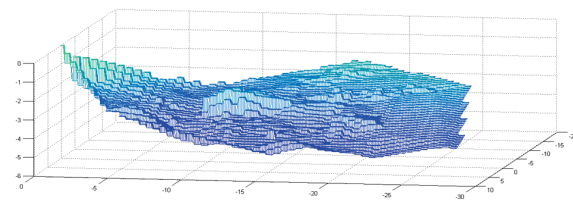
Figure 4-3 visualizes the DEM grids generated with the three interpolation methods. The linear interpolation was computationally economic, and the DEM generated corresponds to reality in most topographic features, except for the rigid land surface presented. The nearest-neighbour interpolation generated a DEM with some distortion, where the jagged surface caused by over-fitting did not correspond with reality. The kriging interpolation resulted in the topographic characteristics of the study area being presented with a smooth and more realistic surface.



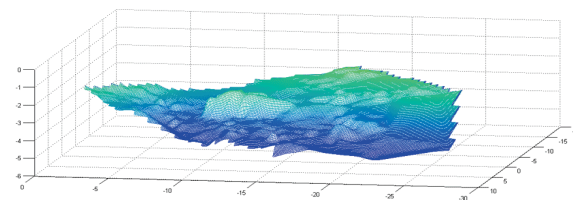
point cloud



linear interpolation



nearest neighbor interpolation



kriging interpolation

Figure 4-3 DEMs generated with the linear, nearest neighbour, and kriging interpolation methods

Table 4-2 shows the details of the accuracy of the DEMs generated from 2000 points from the first scan. The root mean square error between the observed elevation and the interpolated DEM was determined using the independent check points (N=30). The results confirmed that the kriging interpolation resulted in a DEM with the highest vertical accuracy.

Table 4-2 The root mean square error between the observed elevation at independent check points and the DEMs generated with the different interpolation methods

Interpolation method	linear	nearest neighbour	kriging
root mean square error (m)	0.30	0.36	0.28

The elevation errors between the interpolated DEMs and the measured check points (N=30) were plotted in Figure 4-4, against the distance between the points to the observation point. The vertical errors increased with the increasing distance. At 10 m distance from the observation point, the elevation error was about 0.10 m; at 26 m, for example, the error increased to 0.59 m.

A one sample t-test was performed between the averaged errors (+0.15 m) and the expected value of 0. A significant difference was observed (N=30,  $p=0.0042$ ), which was an evidence of a positive bias in the errors.

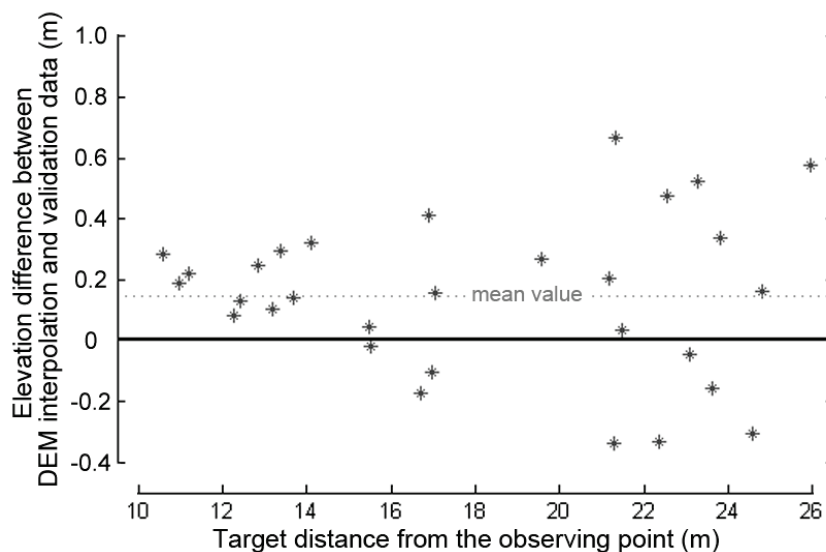


Figure 4-4 Relationship between the target distance and the elevation errors

### 4.3.2 DEM Generated with Two Scans

Figure 4-5 presents the DEM grid generated by the merged point clouds from two scans using the kriging interpolation method. Compared to the DEMs from one scan, more detail can be discerned visually, and the root mean square error decreased slightly from the previous 0.28 m to 0.20 m (Figure 4-6); however, no significant difference was found (N=30,  $P=0.1280$ ) (Figure 4-7).

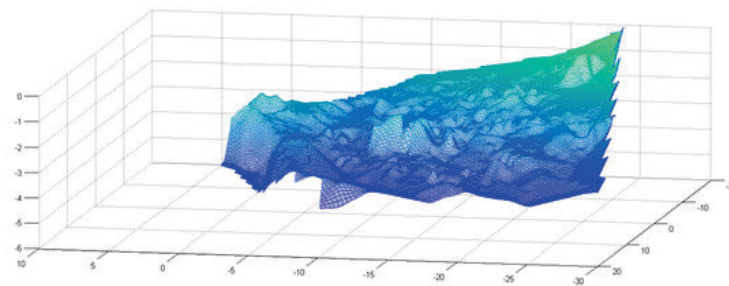
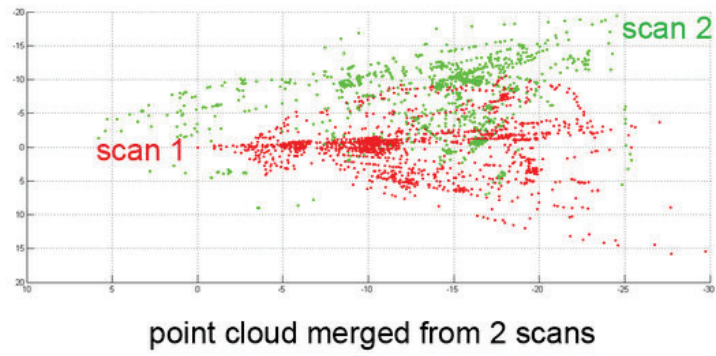


Figure 4-5 DEM generated by the merged point clouds from two scans, using the kriging interpolation method

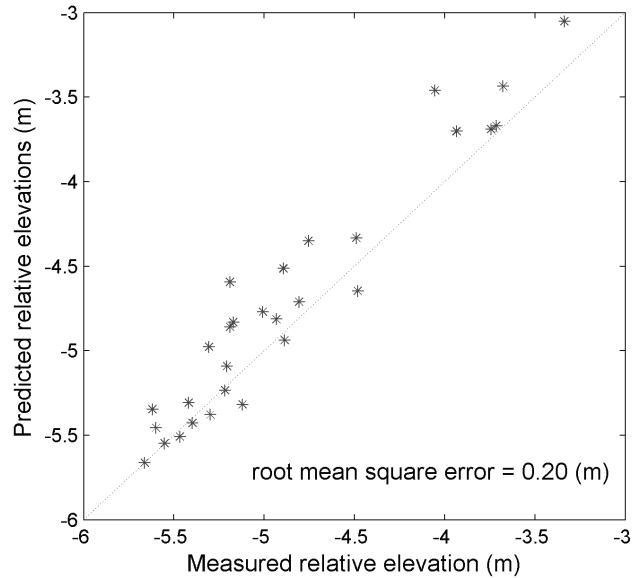


Figure 4-6 Level-measured elevation at independent check points vs. DEM interpolations at these points.

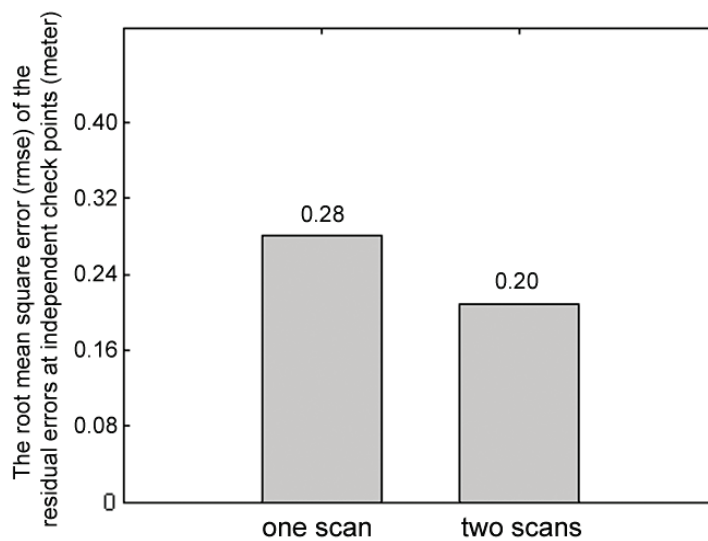


Figure 4-7 Using two scans, the error of the DEM decreases from 0.28 m to 0.20 m, but with no significant difference

To test the optimal number of reference points needed, independent test points (N=30) in the study area were measured twice from two observation points for their positions. The two results were aligned based on an increasing number of

reference points (from 1 to 12), and the average horizontal errors between the two results were computed and illustrated in Figure 4-8.

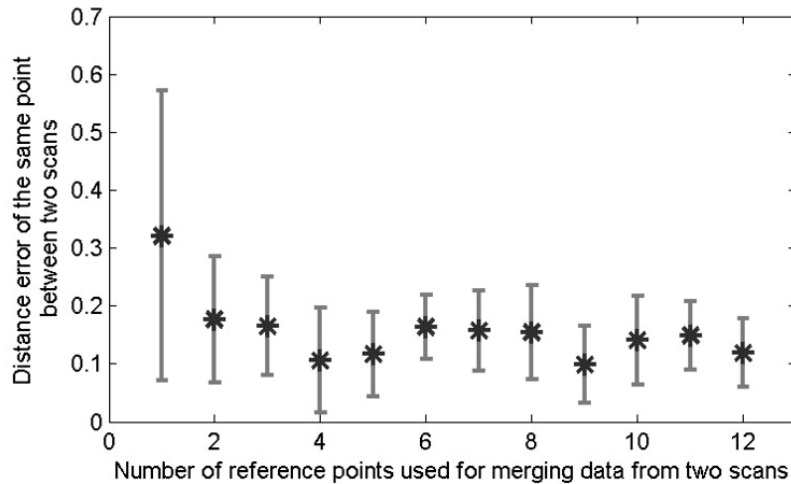


Figure 4-8 Horizontal error between two scans, with different numbers of reference points

It showed that 4 reference points could reduce the horizontal error from 0.31 m to about 0.10 m, while more than 4 reference points did not result in any further significant reduction in the horizontal error.

#### 4.4 Discussion and Conclusions

In this study, an economic yet fast method was proposed as an alternative way to generate a digital elevation model for a small area (less than 1000 m<sup>2</sup>). It can be implemented quickly and easily in the field and several features make this method unique:

Firstly, it is inexpensive. The whole system consists of a handheld infrared rangefinder, a tripod, a laptop with Bluetooth module (or a smartphone in the near future) and several distinguishable marks (painted iron nails in this case) as reference points. Secondly, it works relatively fast, compared with levelling. Within one hour, the 3D locations of more than 1000 points can be collected, while by levelling, it took us more than one hour to measure only 30 points. Thirdly, users have some degree of control over the accuracy of the DEM. When a land feature is important to the user, densely distributed points can be collected to capture those detailed topographic features such as rock edges or

creek beds; when the topography is smooth, the user may collect points with less density to save time. The points collected can be shown on the computer screen on the fly, allowing the user to monitor the process and decide whether enough points have been collected. Last but not the least, the method is flexible. It needs only one person, and about 10 minutes to install the instruments before collecting data. Moreover, additional scans can be initiated at any position and angle to collect supplementary data of the study area. The wireless connection between the laptop and the rangefinder allows the user to move the rangefinder between observation points without carrying the computer.

The vertical accuracy of the final DEM in our test is around 0.2 m, depending on the interpolation method, the number of scans performed and the distance of the target points from the rangefinder. It turned out that the accuracy of the elevation decreases with increasing distance between the sensor and the measuring point (Figure 4-4). The possible reasons for this might be twofold: 1. compared with near targets, the spatial locations of distant objects require more accurate measurement of the incline angle of the rangefinder, while the accuracy of the inclination measurement is limited by the built-in tilt sensor. 2. As the laser rangefinder measures the distance based on timing the delay of a reflected laser pulse, the optimal accuracy only occurs when the returning signal is strong. The further away the measured target, the more likely the flat surface of the target will be shot at a sharper angle, which results in a weaker returning signal, resulting to a lower accuracy. These two possible errors can be reduced by increasing the height of the observation position, either by raising the tripod or by choosing advantageous terrain points. Additionally, if multiple scans are performed for the same area, more weight can be applied to the points closer to the rangefinder when interpolating the land surface from the point cloud, as they have smaller confidence intervals.

As reported in the results, there was a significant positive elevation bias between the generated DEM and the land surface. The possibility that the device had a systematic error was excluded by an indoor calibration of the device. The distances recorded were not necessarily representatives of the ground surface, but whatever was first encountered by the laser beam in the field. Therefore, the elevations of the first-reflected surface, for example standing grass, were measured as the elevation of the land surface. As a result,

some of the points collected in the field were representing the top of the grass instead of the earth surface; hence, the elevation in the DEM became significantly overestimated. To overcome this problem in future studies, it is possible to apply filtering algorithms developed to remove off-ground points from the point cloud (Zhang et al., 2003; Kobler et al., 2007).

This study illustrates a method by which the DEM of a small area (less than 1000 m<sup>2</sup>) can be efficiently derived using a lightweight, low-cost infrared laser rangefinder which communicates with a portable computer. The vertical error of the elevation model generated is about 0.2 m and has the potential to be further reduced by post-processing with a data filtering technique. The DEMs generated by this method could be useful for many fine-scale biological/ecological field work applications.

# CHAPTER 5

## MODEL THE LAND SURFACE TEMPERATURE OF LIZARD MICROHABITAT USING MICROCLIMATE DATA

---

This chapter is based on: Fei, T., Skidmore, A.K., Wang, T.J., Toxopeus, A.G., Venus, V., 2012, Accurate land surface temperature modelling using microclimate data. *Journal of Environmental Earth Science* (in review).

## **Abstract**

Land surface temperature (LST) is one of the core variables in the physics of land surface processes, which influences energy balance and water cycles of the ecosystem. However, a lack of land surface temperature observations at a fine resolution has been a persistent problem in various studies associated with environmental science. This study presented a method to predict local land surface temperature dynamics using an artificial neural network (ANN) in combination with meteorological data and topographical information. Seven predictive terms were selected by the ANN model: air temperature, solar radiation, relative humidity, soil moisture, gust speed, time of a day and cosine of solar angle. The model was validated by independent test data collected on-site during an 8 days experiment, and the standard error of the prediction was less than 1.5 K for the surface temperature of bare soil.

## 5.1 Introduction

Land surface temperature (LST) is one of the core variables in the physics of land surface processes, which influences energy balance and water cycles of the ecosystem (Huang et al., 2008). However, a lack of land surface temperature observations has been a persistent problem in various studies associated with environmental science. To overcome the shortages of the sparse data observation, LST products have been derived from satellite data with thermal infrared sensors (Qin et al., 2001; Sobrino et al., 2004; Mao et al., 2005; Kerr et al.). For example, using Moderate Resolution Imaging Spectroradiometer (MODIS) thermal infrared (TIR) sensors, LST maps in more than 20 clear-sky cases were derived with accuracies better than 1K in the range from 263 to 322 K (Wan et al., 2004). With Envisat/Advanced Along-Track Scanning Radiometer (AATSR) thermal bands, the LST production yielded an average error of 0.9 K (Coll et al., 2005).

However, remote sensing has its shortcomings in LST retrieving. Firstly, remote sensing observation is instantaneous, so the continuous dynamics of land surface temperature cannot be captured from remotely sensed thermal images. Secondly, the surface temperature accuracy is constrained by the resolution of remote sensing data. Remote-sensing systems typically average information over a large area (Turner et al., 2003). When the surface temperature distributes heterogeneously, as in most cases, the surface temperature of a pixel retrieved from remote sensing data can be diverse largely from its true value. In addition, the accessibility of thermal infrared remote sensing data is strongly influenced by weather condition such as cloud, which limited the use of remote sensing data for LST retrieval under such weather conditions.

Instead of direct observation, land surface temperature may be obtained by modelling. Physical models uses knowledge of underlying physical principles to provide a complete description of the process of energy exchange of the land-atmospheric interface (Bastiaanssen et al., 1998) (Su, 2002), however the data and skill required to solve the various terms in the model are prohibitive for operational applications (Sobrino et al., 2004). In addition, errors in the initial conditions of the model will accumulate gradually and the LST estimation will diverge from the true state as time passes (Sobrino et al., 2004).

Although the data on daily variation of LST is little, the microclimate data including air temperature, relative humidity, wind speed, and soil moisture can be easily obtained by a local meteorological station. Previous studies have found strong relationships exist between the LST and environmental factors such as air temperature (Kawashima et al., 2000), relative humidity (Lakshmi et al., 1998) and wind speed (Su, 2002), however, the potential of modelling the LST by using these meteorological data is less studied.

Artificial neural networks (ANN) have been shown to be powerful when modelling nonlinear behaviours (Keiner and Yan, 1998). In addition, this method has high error tolerance. From this background, some studies have explored the potential of neural networks for function fitting and for relationship building. For instance, ANN modelling methods has been applied by Yi (Yi et al., 2007) to the monitoring of rice nitrogen status using leaf level hyperspectral reflectance; Mutanga (Mutanga and Skidmore, 2004) mapped grass quality in an African savanna rangeland using ANN method based on airborne hyperspectral imagery.

This study aims to seek for the possibility to predict the continuous land surface temperature by using microclimate data, while the land surface temperature is not measured directly.

## **5.2 Methods**

### **5.2.1 Study Area**

The 100 by 100 meters study area was located at El Torcal de Antequera, Málaga, Spain (latitude +36°59'5", longitude -4°31'38"). The site is situated by the north foot of the limestone mountain of El Torcal. The region is characterized by Mediterranean semiarid landscape: dry and firm soil, sparse herbaceous plants and thinly scattered woody plants (mostly *Retama sphaerocarpa* and some scattered European fan palms *Chamaerops humilis*). The topography of the study site was complex, with bare soil and rocks, as a related research about lizard's microhabitat required (Figure 5-1)

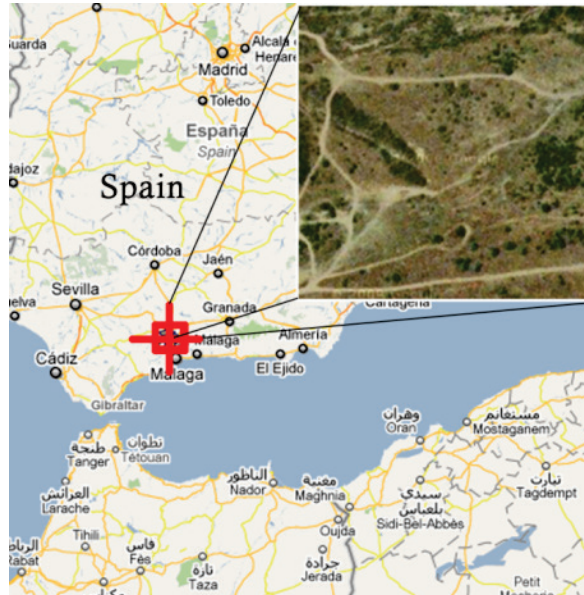


Figure 5-1 The location of the study area

### 5.2.2 Data Collection

Air temperature, total solar radiation on flat surface, relative humidity of air, soil moisture, wind speed and gust speed were measured from 17:00, September, 18<sup>th</sup>, 2009 to 10:30, September, 26<sup>th</sup>, at a time interval of 30 seconds. The sensors were connected to a data logger (15-channel Onset HOBO Weather Station), and the logger was mounted in a 1.5m high tripod which was located in a flat area with open sky. The data collected in the logger were representative of the study area. The sensors that collected these local meteorological data were listed in Table 5-1.

Table 5-1 Detail of data collection

<b>Microclimate variables</b>	<b>Sensor</b>	<b>Accuracy</b>
<b>Air Temperature</b>	HOBO 12-Bit Temperature Sensor	±0.2°C
<b>Total solar radiation on flat surface</b>	HOBO Silicon Pyranometer (Solar Radiation) Smart Sensor	±10.0 W/m <sup>2</sup> or ±5%, whichever is greater
<b>Relative humidity</b>	HOBO 12-Bit Temperature RH Smart Sensor	±2.5%
<b>Soil moisture</b>	HOBO Soil Moisture Smart Sensor	±0.041 m <sup>3</sup> /m <sup>3</sup> (±4%)
<b>Wind speed</b>	HOBO Wind Speed Smart Sensor	±1.1 m/s
<b>Gust speed</b>	HOBO Wind Speed Smart Sensor	±1.1 m/s
<b>Land surface temperature</b>	Hot-wire contact surface temperature sensors	±0.2°C at 0°C

Land surface temperatures, were recorded by contact surface temperature sensors at 10 different locations. The aspect and slope of the surfaces where we place the sensors were recorded. At least one land surface temperature sensor in each land type was placed on flat surface. The LST data were measured from 16:00, September, 18<sup>th</sup>, 2009 to 10:30, September, 26<sup>th</sup>, at a time interval of 30 seconds.

### **5.2.3 Input Data Selection**

#### *Meteorological data*

As meteorological variables are correlated (Chang and Root, 1975), firstly the autocorrelation between the weather condition data were tested. The normality of each parameter was also tested. Although the neural network used in this study can select the inputs with the strongest relation to the land surface temperature by adjusting weighting variables, and ignoring non-significant relations, this may result in the inclusion of input variables which have no causal relation to the variation of the land surface temperature. Therefore specific input variables were extracted to be the input to for a neural network. The selected input meteorological data were based on an examination, in which all possible combinations ( $2^6-1=63$ ) of meteorological data were tested one by

one as inputs to 9 different structured artificial neural networks. Nine back-propagation neural networks were trained to predict the LST from different combinations of meteorological data, with the number of neurons in the hidden layer ranges from 2 to 10.

The earlier stop technique was applied in this study to avoid over-fitting (Coleman et al., 1999). In this technique the available data is divided into three groups: the training dataset (40%), the validation dataset (40%) and the test dataset (20%). The training dataset is used for computing the gradient and updating the network weights and biases. The validation dataset is used to decide when to stop the training. When the network starts to over-fit the training data, the error on the validation set begins to rise as a result. In this study, if the validation error increased continuously for 6 iterations, the training was stopped and the weights and biases at the minimum of the validation error are applied for the neural network. Two measures were taken to speed up the training process of neural networks models. Firstly, the input data of chemical concentrations were normalized between 0 and 1:

$$Y_{input} = \frac{Y_i - Y_{min}}{Y_{max} - Y_{min}} \quad (\text{Eq. 5-1})$$

Where  $Y_{input}$ = normalized input meteorological data,  $Y_i$ = meteorological data,  $Y_{min}$ =Minimum of the measured meteorological data, and  $Y_{max}$ =Maximum of the measured meteorological data. Secondly, a training method named Levenberg-Marquardt training was applied, for the fast training speed (Moré, 1977). The performance of the neural network models with different input parameters was evaluated by the determination coefficient ( $R^2$  values) between the predicted and measured land surface temperature based on the test dataset, and the best (highest  $R^2$  value) combination of input data was selected as the prediction factors.

#### *Additional variable*

Additional data were tested for whether they can significantly improve the prediction accuracy. Time and solar angle information were considered as the candidate of additional inputs, for their close relationship to the land surface temperature. Two way T-test were performed to test if these additional input data can improve the result.

### *Time*

The information of time in a day can be important to the prediction of surface temperature because the overall pattern of daily temperature variation is highly regular along with the time: In cloud free days, the surface temperature starts to rise in the morning and reaches its max peak in the early afternoon before goes down. Giving this information may help the neural network fit this overall pattern.

The time data have been linearly normalized between 0 and 1. 0 represents 0:00:00, 0.99998 represents 23:59:59, and 0.5 represents 12:00:00.

### *Solar Angle*

The daily cycle of net radiation is the primary factor that determines the normal daily cycle of temperature. The intensity of solar radiation that received by the surface of land objects is proportionally affected by the solar angle, more accurately, the cosine of the angle of incidence between the solar rays and the normal to the land surface ( $\cos i$ ). For example, in the study area, September, 15th, 2009, the daily cosine value of the sun angle to target land surfaces are illustrated below, in Figure 5-2.

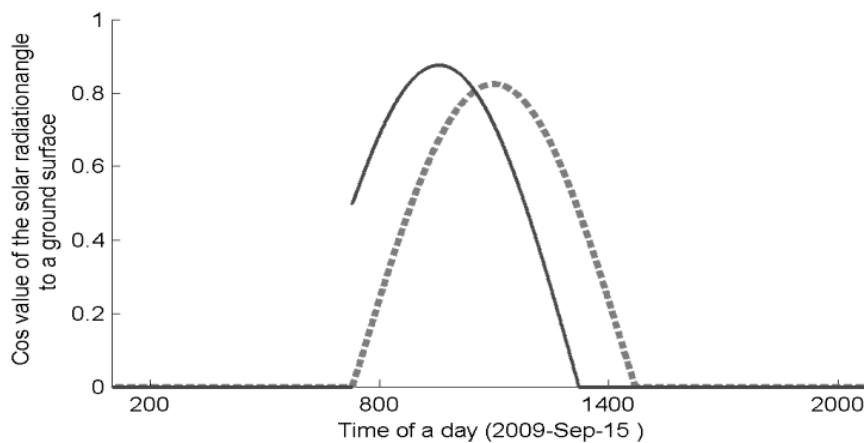


Figure 5-2 The daily cosine value of the sun angle to land surface with different orientations

The dotted line represents the daily sun angle to a flat surface, while the solid line represents the relative daily sun angle to a 30 degree east-facing surface. In this study,  $\cos(i)$  was calculated by:

$$\cos i = \sin\theta\cos\alpha\cos(\alpha - \alpha_s) + \cos\theta\sin\alpha \quad (\text{Eq. 5-2})$$

Where  $\theta$  is surface slope angle,  $a$  is the altitude angle of the sun,  $\alpha$  is the azimuth of the sun, and  $\alpha_s$  is the aspect of the surface (Hetrick et al., 1993).

The altitude angle of the sun ( $a$ ) and the solar azimuth  $\alpha_s$  can be calculated from:

$$\sin a = \sin L \sin \alpha + \cos L \cos \alpha \cos h \quad (\text{Eq. 5-3})$$

$$\sin \alpha_s = \cos \delta_s \sin h_s / \cos \alpha \quad (\text{Eq. 5-4})$$

Where  $L$  is the latitude of the site,  $h$  is the hour angle and  $\delta_s$  is solar declination. The hour angle describes how far east or west the Sun is from the local meridian. It is zero when the Sun is on the meridian and decreases at a rate of 15 degree per hour. The solar declination can be derived from (Kreith and Kreider, 1978):

$$\delta_s = 23.45 \left( 360 \frac{284+N}{365} \right) \quad (\text{Eq. 5-5})$$

where  $N$  is the day number, 1 January being day 1 and 31 December being day 365.

The cosine of the solar angle to the normal of target surface was tested as an additional input to exam if this information can increase the accuracy of the surface temperature prediction.

#### 5.2.4 Optimizing Neural Network

In this study, we have used a one-layer, feed-forward, error-back-propagation artificial neural network implemented in the Matlab 7.1, to predict the surface temperature for bare soil, using all possible combinations of meteorological data and useful additional data.

To make sure the ANN structure is sophisticated enough to learn the pattern between input data and land surface temperature, yet not too complex to over-fit the noise exists in the training data, 9 ANN structures, with the number of neurons in the hidden layer from 2 to 10, were tested. The architectural that provided best (highest  $R^2$  value) prediction result was selected as the optimal architectural for the ANN.

### **5.2.5 Model Validation**

The test dataset was prepared for the input of the model validation and has never been used in the modelling phase. The output from the ANN model corresponding to these input were then compared with real land surface temperature measurements. The root mean square error (RMSE) between the prediction and the observation was calculated as an index of the prediction accuracy. The root mean square error was calculated by:

$$\text{RMSE} = \sqrt{\frac{\sum_{i=1}^n (T_p - T_o)^2}{n}} \quad (\text{Eq. 5-6})$$

Where  $T_p$  is the surface temperature predicted by the model, and the  $T_o$  is the observed real surface temperature.

## **5.3 Results**

### **5.3.1 Input Data Selection**

#### *Microclimate variables*

The autocorrelation between microclimate data recorded by the on-site meteorological station were plotted in (Figure 5-3). Strong correlations exist between: (1) air temperature and air relative humidity; (2) wind speed and gust speed.

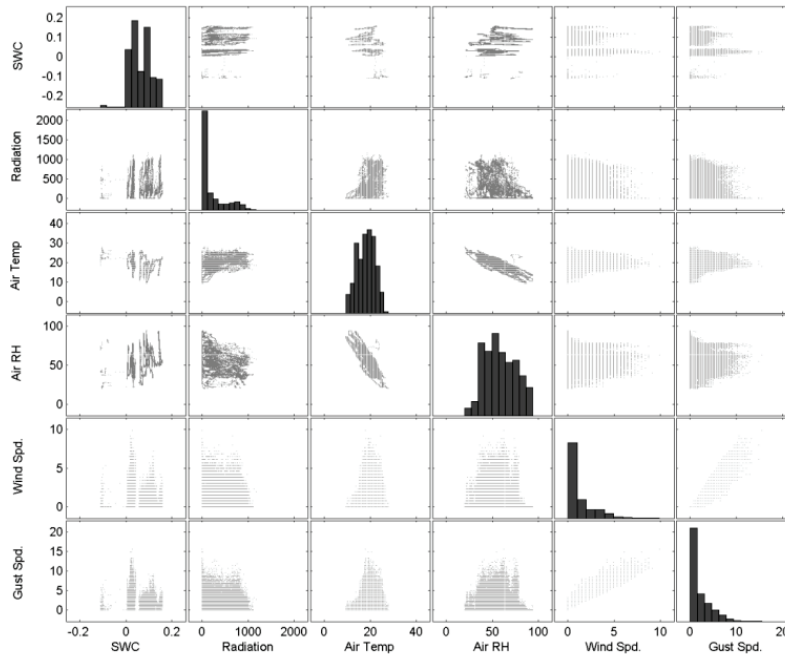


Figure 5-3 The correlation between meteorological data (SWC: Soil water content, Radiation: Solar radiation, Air Temp: Air temperature, Air RH: Air relative humidity, Wind Spd.: Wind speed, Gust Spd.: Gust speed)

The performance of the neural networks with different input parameter combinations evaluated by the determination coefficient ( $R^2$  values) between the predicted and measured land surface temperature was illustrated in Figure 5-4. The best combination with highest  $R^2$  value of input data was: air temperature, solar radiation, air relative humidity, soil moisture and gust speed for land surface temperature retrieving.

The pattern of the predictive power of the artificial neural network with different input combination was illustrated in Figure 5-5. The highest accuracy of temperature prediction was achieved by the neural network with 8 neurons in the hidden layer.

For soil surface temperature prediction, we noticed that air temperature in the input parameter can significantly enhance the predictive power. However, the air temperature alone does not predict the surface temperature accurately. In fact, any microclimate factor alone we collected does not predict the surface

temperature with high accuracy by its own, as we underlined in the Figure 5-5. This finding stands for both the surface temperature of soil and rocks.

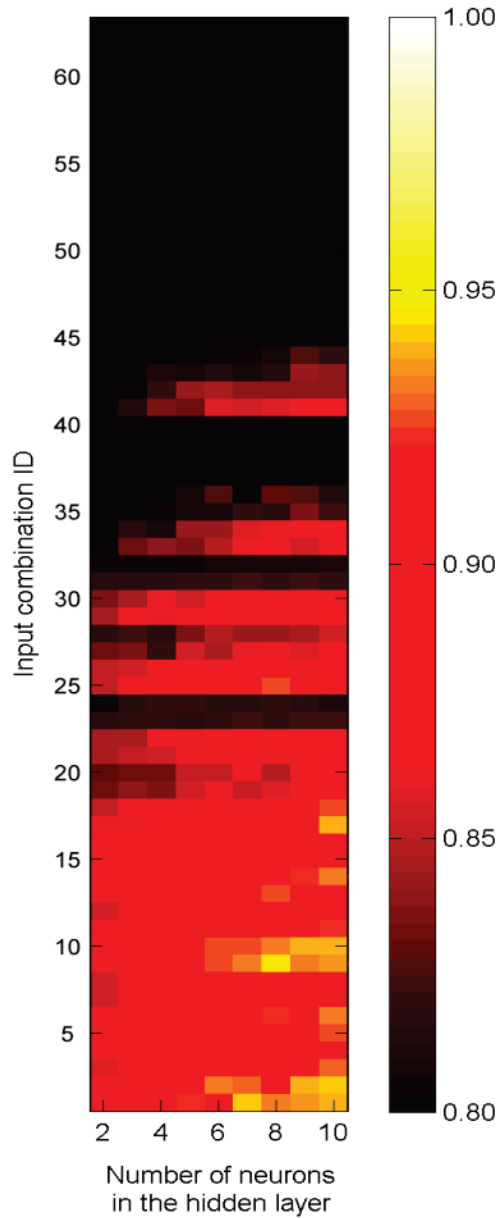


Figure 5-4 The performance of the neural networks with different input parameter combinations evaluated by the determination coefficient (R2 values) between the predicted and measured land surface temperatures

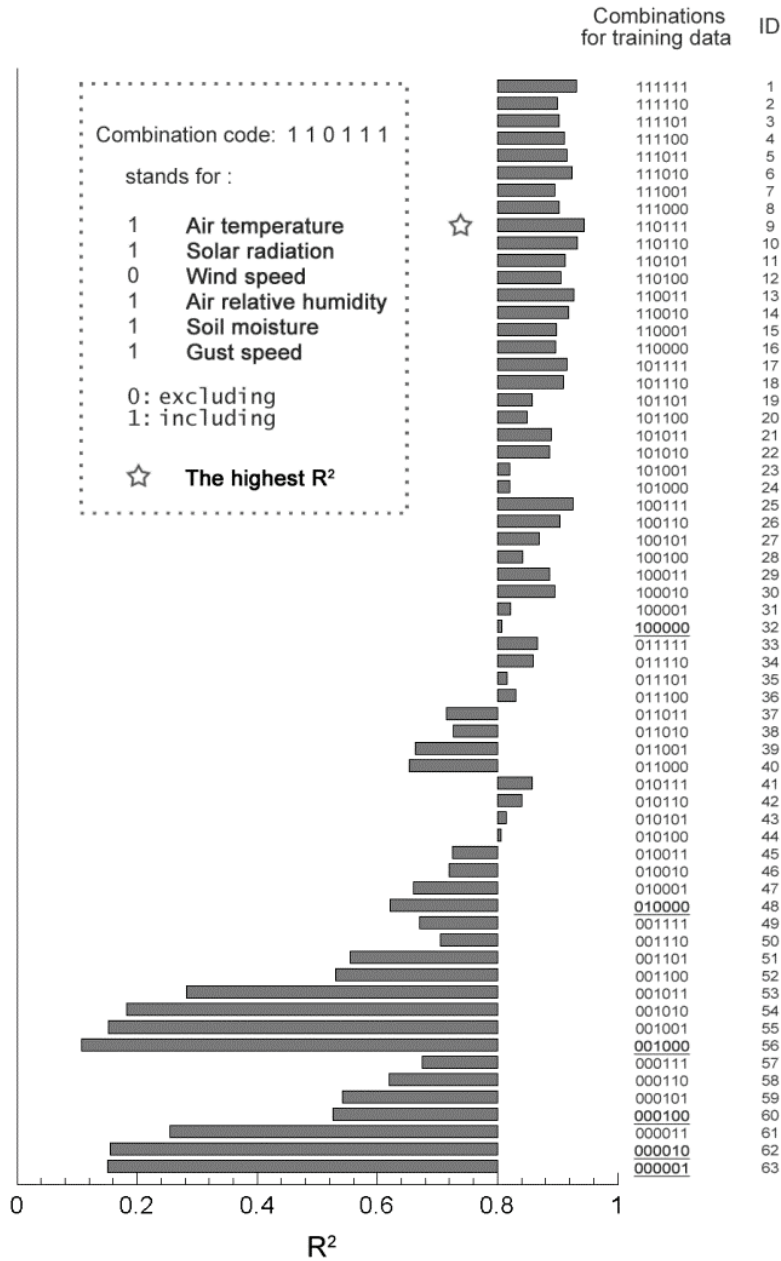


Figure 5-5 The impact of the input combinations on the predictive power for land surface temperature. The combination codes include 6 numbers described microclimate data used as input of the ANN model. The code '1' represents presence of a data type and '0' stands for absence of it. The combination that leads to the highest R<sup>2</sup> is marked with a star.

### Additional input variables

Figure 5-6 showed that each additional input data increased the prediction accuracy of ANN significantly. With both the time of a day and the cosine of solar angle as inputs, the smallest root mean square error between observatory surface temperature and the model prediction was achieved. Two way t-test for the RMSE showed compared with the second best input combination, the best one improved the prediction accuracy significantly ( $p=0.02$ ,  $N=30$ ), and the lowest RMSE was 1.25 degree Celsius.

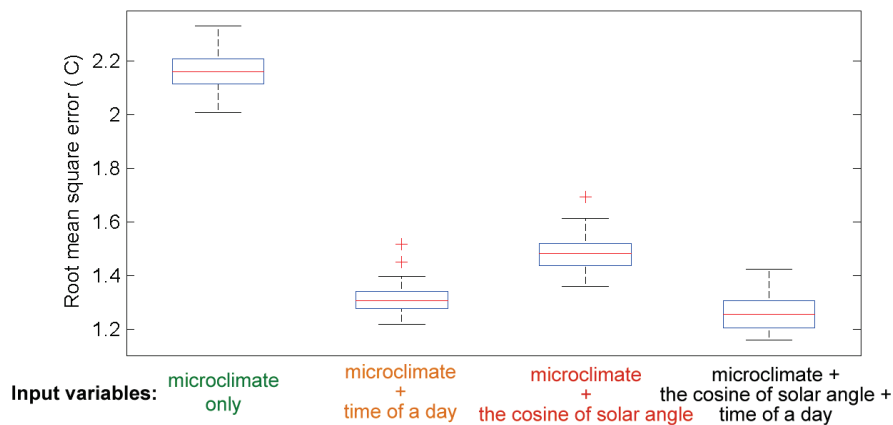


Figure 5-6 The improvement of surface temperature prediction brought by importing additional input data

### 5.3.2 Optimizing Neural Network Setting

An artificial neural network with 8 nodes in one hidden layer, 7 inputs and 1 output, and with the parameters of a momentum of 0.8, a learning rate of 0.7 and 1000 epochs, was the final selection to predict the land surface temperature.

### 5.3.3 Prediction Accuracy

Figure 5-7 plotted the temperature prediction against observation for both flat and sloped land surface. The  $R^2=0.97$  and the root mean square error was 1.25 degree Celsius.

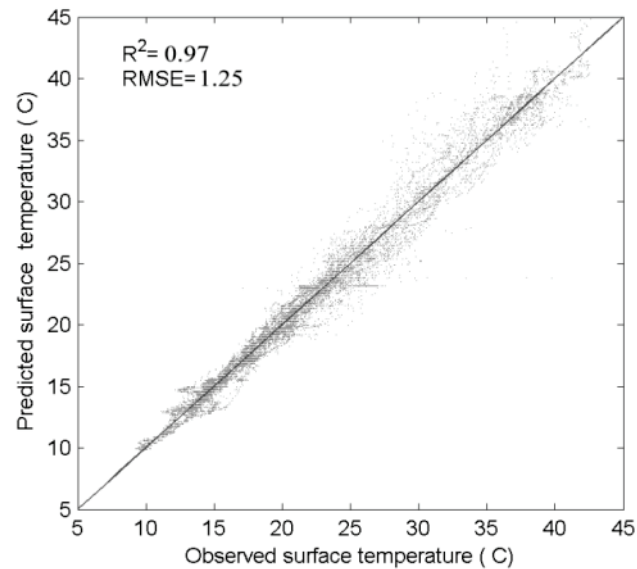


Figure 5-7 The prediction of the land surface temperature vs. the observation

Figure 5-8 exemplified the model performance on a tilt land surface (east faced, 30 degree). The grey line represented the observed LST, while the blue dot stands for the prediction.

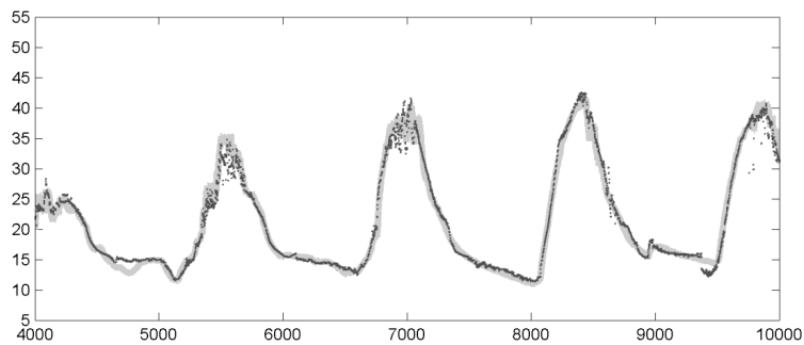


Figure 5-8 The predicted vs. observed daily land surface temperature on a sloped (East,30-degree) land surface

## 5.4 Discussion and Conclusion

On flat terrain and under clear-sky conditions, the downwelling shortwave radiation is nearly the same from point to point over relatively large areas and so one measurement can be taken to be representative of the entire area. However, on complex topography, the surface temperature distribution among

different slope is heterogeneous. By using microclimate data alone, the accuracy to predict the surface temperature is 2.18K in terms of RMSE. Adding time and solar angle information to the ANN inputs has largely improved the accuracy of prediction (RMSE=1.25K).

Figure 5-9 illustrated the observed and predicted surface temperature for flat soil surface vs. the surface temperature for an east faced (30 degree) slope in two days. From the figure, the pattern of daily surface temperature variation is clear: in the morning shortly after the sun rise, the east faced surface received more intensive radiation and the surface temperature rises quicker than that of the flat surface, and reaches its peak value at about 11:00. However, the higher surface temperature occurred on flat surface in the afternoon (14:00) because the sun gets lower in the sky and the earth surface gets warmer. Therefore the net radiation (the difference between the radiant energy absorbed and the radiant energy emitted) will decrease to zero. At this point the surface temperature stops to increase and the maximum temperature occurs. The pattern can be easily recognized also in the model prediction.

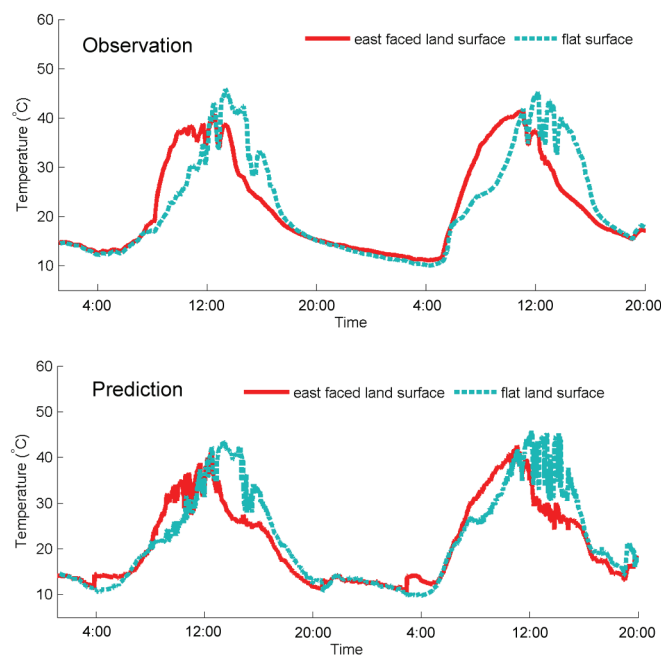


Figure 5-9 The observed and predicted land surface temperature dynamics for flat soil surface (dotted line) and east faced (30 degree) surface.

The inputs of ANN were 7 factors: air temperature, solar radiation, relative humidity, soil moisture, gust speed, time of a day and the cosine of solar angle. Figure 5-5 illustrated that except for 'air temperature', any of other meteorological factors alone does not predict the surface temperature with the determination coefficient  $R^2$  larger than 0.8. That may due to the fact that the air temperature is the direct consequence of the land surface temperature (the land surface heats the air near surface), while other factors such as radiation, wind gust, relative humidity and soil moisture are merely one of many causes of the land surface temperature.

Solar radiation is the ultimate heat source for land surface temperature. By using solar radiation alone, one can explain more than half (63%) of the variation occurred in land surface temperature. However, the diffuse radiation, vary only slightly from slope to slope within a small area (Kumar et al., 1997), so this study assumed it to be a constant to all land surface. The reason that soil moisture was determined as an important factor for LST may be the fact that on the one hand, soil moisture has an impact on the evaporative cooling process of land surface (Price et al., 1999); on the other hand, the moisture soil will change its specific heat capacity, which in turn affects the land surface temperature.

The reasons that gust speed is a better predictive factor than the wind speed need further investigation. As wind speed and gust speed are highly correlated (Figure 5-3), the predictive power of the two were expected to be similar. A possible explanation is the surface energy took by convection (wind) is not proportional to the wind speed.

This study presented a method to predict the land surface temperature dynamics with meteorological data and topographical information with artificial neural network, and the accuracy of the prediction is less than 1.5 degree Celsius. In future studies, the method presented in this paper can be integrated with a solar radiation model which computes potential solar radiation (the amount of shortwave radiation received under clear-sky conditions) over a large area using only digital elevation model (DEM). In this way, with the DEM of a study area and the meteorological data, we can map the daily land surface temperature dynamics over the area. On the other hand, as the land surface temperature is also related with the thermal properties of surface materials such as specific heat

capacity, in future studies, different surface materials or land type will be modelled using the methodology applied in this study.

# CHAPTER 6

## PREDICTING THE SPATIAL USE OF LOCAL HABITAT OF A LIZARD USING THERMAL ROUGHNESS INDEX

---

This chapter is based on: Fei, T., Skidmore, A.K., Wang, T.J., Toxopeus, A. G., Venus, V., Bian M.. 2012, Predicting the Spatial Use of Local Habitat of a Lizard using Thermal Roughness Index. *Landscape Ecology* (in review).

## **Abstract**

A new index of ‘thermal roughness’ is proposed to represent the thermal heterogeneity (variance) as well as the thermal contrast of the local habitat of ectotherms. As ectotherms often shuttle between places with very different thermal properties to maintain their body temperature, the places often occupied and used to perform thermoregulation can be highlighted by the thermal roughness index. The hypothesis that the local habitat occupancy of a lizard can be predicted using thermal roughness index was tested, by comparing the calculated thermal roughness index with a lizard occupancy map simulated using an existing model, and with field observations. The results show that the thermal roughness index offers a fast and accurate method to predict ectotherm habitat occupancy, however for lizards at different size, calculating the index with different resolution is suggested.

## 6.1 Introduction

The study of how and why organisms select particular habitats has long been central to ecology. One special interest in ecology was the concept of limiting factors: which physical factors limit the occurrence of organisms to particular habitat (Huey, 1991a). A habitat with a suitable thermal environment is of importance for ectotherms, as thermal conditions play an important role in various aspects of the physiology, biology and ecology of ectothermic species. Previous studies have shown that thermal conditions can influence the growth and development as well as the survival of embryos (Angilletta et al., 2009), metabolic processes such as digestion (Harwood, 1979), behavioural processes such as activity (Waldschmidt and Tracy, 1983; Nicholson et al., 2005; Sears, 2005; Rouag et al., 2006), microhabitat selection (Angilletta et al., 2009; Schofield et al., 2009) and distribution and life history traits of populations (Porter and Tracy, 1983; Kearney and Porter, 2004; Medina et al., 2009). Some studies suggested that when temperature is not a primary consideration in habitat selection of ectotherms, its effects are often mediated through other behavioural responses (Bevelhimer, 1996).

The quantification of species–environment relationships is one core task in predictive modelling in ecology, and to model the habitat of organisms has long been central to geographical ecology (Guisan and Zimmermann, 2000). In practical, the application of habitat models is a highly influential tool used by natural resource managers and decision makers to manage wildlife (Brooks, 1997). One special interest in the ecology was the concept of environmental factors: physical factors limiting the occurrence of organisms to particular habitat (Huey, 1991a). The use of statistical models to predict the likely occurrence or distribution of species based on relevant variables of environmental factors is an important tool in conservation ecology and wildlife management. In the past, a lot of empirical models have been developed to predict the animal occurrence or distribution (Table 6-1).

Table 6-1 Example of existing empirical animal distribution models

Model	Reference	Algorithms*
BIOCLIM	(Busby, 1991)	CE
BAYES	(Aspinall, 1992)	BA
BIOMAPPER	(Hirzel et al., 2002)	ENFA
BIOMOD	(Thuiller, 2003)	GLM, GAM, ANN
CART	(Skidmore et al., 1996)	CART
Disperse	(Carey, 1996)	CE
DIVA	(Hijmans et al., 2001)	CE
DOMAIN	(Carpenter et al., 1993)	CE
GARP	(Stockwell, 1999)	GA (with CE, GLM,
GDM	(Ferrier et al., 2002a; Ferrier et al., 2002b)	GDM
GRASP	(Lehmann et al., 2002)	GLM, GAM
MAXENT	(Phillips et al., 2006; Phillips and Dudík,	ME
SPECIES	(Pearson et al., 2002)	ANN
Shift	(Iverson et al., 1999)	CART

\* ANN, artificial neural networks; BA, Bayesian algorithms; CE, climate envelope algorithm; CART, classification and regression tree; ENFA, ecological niche factor analysis; GA, genetic algorithm; the GAM, generalized additive model; GDM generalized dissimilarity model; GLM, generalized linear model; ME, maximum entropy model.

Statistical models describe the relations between the environment and the distribution of organisms (Heikkinen *et al.*, 2006). Although prevailing, the statistical models are not suitable tools to model the effect of thermal habitat on ectotherms for the two reasons below. Firstly, compared with other environmental factors, the thermal environment is highly dynamic at different temporal scales, which makes it difficult to describe as a static environmental factor (Fei et al., 2012b). Secondly, for ectotherms, they use behavioural thermoregulation as a way to control body temperature, which means they take advantage of places with very different thermal properties to maintain their body temperature. While the static model takes environmental factors within a range within which the animals survive, most of them simply assume that one ‘most suitable value’ (average) exists for every environmental factor for each species.

An alternative to static modelling is the dynamic approach. A number of studies have been conducted in terms of species response to dynamic environmental change, including the simulating of vegetation distribution dynamics (Moore and Noble, 1993), the movement of ants on a trail (Kunwar et al., 2004), the flying path of birds during a breeding season (Betts et al., 2008) and the

movement and thermal habitat use of lizards under laboratory conditions (Fei et al., 2012b). However, the main problem of dynamic models is the computational load of running an individual based dynamic model, so that any attempt that tries to transplant the model to cover a larger spatial area is a challenge. Take the lizard movement model (Fei et al., 2012b) for example: In order to simulate the movement of a lizard in 10 days, it took nearly 24 hours for a main-stream PC to complete the calculation. The second problem is posed by the fact that dynamic models normally require more fixed parameters as prior knowledge which are often unavailable.

Instead of simulating the movement of target animal in response to the thermal habitat using a dynamic model, here we propose a new index, namely ‘thermal roughness’ to represent the thermal heterogeneity (variance) as well as the thermal contrast of an ectotherms’ habitat. To explain the term ‘thermal roughness’, the term ‘operative temperature’ needs to be introduced. Operative temperature ( $T_e$ ) is defined as the temperature of an inanimate object of zero heat capacity with the same size, shape and radiative properties as an animal exposed to the same microclimate (Bakken and Gates, 1975). Operative temperature provides a meaningful measure of thermal environment compared with simple measures of air or ground temperatures, because it integrates the array of radiative, convective and conductive heat exchange (Christian et al., 2006).

The thermal roughness can be understood as the fluctuations of a greyscale image where the grey levels correspond to the operative temperatures. A darker pixel corresponds to a lower  $T_e$ , and a brighter pixel corresponds to a higher  $T_e$ . If an area has a smooth ‘relief’, this area has a less variation in its thermal condition; in contrast, if an area has a complex and has an uneven ‘relief’, the area can be seen as thermally rough. The degree of roughness of a surface can be calculated by Laplacian of Gaussian (LoG) filter at multiple scales.

In this study, we hypothesized that the thermal roughness index can be used as a surrogate measure to explain and predict the spatial pattern of local habitat usage of lizards. To do so, the thermal roughness map extracted from the thermal landscape was tested against the habitat occupancy map generated from a dynamic lizard movement model. The similarity between the two was

measured using the moment invariants technique. Finally, field data was used to validate if the thermal roughness index represent the use of thermal landscape by lizards.

## **6.2 Materials and Methods**

### **6.2.1 Thermal Landscape Simulation**

The landscape is a complex, multi-scalar product of environmental variables. It is the totality of natural features (soils, vegetations, landforms etc.) and may include specific environments and ecotones (Farina, 2006). Among these natural features, thermal energy, which is our concern, is always present and can be measured. Thermal variables including air temperature, radiation intensity, surface temperature and the convective thermal flow at one spatial location determines largely the body temperature of an organism at that point. In combination, the thermal variables at each point across the landscape form the so called ‘thermal landscape’.

A grid based dynamic thermal landscape was applied to simulate diurnal thermal environmental changes for ectotherms and has four elements: air temperature, radiation, surface temperature and convection. In natural condition, the ultimate energy source is solar radiation, with the radiative energy heating up land surface as well as the air near the land surface. Due to the complexity of the topography, the energy distribution over the landscape can be complex and heterogeneous at multiple scales. With the purpose of simulating the heterogeneity at multiple scales, we simulated a thermal pattern, from a simple template containing 2x2 pixels of different thermal conditions values. For simplicity, they were set to: [-2 -1 1 2] (Figure 6-1):



Figure 6-1 A thermal template with four values

This template was then iterated 8 times. At each iteration, a template with a factor of 0.2 was added to each pixel, splitting each pixel to four new pixels. It resulted in a fractal thermal pattern of 256 x 256 pixels as the pattern repeats itself in every scale. All the values in the template were then linearly

normalized to 0 to 1. Based on this thermal pattern, solar radiation, air temperature and land surface temperature were simulated.

Solar radiation of the thermal landscape was set to vary on a daily basis. The thermal pattern was multiplied with a cosine function and a factor coefficient. The coefficient was adjusted to limit the radiation intensity starting from a minimum value of 0 (completely dark) to a maximum value of  $1000 \text{ Wm}^{-2}$  (it is the maximum solar radiation recorded at noon time of June, 2010, during a fieldwork in Spain).

Air temperature and land surface temperature were also simulated following the normalized thermal pattern, with a changing factor of cosine function. The air temperature was adjusted to between 10 to 30 degree Celsius and the land surface temperature was controlled between 10 to 60 degree Celsius following the cosine pattern, but with a 2-hours lag in the solar radiation. In other words, the simulated solar radiation reaches the maximum at 12:00, while the air temperature and land surface temperature peaks at 14:00.

Convection results in the transfer of heat between the environment and the organisms. When the animal size (surface area), body temperature, and environmental temperature are given, the only environmental factor that influences the energy convection is the wind speed in Porter's bio-physical model (Porter and Gates, 1969). The wind speed in the simulation was assumed to be less than 0.5m per second, and resulted in a convective heat transfer coefficient  $h_L=10.45 \text{ Wm}^2\text{K}^{-1}$  (Porter et al., 1973).

Under the natural conditions, thermal energy is usually distributed unequally across the landscape of animal's habitat. Since operative temperature can be calculated as a representative of thermal environment by heat transfer models, in this study, a bio-physical body temperature model for lizard (Fei et al., 2012a) was applied to generate an averaged operative temperature map of the simulated area.

### 6.2.2 Calculation of Thermal Roughness Index

In this study, Laplacian of Gaussian (LoG) filter was used to extract the thermal roughness from the image of thermal landscape (i.e., the distribution of operative temperatures). Laplacian filters are derivative filters used to find areas of rapid change in images and usually be used for edge detections in the field of image processing (Chen et al., 1987). Since derivative filters are very sensitive to noise, it is common to suppress the noise (e.g., using a Gaussian filter) before

applying the Laplacian. This two-step process is called the Laplacian of Gaussian operation. By combining the Laplacian and Gaussian functions we obtain a single equation:

$$\text{LoG}(x, y) = -\frac{1}{\pi\sigma^4} \left[ 1 - \frac{x^2+y^2}{2\sigma^2} \right] e^{-\frac{x^2+y^2}{2\sigma^2}} \quad (\text{Eq. 6-1})$$

in which  $\sigma$  is the width of Gaussian kernel to smooth the image. The Laplacian of Gaussian operator takes the second derivative of the image. Where the image is uniform, the Laplacian of Gaussian is zero. Wherever a change occurs, the Laplacian of Gaussian will give a positive response on the darker side and a negative response on the lighter side. The magnitude of the values represents the intensity of changes in the thermal image. 2D Laplacian of Gaussian can be approximated by an n-by-n convolution kernel which can be obtained by approximating the continuous expression of Laplacian of Gaussian given above. Since the appropriate scale(s) at which the thermal roughness should be calculated is not known yet, we have calculated the thermal roughness at five different scales, by varying the size of Laplacian of Gaussian convolution kernel, in which  $n = 3, 5, 7, 9$  and  $11$  pixels were tested. After the operative temperature was filtered by Laplacian of Gaussian filter, the output was normalized to  $-1$  to  $1$ . To generate the thermal roughness map, the values above a threshold of 2 times standard deviations was retained. As the extreme negative and positive values (i.e.  $-1$  and  $1$ ) in the filtered image represent a sharp change of thermal conditions within very short distance, all negative values were converted to positive by taking only the absolute values. These values range from  $0$  to  $1$  and represent the thermal roughness index.

### 6.2.3 Habitat Occupancy Simulation of a Lizard

A physically based, behavioural thermoregulation driven reptile movement model (Fei et al., 2012b) was applied to map the habitat occupancy of lizards. The method is based on a spatially explicit dynamic model, which simulates the change of thermal landscape and the behavioural response of reptiles by a 10 seconds' interval for 10 days. This model simulates the sequential movements of a lizard, which finally leads to the map of its habitat utilization. All simulated thermal environmental factors such as radiation intensity, air temperature and land surface temperature were fed into the model. At the same time, the movements of three different sized lizard including a juvenile, a normal sized adult and a extremely large sized adult ocellated lizard (*Timon lepidus*) were

simulated. The related parameters of the lizards were adapted from (Chato, 1966; Barlett and Gates, 1967; Beckman et al., 1973; Porter et al., 1973) and adjusted according to (Fei et al., 2011a). See Table 6-2 for details.

Table 6-2 Estimated thermal related parameters of three *Timon Lepidus* used in this study

Parameters	Value *	Unit
SLV	50/150/450	(mm)
Body mass	2.5/73.8/1009.4	(g)
Skin absorbance	$9.36 \times 10^{-2}$	--
Specific heat capacity	3.76	(JK <sup>-1</sup> g <sup>-1</sup> )
Heat transfer coefficient. (conduction)	0.50	(Wm <sup>-1</sup> K <sup>-1</sup> )
convection coefficient	10.45	(Wm <sup>-2</sup> K <sup>-1</sup> )
Emissivity of lizard skin	0.95	--

\* if different, values for three sized lizards were separated by back slash '/'

To prevent the simulation from being trapped in a local optimization, random moves were introduced into the algorithm to reposition the lizard within the simulated area at a low probability of 1%. And each simulation was repeated 10 times and the results were averaged to form the probability of habitat occupancy. Note that the body mass parameters were inferred from the snout-vent-length based on an empirical formula (Meiri, 2010). By the reptile movement model, the probability of local habitat occupancy of the three different sized lizards in 10 days was computed and shown in an image of 256 x 256 grids.

#### 6.2.4 Comparing the Thermal Roughness Index with Simulated Habitat Occupancy

Moment invariants were introduced to the pattern recognition community by Hu (1962) who employed the results of the theory of algebraic invariants and derived his seven famous invariants to rotation, scaling and general affine transform of 2-D objects. The basic idea behind it is to describe the images by a set of features which are not sensitive to particular deformations and which provide enough discrimination power to distinguish among objects from different classes. This algorithm has been used in many applications including feature recognition (Dudani et al., 1977; Belkasim et al., 1991), satellite image registration (Goshtasby, 1985; Flusser et al., 2009), texture classification and image similarity calculation (Papakostas et al., 2010)

In this study, the classical seven invariants proposed by Hu (1962) were employed to calculate the similarity between images, in this case, between the thermal roughness map we extracted from thermal landscape and the habitat occupancy map generated by the dynamic reptile movement model. For each of the three different sized lizards, the corresponding habitat occupancy map was compared with all the five thermal roughness images extracted at different scales. The seven variables of invariants formed a seven dimensional space, in which seven unique features of one image can be mapped to a dot in that space. The similarity of two images can be measured by the Euclidean distance in the 7D space between the two dots mapped from their moment invariants. The shorter the distance between the two dots, the more similar the two images are. The Euclidean distance in multiple dimensional space can be denoted as:

$$d(x,y)=\sqrt{\sum_{i=1}^n(x_i - y_i)^2} \quad (\text{Eq. 6-2})$$

### **6.2.5 Test the Thermal Roughness using Field Observation**

#### *Field data collection*

A field campaign was carried out on a sunny day of July, 2010 at the El Torcal de Antequera, Málaga, Spain (latitude +36°59'5", longitude -4°31'38"). The region is characterized by a Mediterranean semiarid landscape: dry and firm soil, sparse herbaceous plants and thinly scattered woody plants (mostly *Retama sphaerocarpa* and some scattered European fan palms [*Chamaerops humilis*]). The topography of the study site was complex, with rocks and dried herbaceous plants.

*Timon lepidus* is a ground-dwelling lizard that is widely distributed in Spain, Portugal, southern France and north-western Italy. The skin colour of an adult has a camouflaged effect comprising mottled blue, green and brown patches interspersed with brighter spots (Figure 6-2). The microhabitat usage pattern can largely be explained by the behavioural thermoregulation (Fei et al., 2012b). In the wild, it feeds on insects, snails, newly hatched birds and fruits (Pleguezuelos et al., 2008).

A thermal infrared imager (NEC thermo tracer H2640 with a resolution of 320x240) were mounted on a platform of a lifter at about 10m above the ground surface, pointing down with a field-of-view (FOV) covering a rectangular area of 1.6 x 1.2m. When recording, the imager captured the land surface

temperature, the lizard's body temperature when it showed up, as well as the lizard's position within the field-of-view.



Figure 6-2 locations, instruments used and the target species of the field data collection

Other thermal environment factors including air temperature, solar radiation intensity and wind speed were collected using a Hobo™ micro weather station connected with temperature sensors, a silicon pyranometer smart sensor and a wind speed sensor. All data were recorded by a sampling interval of 10 seconds. Two study sites of the microhabitat of the lizard *Timon Lepidus* were selected. A juvenile (SVL=37mm) was dwelling at site one. Site two was occupied by an adult (SVL=270mm) of the target species. At each site, thermal environmental factors were recorded for 12 hours from 6:00 am to 18:00 pm by the instruments mentioned above, and the movement of the target species were also recorded when they were active and exposed to the camera. Later, from the video recording we located the lizard positions frame by frame and marked them whenever visible for the 12 hours (Figure 6-3).

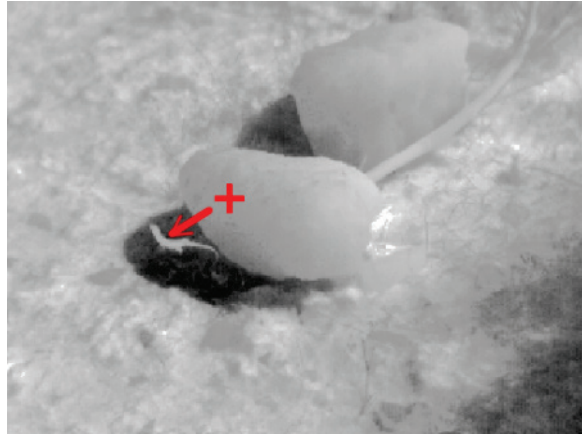


Figure 6-3 With the help from thermal infrared imager, the position of the lizard was marked in a frame with a red cross. The 12-hour habitat occupancy of the lizards in two sites were mapped frame by frame.

#### *Thermal roughness extraction*

The Laplacian of Gaussian filter was used to extract the ‘thermal roughness’ from the thermal landscape (the averaged operative temperatures of the 12 hours in the day time). Three different sized Laplacian of Gaussian filters were used: 25 mm (5 pixel), 50mm (10 pixel) and 500 mm (100 pixels). The thermal roughness was then mapped and compared with the actual habitat occupancy of the two *Timon Lepidus*.

## **6.3 Results**

### **6.3.1 Simulated Thermal Habitat**

The simulated thermal landscape is a 256 pixel by 256 pixel gray scale image of averaged operative temperature of lizards. Each pixel represents an area of 25 cm<sup>2</sup> (5 by 5 centimetres). As illustrated by pseudo-coloured Figure 6-4, the landscape is in general warmer in the upper-left portion and cooler at lower-right portion of the study area.

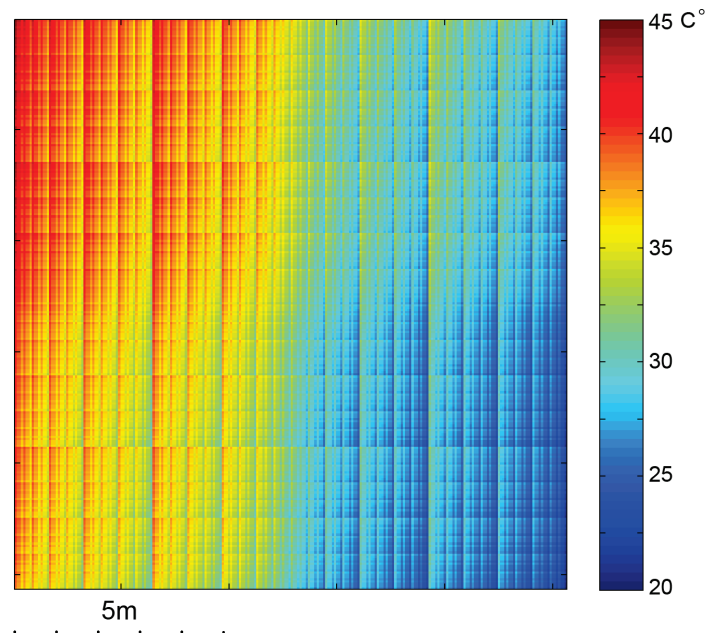


Figure 6-4 Normalized pattern of thermal landscape simulation

### 6.3.2 Thermal Roughness Map

As the thermal environment for lizards was represented by the operative temperature over the area, the thermal roughness was extracted from the operative temperature by Laplacian of Gaussian filter with different kernel sizes of 3,5,7,9,11 pixels. Linearly normalized results show that the larger the scale (larger filter kernel size), the less the thermally rough area, as shown in Figure 6-5.

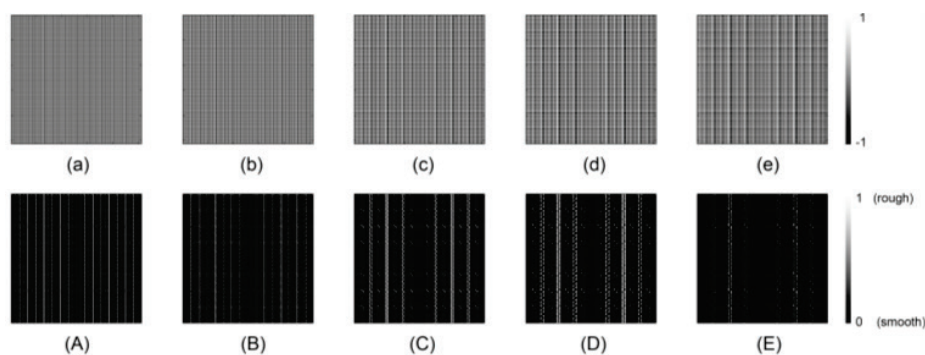


Figure 6-5 Operative temperature map filtered by Laplacian of Gaussian (LoG) with different filter size of 3,5,7,9,11 pixels (corresponding to sub-plot: a,b,c,d,e respectively). At each scale, the areas with sharp changes of thermal conditions were retained, as thermally rough area (subplot: A,B,C,D,E)

### 6.3.3 Habitat Occupancies Simulated by Animal Movement Models with Different Sized Lizards

When simulating the habitat occupancy, three lizards with different sizes and weights were parameterized, leading to a habitat occupancy map for each lizard. The results showed that the smallest lizard occupied more area than larger ones. Conversely, larger lizards tend to use less spots in thermal landscape for thermoregulation but spend more time on these spots (Figure 6-6).

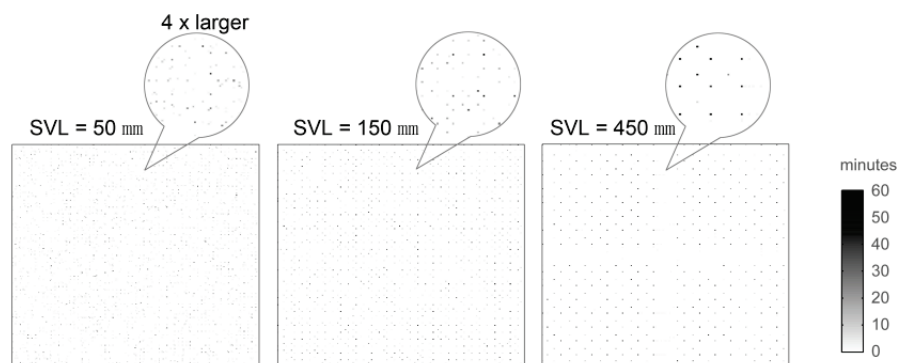


Figure 6-6 Habitat occupancies simulated by a bio-physical animal movement model for lizards in three sizes (snout-vent-length = 50 mm, 150 mm and 450 mm). Local areas were 4X zoomed in for details.

### 6.3.4 Comparing the Thermal Roughness Index and Habitat Occupancies

Euclidean distance of moment invariants between the thermal roughness maps and habitat occupancy simulations were used to compare similarity between the two maps. A smaller distance is interpreted as a more similar pattern. The result showed that a similar pattern between the thermal roughness and the simulated habitat occupancies does exist at certain scales. In our case, for the smallest lizard, when the size of moving window in Laplacian of Gaussian filter was 3 pixels, a maximum of similarity was obtained between the thermal roughness index and the habitat occupancy map. For the median sized lizard, 7 pixels is the best moving window size in terms of the maximum similarity; and for the largest lizard, the best parameter of the moving window size is 11 pixels (Figure 6-7).

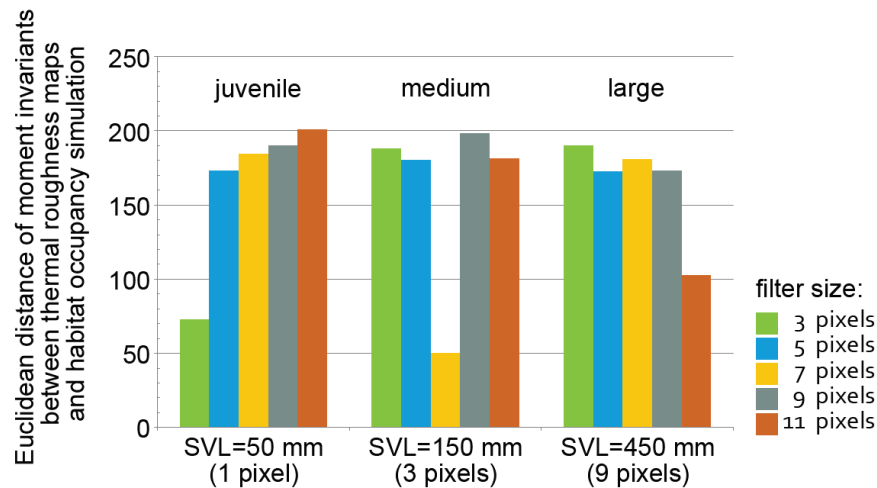


Figure 6-7 For each of the 3 different sized lizards, the thermal roughness map of lizards derived with different parameters were compared with the habitat occupancy simulations, in terms of the similarities between the two. Shorter bars indicate a closer patterns between them.

### 6.3.5 Thermal Roughness Maps versus Actual Habitat Occupancy of Lizards

Thermal roughness maps were extracted for the two field sites at three different scales, using the Laplacian of Gaussian filter. The actual positions of the lizards as recorded during the experiment were mapped. As demonstrated in Figure 6-8, (a1) to (a3) are the thermal roughness maps for the smaller juvenile lizard found in site 1, using different sized Laplacian of Gaussian filters (25 mm, 50mm, 500mm). (b1) to (b3) are the thermal roughness maps for the larger adult lizard found in site 2, using same set of filters as for the lizard in site 1. (a4) and (b4) are the lizard's positions recorded, represented by a red cross for each record.

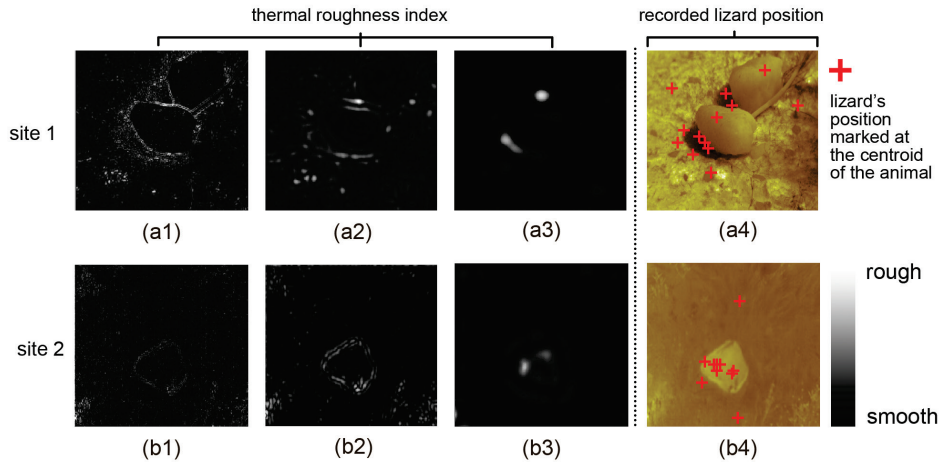


Figure 6-8 The thermal roughness extracted at different scales for site 1 (a1-a3) and site 2 (b1-b3). (a4) and (b4) are drawn from observed data of the actual positions visited by the two lizards in 12 hours. Each red cross represents the centroid of the target animal that appeared in one frame.

## 6.4 Discussion

The (micro)-habitat occupancy of a lizard in the field can be accurately approximated by a thermal roughness index calculated from its thermal landscape. The micro-habitat usage during the course of a day predicted by thermal roughness index was compared with a model simulation of lizard movement and a field observation. It is found that thermal roughness explains a large portion of lizard's habitat occupancy, when calculated at appropriate scales.

The results from field observation showed that the smaller lizards were less selective in their use of the thermal environment compared with larger lizards. Conversely, larger lizards tend to use fewer spots in the thermal landscape for thermoregulation but spend more time at these spots (Figure 6-8. (a4) and Figure 6-8. (b4)). Both the lizard movement model as well as the proposed thermal roughness index agreed with this pattern (Figure 6-5 (A)-(E) and Figure 6-6). Our results were consistent with previous investigations that have examined the relationship between the lizard's habitat usage and its size/age (Irschick et al., 2005). This might be explained by a combination of factors. Firstly, larger lizards usually have higher thermal inertia so it warms up and cools off at a much slower rate. Therefore it takes larger lizards longer to regulate to their preferred body temperature than smaller lizards. Secondly,

smaller lizards are able to use small parcels of thermal resources such as solar luminous spot, a piece of small hot rock or a small shadow/rock crevice to quickly rise/decrease its body temperature, while larger lizards cannot use these specific thermal environment due to the larger body size. In other words, smaller lizards are capable of finding the “local optimal” thermal environments all over the thermal landscape while larger lizards have to find much limited optimal thermal conditions at larger spatial scales.

Our results also accord with intuition, in that the ectotherms prefer highly contrasted thermal environment to perform behavioural thermoregulation. When the thermally contrasted spots are close to each other, the energy as well as risks related to thermoregulation can be reduced. By calculating thermal roughness index, these sharply changing thermal conditions in the landscape can be highlighted. The thermally rough area provides two important environmental characteristics for lizards: 1, highly contrasted thermal conditions and 2, the proximity between them. Moreover, high thermal roughness is typically caused by complex and rough landforms, which usually provides ideal shelters for lizards. As a result, the thermal roughness index can be seen as a useful tool to predict the habitat usage and the micro-habitat distribution of lizards.

Interestingly, this study highlighted the importance of examining spatial scale when developing a landscape index to predict the animal distribution. Figure 6-7 showed that if we calculate the thermal roughness at an appropriate scale, the roughness index can predict the habitat occupancy of a lizard. And the most appropriate scale to extract thermal roughness relates to the body size of the target lizard. According to our experiments, the optimal resolution to extract the thermal roughness index is to set the moving window size of Laplacian of Gaussian filter at the same magnitude of the lizard’s snout-vent-length but 2 to 3 times larger. However, given the limited nature of this result in terms of the number of species tested and spatial/temporal coverage, it could be premature to draw a definite conclusion about the appropriate parameter for the thermal roughness index calculation. Further research is needed.

The thermal roughness index proposed in this study also has some limitations. Animals usually face a number of important, yet conflicting demands. Many

animals especially ectotherms must also seek out habitats with a very specific thermal landscape in order to regulate body temperature (Huey, 1991a). However, it is obvious that avoidance of predators was a higher priority than thermoregulation (Downes and Shine, 1998). Besides, social dominance also interacts with thermal benefits in determining the habitat occupation. Moreover, food distribution, courtship behaviours and other environmental factors such as rainfall also shape the spatial usage of animal's local habitat. Nature is complex, so we did not expect the habitat occupancy of ectotherms to be dominated by a sole landscape index i.e. the thermal landscape. To map the habitat selection and the habitat occupancy more accurately, our next work will include other factors such as introducing animal territory, community interactions, distance to other natural resources, retreating path and site, and assess the impact of these explanatory variables on the explained variance of the occupancy model by lizard in its natural habitat using animal experiments.

## **6.5 Conclusion**

The results showed that the thermal roughness index offers a fast and accurate method to predict ectotherm habitat occupancy, if the scale to calculate the index is appropriate. The appropriate scale to determine the thermal roughness can be inferred from a reptile's body size. According to our study, the optimal scale to extract the thermal roughness index is to set the size of Laplacian of Gaussian filter at the same magnitude of the lizard's size but 2 to 3 times larger. As the dynamic model of lizard movement, the thermal roughness index also reveals that the smaller sized ectotherms make use of smaller scaled thermal heterogeneities, while larger sized ectotherms take advantage of thermal heterogeneities at larger scales.

# **CHAPTER 7**

## **SYNTHESIS**

Modelling the response of lizards to thermal landscapes



## 7.1 Introduction

Reptiles make up an important component of global biodiversity (Mittermeier et al., 1992). In recent years, however, these animals are facing a number of serious threats (Seburn et al., 2000) that cause decline of their population on a global scale (Gibbon et al., 2000). Among these threats, climate change may have a disproportionately large impact on ectotherms (Araújo et al., 2006). One significant consequence of climate change for reptiles is the change of their habitat's thermal environment (Walther et al., 2002).

The thermal environment is especially important for reptiles at different spatial scales and every aspect of their life history (Sabo, 2003; Row and Blouin-Demers, 2006). At individual level, it is known that the thermal environment influences reptiles' growth, development and survival of embryos (Angilletta et al., 2009), metabolic processes such as digestion (Harwood, 1979), behavioural processes such as activity (Stephen and Porter, 1993; Nicholson et al., 2005; Sears, 2005; Rouag et al., 2006) and locomotion (Waldschmidt and Tracy, 1983). At the microhabitat scale (within individual territories), evidence shows that the thermal characteristics of habitat components such as rocks (Schlesinger and Shine, 1994) and shrubs (Kerr et al., 2003) may influence the habitat occupancy of reptiles (Porter and James, 1979; Angilletta et al., 2009; Schofield et al., 2009). At the macrohabitat scale, studies show that the change in thermal landscape affects the spatial distribution and life history traits of the whole populations (Porter and Tracy, 1983; Kearney and Porter, 2004; Medina et al., 2009). At the global scale, the species richness co-varies with the latitude: it is highest at low latitudes, where the thermal environment is warmer in general (Barnosky et al., 2001; Boyles et al., 2011; Sears and Angilletta, 2011).

As a result, climate change may have a significant effect on reptiles through the proxy of thermal environment. And the responses of reptiles to environmental change have become an important topic in ecological and animal conservation studies (Medina et al., 2009). To model the spatial response of reptiles to their environment, many researchers have employed the concept of niche, which is a set of unique preferences or requirements of a species of the environment (Guisan and Zimmermann, 2000; Kearney and Porter, 2004; Wiens et al., 2009). With this set of preferences, correlative species distribution models can locate the areas where all environmental variables satisfy the species, and map

the (potential) distribution of the species (Phillips and Dudík, 2008; Elith and Leathwick, 2009; Kearney et al., 2010; Sinclair et al., 2010). Among other preferences, the thermal environmental variable is usually an important component in such a model to predict the distribution of animals (Sinclair et al., 2010).

It should be noted that detailed information concerning specific thermal habitat needs, habitat occupancy, and dispersal pattern is lacking for many species of reptiles (Seburn et al., 2000). Knowledge about reptile responses to the thermal landscape is needed through ecological studies of reptiles. To apply such knowledge, the thermal landscape of the reptile habitat needs to be defined and measured.

Heat transfer processes including radiation, convection and conduction. These processes dominate the energy exchange between a reptile and its environment (Porter et al., 1973). However, in portraying the thermal landscape most studies did not take into account all of the thermal sources that affect the body temperature of animal. For example, Schlesinger and Shine (1994) used the surface temperature of rocks as representative of thermal conditions; while Barnosky (2001) simplified the thermal landscape to (averaged) air temperatures. In these studies, the thermal variables mapped (surface temperature/air temperature) were merely an approximation of the thermal landscape.

In this study, thermal landscape has been defined as the spatial pattern of the thermal environment which combines the effects of all significant thermal sources including radiation, convection and conduction received by animals (Fei et al., 2012a). By this definition, we are able to accurately calculate the body temperature of a reptile in a given thermal landscape at any time, with the help of a bio-physical model. Various bio-physical models developed since the 1970s describe energy exchange between reptiles and their environment (Beckman et al., 1973; Tracy, 1982; Gates, 2003; Boyles et al., 2011; Lutterschmidt and Reinert, 2012). However, these models only calculate how the body temperature responds to the thermal landscape. The question of how the thermal landscape affects the spatial utilization of reptiles still remains unanswered. This study attempts to answer this question at a microhabitat scale,

with the help of physiological knowledge about reptile's "behavioural thermoregulation".

Reptiles are ectothermic, which are organisms that regulate their body temperature largely by exchanging heat with their surroundings, as their internal physiological sources of heat are of relatively small or quite negligible importance in controlling body temperature (Davenport, 1992). They control their body temperature mainly by behavioural thermoregulation: (Waldschmidt and Tracy, 1983): they alter their location continuously by behavioural means (e.g. basking or seeking shade) to maintain their normal body temperature which optimize their physiological functions (Raymond and Montgomery, 1976). This interesting feature of reptiles links the physiological process of the animal (body temperature) to their spatial utilization. Therefore, by simulating the behavioural thermoregulation, the movement pattern and microhabitat utilization of reptile, as a spatial response to the thermal landscape, can be modelled.

As mentioned above, the thermal landscape for reptiles needs to be measured or modelled. It is relatively easy to measure the thermal landscape in laboratory conditions where all the thermal factors are under control (see Chapter 2, 3). However, in field conditions, thermal related factors such as ground surface temperature are highly dynamic and heterogeneously distributed, and thus difficult to measure. Although at large scales, surface temperature may be retrieved by remote sensing technique (Qin et al., 2001; Sobrino et al., 2004; Coll et al., 2005; Kerr et al., 2010), the spatial resolution usually does not meet the requirement – thermal images derived from remote sensing satellites rarely resolve pixels to less than 50 m (Sobrino et al., 2004), while most organisms interact with local thermal environment at much smaller scales (Sears et al., 2011). In this thesis, a flexible, inexpensive yet accurate method to measure the digital terrain model was developed to measure the topographic characteristics of the animal's microhabitat (Chapter 4). Furthermore, based on the topographic information that can be derived from the digital terrain model, a simple yet accurate Artificial Neural Network based model was developed and tested to compute the dynamics of land surface temperature over the microhabitat of the target animal (Chapter 5). The practical techniques developed in this study to

model the key factors of thermal landscape are expected to benefit future studies related to thermal ecology at microhabitat scale.

## **7.2 Species Distribution models**

Ecological modelling has a long history in Earth sciences. Models have been developed to examine phenomena at multiple scales, from physiological systems and individual organisms to global ecosystems. Among these models, species distribution models which predict the species' distribution across a landscape have received special attention (Sinclair et al., 2010). Among the different species distribution models, two general classes can be identified: inductive models and deductive models ( Chapter 1.1; Loomis et al., 1979).

An example of an inductive model is a regression equation relating the distribution of one species to altitude and/or air temperature (Barnosky et al., 2001). When the environmental factors involved in the regression equation have a strong relationship with the prediction variable (spatial distribution of a species in this case), such a model can be rather accurate (Guisan and Zimmermann, 2000). However, it does not explain the operation of the system, and the model may lose its accuracy or even be inapplicable to conditions outside the environmental envelope that are used to parameterize the model, such as found in a different eco-system (Buckley et al., 2010).

In many fields of ecology what is taken to be a satisfactory explanation requires providing a description of a mechanism (Machamer et al., 2000). The deductive approach offers these explanations. It is a bottom-up approach that starts with the 'parts' of a system and then attempts to model how the system's properties emerge from the interactions between these parts (Loomis et al., 1979). However, it requires substantial knowledge of the system to be modelled (Buckley et al., 2010).

However, most models are neither purely inductive nor deductive models, but rather hybrids of the two, usually containing empirical relationships or parameters, linked according to theory (Kearney et al., 2010). For example, many parameters in mechanistic models are simply empirically determined quantities that have been repeatedly tested and that are consistent and linked with the consolidated body of principles or laws in ecology (O'Connor and

Spotila, 1992), such as the parameter of specific heat capacity of the lizard in this study.

### 7.3 Model Animal Responses to the Thermal Environment in a Laboratory

Ectotherms in general respond to the change in thermal environment at different scales, such as by body temperature responses, activity status changes and habitat occupancy pattern.

#### Response of body temperature to the thermal environment

In Chapter 2, a physically based model was built to predict the response of the transient body temperature of lizards to a changing thermal environment. The model took into account six energy transfer terms, including shortwave solar radiation, convective heat flow, long wave radiation, conductive heat flow, metabolic heat gain and respiratory energy loss. The result was that the model predicted a lizard's transient temperature with a root mean square error of  $0.59^{\circ}\text{C}$  (Figure 7-1).

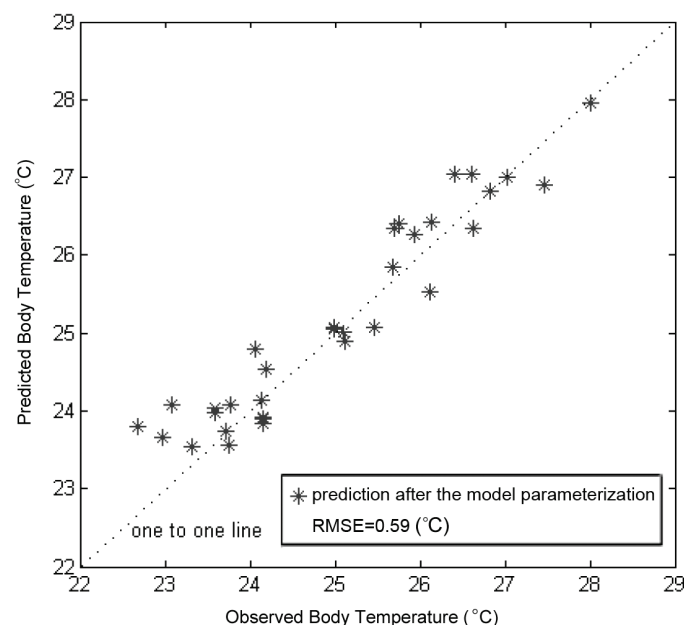


Figure 7-1 Observed vs. predicted body temperature using an independent dataset

In order to enhance the model's predictive power, a *Monte Carlo* simulation was employed to calibrate the bio-physical parameters of the target animal,

increasing the model prediction accuracy from  $1.35^{\circ}\text{C}$  to  $0.59^{\circ}\text{C}$  in terms of root mean square error. This parameterization technique, not often used in ecological studies, showed the potential to retrieve key parameters from remotely sensed data. Because the model presented in Chapter 2 is based on physical principles, it should also be useful in modelling a lizard's body temperature responses to a more complex thermal landscape.

#### Response of activity patterns to the thermal environment

Ectotherms also respond to variations in the thermal environment by altering their activity status. Porter (Porter et al., 1973) simulated the activity pattern of a lizard, a desert iguana, for every month of the year in California. The predicted behavioural pattern was plotted as a function of time of day and month of the year. In early spring, the target species was predicted and observed to be active in the middle of the day, and this pattern progressed to a morning and afternoon pattern in the middle of the summer, because the thermal environment is too hot at noon and the animal retreats into its burrow (inactive). In the autumn, the spring pattern again emerges. (Figure 7-2).

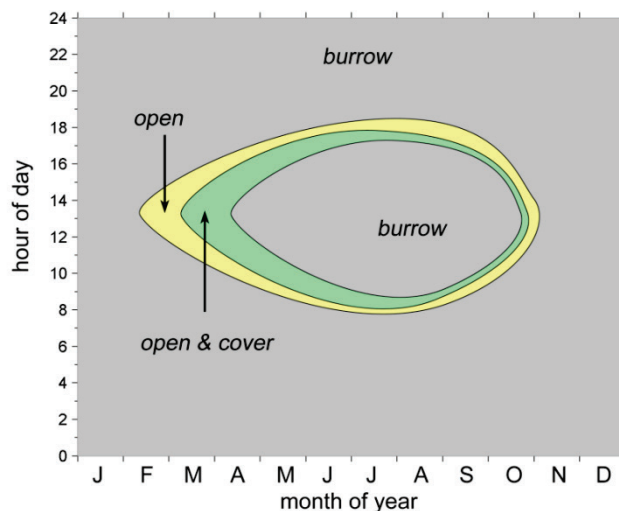


Figure 7-2 Predicted seasonal behavioural pattern for *Dispsosaurus dorsalis* after Porter (1973)

#### Response of habitat occupancy to the thermal landscape

Lizards use behavioural thermoregulation as a means of controlling body temperature, by taking advantage of places with very different thermal properties to maintain their body temperature (Templeton, 1970). In Chapter 3

we quantified the local habitat occupancy of a lizard responding to a dynamic thermal landscape. A spatially explicit model based on a cellular automaton (CA) algorithm was developed to simulate the movement of a lizard. The model assumed that the lizard tries to maintain its preferred body temperature in a dynamic thermal environment by continuously selecting positions with different thermal conditions. The sequence of chosen positions formed a chain defining the individual's path, which was later aggregated into a map of thermal habitat use. The body temperature model developed in Chapter 2 was embedded in the CA algorithm, allowing an accurate calculation of the transient body temperature of the target animal.

The prediction result was tested against observations made in a laboratory-based animal experiment. The predicted overall pattern of the micro-habitat occupancy of the lizard over four days matched these observations at an overall accuracy of 75.7%. This result suggested that local habitat occupancy responses to the thermal landscape may be modelled and predicted by a model which integrates the lizard's body temperature and the CA algorithm (Figure 7-3).

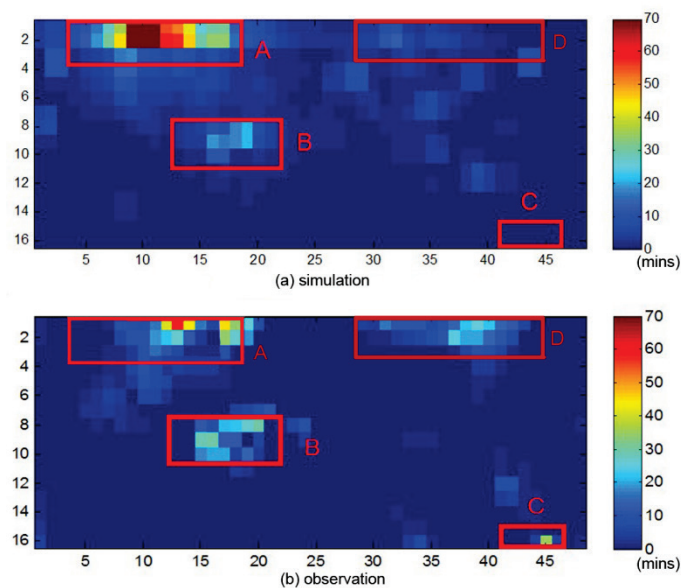


Figure 7-3 Simulated lizard's habitat occupancy (a) vs. observed lizard's habitat occupancy (b). The colours represents microhabitat occupation in terms of time the centroid of the lizard spent at each cell (in minutes) over four days. Each grid cell represents an area of 4.4cm<sup>2</sup>

## **7.4 Modelling the Key Factors of the Thermal Landscape in the Animal's Natural Habitat**

The thermal landscape is one of the most important abiotic determinants of organismal distribution and physiological performance, and especially for ectotherms (Williams and Morritt, 1995). Thermal factors such as air temperature, wind speed, solar radiation, and surface temperature of substrate interact to drive the flux of heat into and out of an organism (Helmuth and Hofmann, 2001). In ecological studies, these factors were measured or modelled by various means (Shine and Kearney, 2001; Skidmore, 2002; Guthery et al., 2005; Zeng et al., 2010). Nevertheless, a majority of thermal studies were conducted at landscape or larger spatial scales (Sobrino et al., 2004; Wan et al., 2004; Coll et al., 2005; Kerr et al., 2010), while at fine scales such as microhabitat scale, modelling the spatial heterogeneity of thermal factors is rarely seen (but see (Huey et al., 1989; Sabo, 2003)). At the scale of a microhabitat of a reptile, some thermal factors such as air temperature and wind speed can be seen to be dimensionless variables because they vary little within a small area (O'Connor and Spotila, 1992). However, the land surface temperature can be very heterogeneously distributed, as a result of complex topography and the different thermal properties of land objects (Lutz, 1997; Guthery et al., 2005; Sears et al., 2011).

Our study have solved some of the difficulties encountered in similar field studies by offering flexible and economical methods for building natural terrain elevation models and for modelling the local surface temperature from in-site meteorological data.

In Chapter 4, a low-budget, fine-scale natural terrain elevation modelling technique was developed. The chapter illustrated a method by which the digital elevation model (DEM) of a small area (around 1000 m<sup>2</sup>) can be efficiently derived using a lightweight infrared laser rangefinder that communicates with a laptop computer. Quantitative evaluations were performed with independent check-points (ICPs) measured by level, and the vertical accuracy of the DEM was about 0.2 m. Based on a DEM measured using this method, the radiation received at the land surface can be calculated. This method could also be useful for many fine-scale biological/ecological fieldwork applications.

Chapter 5 focused on predicting local land surface temperature dynamics using microclimate data and topographical information. As a hot-wire contact thermometer can only make point measurements, the ground-based thermal imagers usually have a very narrow field of view, and the resolution of thermal images from remote sensing is often too coarse, modelling rather than directly measuring the land surface temperature can be a practical alternative. Using the inputs of air temperature, solar radiation, relative humidity, soil moisture, gust wind speed, time of a day and the cosine of solar angle, the artificial neural network-based model was able to predict the surface temperature within an error margin of 1.5K.

## **7.5 Thermal Roughness Index as a Proxy to Indicate Habitat Occupancy by Lizards**

The thermal landscape can be measured directly (Fei et al., 2008), such as the distribution of radiation, land surface temperature and air temperature, or through proxies, such as elevation (Porter, 1989; Fischer and Lindenmayer, 2005), slope aspect (Thomas et al., 1999) and/or seasons (Beckman et al., 1973). Because temperature diversity in a thermal landscape creates an excellent environment for the thermoregulation of ectotherms, this thermal diversity is important for reptiles. To measure the intensity of thermal variation, a thermal roughness index was proposed in Chapter 6.

In chapter 6, a Laplacian of Gaussian (LoG) filter was used to extract the ‘thermally rough areas’ from the image of operative temperatures (defined as the temperature of an inanimate object of zero heat capacity with the same size, shape and radiative properties as an animal exposed to the same microclimate (Bakken and Gates, 1975)). These areas were compared with the habitat occupancy map generated by the methods illustrated in Chapter 3. Field data was also used to validate whether the thermal roughness index represented the use of the thermal landscape by lizards. The results showed that the thermal roughness index offers a fast and accurate method to predict lizard habitat occupancy, if the scale used to calculate the thermal roughness index is appropriate.

Chapters 3 and 6 both predicted local habitat occupancies: one under laboratory conditions and the other using field conditions. However, different approaches

were tested: in Chapter 3 a dynamic model was developed to simulate the movement of lizards, and in Chapter 6 a static index was proposed to capture the intensity of changes in the thermal landscape. This choice was made because of the structure of the lizard’s natural microhabitat is too complex and too computational intensive (including vertical features such as palm tree) for this individual based dynamic model. These two methods can be seen as supplementary to each other, and both methods were successful.

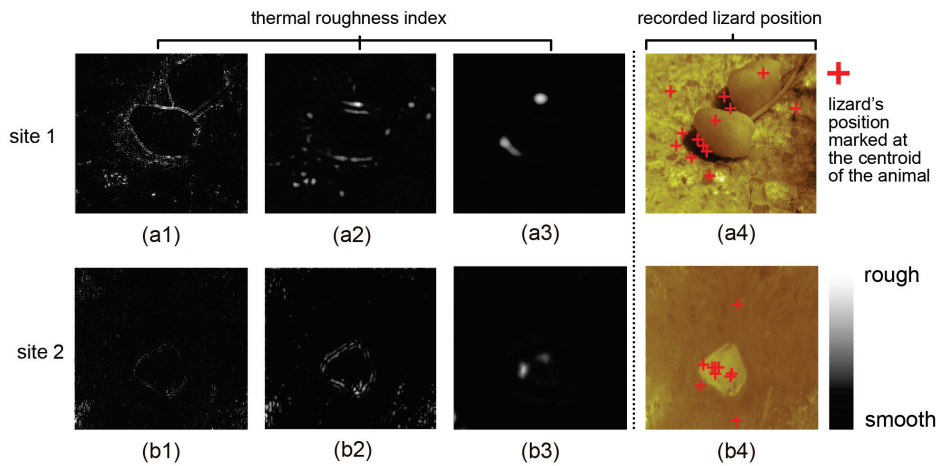


Figure 7-4 The thermal roughness extracted at different scales for site 1 (a1–a3) and site 2 (b1–b3). (a4) and (b4) are drawn from observed data of the actual positions visited by two lizards in 12 hours. Each red cross represents the centroid of the target animal that appeared in a single frame.

## 7.6 Implications

This study provides valuable information for the management of reptile habitats by modelling the thermal landscape and the response of a lizard. It offered a thermal point of view from which the spatial utilization of a lizard within its thermal microhabitat can be predicted. The results obtained in this study may have some implications and here is a few of them:

This study can benefit some future thermal biological/ecological researches. In this study, some hard-to-measure parameters of the model were obtained by inversion techniques rather than measurements. With this technique which is currently not often used in biological/ecological studies, bio-physical modelling can be a more attractive tool for studies meant to provide reasonably precise predictions about an organism, while having limited prior-knowledge about it.

Reptilian conservation may benefit from this study. By applying the deductive modelling approach used in this study, one can model and simulate the responses of reptiles (or in general, ectotherms) to a wide series of different scenarios of thermal regimes of possible futures. Based on these simulated scenarios of reptile's activity patterns, energy expenses, and potential distribution, scientific decisions can be made for animal conservation in the context of global climate change or extreme weather.

In the field of habitat restoration and recreation, the thermal roughness index proposed in this study can be applied to exam whether the recreated thermal landscape enhanced the thermal diversity and to predict if the thermal landscape is in compliance with the animal thermoregulatory requirements.

The method to model the topography and the land surface temperature at microhabitat scale that we developed in this study may provide valuable information on thermal landscape in the field and benefit other thermal ecological studies of terrain animals.

## **7.7 General Conclusion**

This study focused on the spatial relevance between the thermal landscape and the response of ectotherms. It has demonstrated that the response of ectotherms within the thermal landscape can be successfully modelled at different levels, under both laboratory conditions as well as in the field.

A bio-physical model can accurately simulate the transient body temperature of a lizard through monitoring the changing thermal environment. A cellular automaton based spatially explicit model integrated with a bio-physical model is able to simulate the change of thermal landscape and the behavioural response of a lizard. The movement of a reptile can be simulated and finally lead to a prediction of the utilization by a lizard of its microhabitat. The simulation was validated by a laboratory based animal experiment and the result showed that the thermal landscape explains a large portion of the spatial utilization of ectotherms, as demonstrated by the lizard of *Timon Lepidus* in this study. Besides the cellular automaton based dynamic model, a thermal roughness index was proposed, by which the pattern of ectotherm habitat occupancy can also be predicted accurately.

This study also developed some practical techniques on collecting field data: natural terrain elevation and land surface temperature of animal's local habitat can be modelled with satisfactory accuracy by new and practical methods that were developed in this thesis. These methods can be useful also for some future applied ecological investigations in the field.

## BIBLIOGRAPHY

- Agarwal, P., Arge, L. and Danner, A., 2006. From point cloud to grid DEM: a scalable approach. *Progress in Spatial Data Handling*, pp. 771-788.
- Angilletta, M.J.J., Sears, M.W. and Pringle, R.M., 2009. The spatial dynamics of nesting behavior: Lizards shift microhabitats to construct nests with beneficial thermal properties. *Ecology*, 90:2933-2939.
- Araújo, M.B., Thuiller, W. and Pearson, R.G., 2006. Climate warming and the decline of amphibians and reptiles in Europe. *Journal of Biogeography*, 33:1712-1728.
- Arnold, S.J., Peterson, C.R. and Gladstone, J., 1995. Behavioural variation in natural populations. VII. Maternal body temperature does not affect juvenile thermoregulation in a garter snake. *Animal Behaviour*, 50:623-633.
- Aspinall, R., 1992. An inductive modelling procedure based on Bayes' theorem for analysis of pattern in spatial data. *International Journal of Geographical Information Science*, 6:105-121.
- Autumn, K. and Nardo, D.F.D., 1995. Behavioral thermoregulation increases growth rate in a nocturnal lizard. *Journal of Herpetology*, 29:157-162.
- Avery, R.A., 1978. Activity patterns, thermoregulation and food consumption in two sympatric lizard species (*Podarcis muralis* and *P. sicula*) from central Italy. *Journal of Animal Ecology*, 47:143-158.
- Avila, V.L., 1995. *Biology: investigating life on earth*. Jones and Bartlett.
- Bachelet, D., Neilson, R.P., Lenihan, J.M. and Drapek, R.J., 2001. Climate change effects on vegetation distribution and carbon budget in the United States. *Ecosystems*, 4:164-185.
- Bakken, G. and Gates, D., 1975. Heat-transfer analysis of animals: some implications for field ecology, physiology, and evolution. *Perspectives of Biophysical Ecology*, 12:255-290.
- Barlett, P.N. and Gates, D.M., 1967. The energy budget of a lizard on a tree trunk. *Ecology*, 48:315-322.
- Barnosky, A.D., Hadly, E.A., Maurer, B.A. and Christie, M.I., 2001. Temperate terrestrial vertebrate faunas in North and South America: interplay of ecology, evolution, and geography with biodiversity. *Conservation Biology*, 15:658-674.
- Bartholomew, G., 1982. Physiological control of body temperature. *Biology of the Reptilia*, 12:167-211.

- Bartholomew, G.A., 1966. A Field study of temperature relations in the Galápagos Marine Iguana. *Copeia*, 1966:241-250.
- Bartholomew, G.A. and Lasiewski, R.C., 1965. Heating and cooling rates, heart rate and simulated diving in the Galapagos marine iguana. *Comparative Biochemistry and Physiology*, 16:573-582.
- Bastiaanssen, W.G.M., Menenti, M., Feddes, R.A. and Holtslag, A.A.M., 1998. A remote sensing surface energy balance algorithm for land (SEBAL). 1. Formulation. *Journal of Hydrology*, 212-213:198-212.
- Bauwens, D., Hertz, P.E. and Castilla, A.M., 1996. Thermoregulation in a Lacertid Lizard: The Relative Contributions of Distinct Behavioral Mechanisms. *Ecology*, 77:1818-1830.
- Beckman, W.A., Mitchell, J.W. and Porter, W.P., 1973. Thermal model for prediction of a desert iguana's daily and seasonal behavior. *Journal of Heat Transfer, Transactions ASME*, 95:257-262.
- Belkasim, S.O., Shridhar, M. and Ahmadi, M., 1991. Pattern recognition with moment invariants: a comparative study and new results. *Pattern recognition*, 24:1117-1138.
- Bennett, A.F., 2004. Thermoregulation in African chameleons. *International Congress Series*, 1275:234-241.
- Bennett, A.F. and Nagy, K.A., 1977. Energy expenditure in free-ranging lizards. *Ecology*, 58:697-700.
- Betts, M.G., Rodenhouse, N.L., Scott Sillett, T., Doran, P.J. and Holmes, R.T., 2008. Dynamic occupancy models reveal within-breeding season movement up a habitat quality gradient by a migratory songbird. *Ecography*, 31:592-600.
- Bevelhimer, M.S., 1996. Relative importance of temperature, food, and physical structure to habitat choice by smallmouth bass in laboratory experiments. *Transactions of the American Fisheries Society*, 125:274-283.
- Block, B.A., Dewar, H., Blackwell, S.B., Williams, T.D., Prince, E.D., Farwell, C.J., Boustany, A., Teo, S.L.H., Seitz, A., Walli, A. and Fudge, D., 2001. Migratory movements, depth preferences, and thermal biology of Atlantic bluefin tuna. *Science*, 293:1310-1314.
- Blouin-Demers, G. and Nadeau, P., 2005. The cost-benefit model of thermoregulation does not predict lizard thermoregulatory behavior. *Ecology*, 86:560-566.

- Bonnaffe, F., Jennette, D. and Andrews, J., 2007. A method for acquiring and processing ground-based lidar data in difficult-to-access outcrops for use in three-dimensional, virtual-reality models. *Geosphere*, 3:501-510.
- Boyles, J.G., Seebacher, F., Smit, B. and McKechnie, A.E., 2011. Adaptive thermoregulation in endotherms may alter responses to climate change. *Integrative and Comparative Biology*, 51:676-690.
- Broitman, B.R., Szathmary, P.L., Mislán, K.A.S., Blanchette, C.A. and Helmuth, B., 2009. Predator-prey interactions under climate change: The importance of habitat vs body temperature. *Oikos*, 118:219-224.
- Brooks, R.P., 1997. Improving habitat suitability index models. *Wildlife Society Bulletin*, 25:163-167.
- Brown, R.P. and Au, T., 2009. The influence of metabolic heat production on body temperature of a small lizard, *Anolis carolinensis*. *Comparative Biochemistry and Physiology - Part A: Molecular & Integrative Physiology*, 153:181-184.
- Buckley, L.B., Urban, M.C., Angilletta, M.J., Crozier, L.G., Rissler, L.J. and Sears, M.W., 2010. Can mechanism inform species' distribution models? *Ecology Letters*, 13:1041-1054.
- Bujes, C.S. and Verrastro, L., 2006. Thermal biology of *Liolaemus occipitalis* (Squamata, Tropiduridae) in the coastal sand dunes of Rio Grande do Sul, Brazil. *Brazilian Journal of Biology*, 66:945-954.
- Busby, J.R., 1991. BIOCLIM-a bioclimate analysis and prediction system. *Plant Protection Quarterly*, 6:8-9.
- Butler, J.B., Lane, S.N. and Chandler, J.H., 1998. Assessment of dem quality for characterizing surface roughness using close range digital photogrammetry. *The Photogrammetric Record*, 16:271-291.
- Campbell, G.S. and Norman, J.M., 1977. *An introduction to environmental biophysics* Springer, New York, USA.
- Cao, J., Fussmann, G.F. and Ramsay, J.O., 2008. Estimating a predator-prey dynamical model with the parameter cascades method. *Biometrics*, 64:959-967.
- Carey, P., 1996. DISPERSE: a cellular automaton for predicting the distribution of species in a changed climate. *Global Ecology and Biogeography Letters*, 5:217-226.
- Carpenter, G., Gillison, A. and Winter, J., 1993. DOMAIN: a flexible modelling procedure for mapping potential distributions of plants and animals. *Biodiversity and Conservation*, 2:667-680.

- Chang, J. and Root, B., 1975. On the relationship between mean monthly global radiation and air temperature. *Theoretical and Applied Climatology*, 23:13-30.
- Chato, J.C., 1966. A survey of thermal conductivity and diffusivity data on biological materials. *ASME 66-WA/HT-37:1-9*.
- Chen, J., Gong, P., He, C., Luo, W., Tamura, M. and Shi, P., 2002. Assessment of the urban development plan of Beijing by using a CA-based urban growth model. *Photogrammetric Engineering and Remote Sensing*, 68:1063-1071.
- Chen, J., Huertas, A. and Medioni, G., 1987. Fast convolution with Laplacian-of-Gaussian masks. *Pattern Analysis and Machine Intelligence, IEEE Transactions on*:584-590.
- Chinneck, J.W., 2004. *Practical optimization: a gentle introduction*. Ottawa, Canada.
- Christian, J. and Roger, A., 2001. From pattern to process: identifying predator-prey models from time-series data. *Anglais*, 43:229 - 243.
- Christian, K.A., Tracy, C.R. and Tracy, C.R., 2006. Evaluating thermoregulation in reptiles: an appropriate null model. *The American Naturalist*, 168:421-430.
- Claireaux, G., Webber, D.M., Kerr, S.R. and Boutilier, R.G., 1995. Physiology and behaviour of free-swimming Atlantic cod (*Gadus morhua*) facing fluctuating salinity and oxygenation conditions. *The journal of experimental biology*, Vol. 198, No. 1 (1995), p. 61-70.
- Clark, T.D., Butler, P.J. and Frappell, P.B., 2006. Factors influencing the prediction of metabolic rate in a reptile. *Functional Ecology*, 20:105-113.
- Coleman, T., Branch, M.A. and Grace, A., 1999. *Optimization toolbox: for use with MATLAB: user's guide*. The MathWorks, Inc.
- Coll, C., Caselles, V., Galve, J.M., Valor, E., Niclòs, R., Sánchez, J.M. and Rivas, R., 2005. Ground measurements for the validation of land surface temperatures derived from AATSR and MODIS data. *Remote Sensing of Environment*, 97:288-300.
- Conroy, M.J., Cohen, Y., James, F.C., Matsinos, Y.G. and Maurer, B.A., 1995. Parameter estimation, reliability, and model improvement for spatially explicit models of animal populations. *Ecological Applications*, 5:17-19.
- Conway, J., 1970. The game of life. *Scientific American*, 223:120-123.

- Cowgell, J. and Underwood, H., 1979. Behavioral thermoregulation in lizards: A circadian rhythm. *Journal of Experimental Zoology*, 210:189-194.
- Cowles, R.B. and Bogert, C.M., 1944. A preliminary study of the thermal requirements of desert reptiles. *Bulletin of the American Museum of Natural History*, 85:265-296.
- Cramer, W., Bondeau, A., Woodward, F.I., Prentice, I.C., Betts, R.A., Brovkin, V., Cox, P.M., Fisher, V., Foley, J.A., Friend, A.D., Kucharik, C., Lomas, M.R., Ramankutty, N., Sitch, S., Smith, B., White, A. and Young-Molling, C., 2001. Global response of terrestrial ecosystem structure and function to CO<sub>2</sub> and climate change: results from six dynamic global vegetation models. *Global Change Biology*, 7:357-373.
- Davenport, J., 1992. *Animal life at low temperature*. Springer.
- Dawson, W.R. and Bartholomew, G.A., 1958. Metabolic and cardiac responses to temperature in the lizard *Dipsosaurus dorsalis*. *Physiol. Zool.*, 31:100-111.
- De Long, A.J., Greenberg, N. and Keane, C., 1986. Temporal responses to environmental scale in the lizard *Anolis carolinensis* (reptilia, lacertilia, iguanidae). *Behavioural Processes*, 13:339-352.
- Deitschman, G.H., 1973. Mapping of habitat types throughout a national forest. [s.n.], Ogden, 14 p.
- Deutsch, C.A., Tewksbury, J.J., Huey, R.B., Sheldon, K.S., Ghalambor, C.K., Haak, D.C. and Martin, P.R., 2008. Impacts of climate warming on terrestrial ectotherms across latitude. *Proceedings of the National Academy of Sciences*, 105:6668-6672.
- Dorcas, M.E. and Peterson, C.R., 1997. Head-body temperature differences in free-ranging rubber boas. *J Herpetol*, 31:87-93.
- Downes, S. and Shine, R., 1998. Heat, safety or solitude? Using habitat selection experiments to identify a lizard's priorities. *Animal Behaviour*, 55:1387-1396.
- Dudani, S.A., Breeding, K.J. and McGhee, R.B., 1977. Aircraft identification by moment invariants. *Computers, IEEE Transactions on*, 100:39-46.
- Dzialowski, E.M. and O'Connor, M.P., 1999. Utility of blood flow to the appendages in physiological control of heat exchange in reptiles. *J Therm Biol*, 24:21-32.
- Dzialowski, E.M. and O'Connor, M.P., 2004. Importance of the limbs in the physiological control of heat exchange in *Iguana iguana* and *Sceloporus undulatus*. *J Therm Biol*, 29:299-305.

- Edgar, G.J., 1983. The ecology of south-east tasmanian phytal animal communities. IV. Factors affecting the distribution of amphitoid amphipods among algae. *Journal of Experimental Marine Biology and Ecology*, 70:205-225.
- Eifler, D.A., Eifler, M.A. and Harris, B.R., 2008. Foraging under the risk of predation in desert grassland whiptail lizards (*Aspidoscelis uniparens*). *Journal of Ethology*, 26:219-223.
- Elith, J. and Leathwick, J.R., 2009. Species distribution models: ecological explanation and prediction across space and time. *Annual Review of Ecology, Evolution, and Systematics*, 40:677-697.
- Estes, L.D., Reillo, P.R., Mwangi, A.G., Okin, G.S. and Shugart, H.H., 2010. Remote sensing of structural complexity indices for habitat and species distribution modeling. *Remote Sensing of Environment*, 114:792-804.
- Farina, A., 2006. *Principles and methods in landscape ecology: toward a science of landscape*. Kluwer Academic Pub.
- Fei, T., Skidmore, A.K., Venus, V., Wang, T., Schlerf, M., Toxopeus, A. G., van Overjijk, S., Bian, M. and Liu, Y., 2012a. A body temperature model for lizards as estimated from the thermal environment. *Journal of Thermal Biology*, 37:56 - 64.
- Fei, T., Skidmore, A.K., Venus, V., Wang, T., Toxopeus, A. G., Bian, M. and Liu, Y., 2012b. Predicting micro thermal habitat of lizards in a dynamic thermal environment. *Ecological Modelling*, 231:126-133.
- Fei, T., Venus, V., Toxopeus, A. G., Skidmore, A.K., Schlerf, M., Liu, Y., Overdijk, S.v. and Bian, M., 2008. Understanding lizard's microhabitat use based on a mechanistic model of behavioral thermoregulation. In: L. Deren, G. Jianya and W. Huayi (Editor). *SPIE*, pp. 728508 - 728513.
- Ferrier, S., Drielsma, M., Manion, G. and Watson, G., 2002a. Extended statistical approaches to modelling spatial pattern in biodiversity in northeast New South Wales. II. Community-level modelling. *Biodiversity and Conservation*, 11:2309-2338.
- Ferrier, S., Watson, G., Pearce, J. and Drielsma, M., 2002b. Extended statistical approaches to modelling spatial pattern in biodiversity in northeast New South Wales. I. Species-level modelling. *Biodiversity and Conservation*, 11:2275-2307.
- Fischer, J. and Lindenmayer, D.B., 2005. The sensitivity of lizards to elevation: A case study from south-eastern Australia. *Diversity and Distributions*, 11:225-233.

- Fischer, J., Lindenmayer, D.B., Nix, H.A., Stein, J.L. and Stein, J.A., 2001. Climate and animal distribution: a climatic analysis of the Australian marsupial *Trichosurus caninus*. *Journal of Biogeography*, 28:293-304.
- Fitzgerald, M., Shine, R. and Lemckert, F., 2003. A reluctant heliotherm: thermal ecology of the arboreal snake *Hoplocephalus stephensii* (Elapidae) in dense forest. *Journal of Thermal Biology*, 28:515-524.
- Flusser, J., Suk, T., Zitová, B. and Ebrary, I., 2009. Moments and moment invariants in pattern recognition. Wiley Online Library.
- Ford, R.G., Ainley, D.G., Brown, E.D., Suryan, R.M. and Irons, D.B., 2007. A spatially explicit optimal foraging model of Black-legged Kittiwake behavior based on prey density, travel distances, and colony size. *Ecological Modelling*, 204:335-348.
- Gates, D.M., 2003. Biophysical ecology. Dover Publications, New York.
- Georgakarakos, S. and Kitsiou, D., 2008. Mapping abundance distribution of small pelagic species applying hydroacoustics and Co-Kriging techniques. *Hydrobiologia*, 612:155-169.
- Georges, A., 1979. Head-body temperature differences in the Australian blue-tongued lizard, *Tiliqua scincoides* during radiant heating. *J Therm Biol*, 4:213-217.
- Gese, E.M., 2001. Monitoring of terrestrial carnivore populations. *Carnivore Conservation*:372-396.
- Gibbon, J.W., Scott, D.E., Ryan, T.J., Buhlmann, K.A., Tuberville, T.D., Metts, B.S., Greene, J.L., Mills, T., Leiden, Y., Poppy, S. and Winne, C.T., 2000. The global decline of reptiles, Déjà vu amphibians. *BioScience*, 50:653-666.
- Goovaerts, P., 2000. Geostatistical approaches for incorporating elevation into the spatial interpolation of rainfall. *Journal of Hydrology*, 228:113-129.
- Goshtasby, A., 1985. Template matching in rotated images. *Pattern Analysis and Machine Intelligence*, IEEE Transactions on:338-344.
- Guisan, A. and Zimmermann, N.E., 2000. Predictive habitat distribution models in ecology. *Ecological Modelling*, 135:147-186.
- Guthery, F.S., Rybak, A.R., Fuhlendorf, S.D., Hiller, T.L., Smith, S.G., Puckett, W.H., Jr. and Baker, R.A., 2005. Aspects of the thermal ecology of bobwhites in North Texas. *Wildlife Monographs*:1-36.
- Gutiérrez-Estrada, J.C., Vasconcelos, R. and Costa, M.J., 2008. Estimating fish community diversity from environmental features in the Tagus estuary (Portugal): Multiple Linear Regression and Artificial Neural Network approaches. *Journal of Applied Ichthyology*, 24:150-162.

- Hammel, H.T., Caldwell Jr, F.T. and Abrams, R.M., 1967. Regulation of body temperature in the blue-tongued lizard. *Science*, 156:1260-1262.
- Harwood, R.H., 1979. The effect of temperature on the digestive efficiency of three species of lizards, *Cnemidophorus tigris*, *Gerrhonotus multicarinatus* and *Sceloporus occidentalis*. *Comparative Biochemistry and Physiology*, 63:417-433.
- Heikkinen, R.K., Luoto, M., Araújo, M.B., Virkkala, R., Thuiller, W. and Sykes, M.T., 2006. Methods and uncertainties in bioclimatic envelope modelling under climate change. *Progress in Physical Geography*, 30:751-777.
- Helmuth, B.S.T. and Hofmann, G.E., 2001. Microhabitats, thermal heterogeneity, and patterns of physiological stress in the rocky intertidal zone. *The Biological Bulletin*, 201:374-384.
- Hertz, P.E., Huey, R.B. and Stevenson, R.D., 1993. Evaluating temperature regulation by field-active ectotherms: the fallacy of the inappropriate question. *American Naturalist*, 142:796-818.
- Hetrick, W., Rich, P., Barnes, F. and Weiss, S., 1993. GIS-based solar radiation flux models. *GIS Photogrammetry and Modeling*, 3:132-143.
- Hijmans, R., Guarino, L., Cruz, M. and Rojas, E., 2001. Computer tools for spatial analysis of plant genetic resources data: 1. DIVA-GIS. *Plant Genetic Resources Newsletter*, 127:15-19.
- Hirzel, A., Hausser, J., Chessel, D. and Perrin, N., 2002. Ecological-niche factor analysis: how to compute habitat-suitability maps without absence data? *Ecology*, 83:2027-2036.
- Hu, M.K., 1962. Visual pattern recognition by moment invariants. *Information Theory, IRE Transactions on*, 8:179-187.
- Huang, C., Li, X. and Lu, L., 2008. Retrieving soil temperature profile by assimilating MODIS LST products with ensemble Kalman filter. *Remote Sensing of Environment*, 112:1320-1336.
- Huey, R., 1991a. Physiological consequences of habitat selection. *The American Naturalist*, 137:S91-S115.
- Huey, R.B., 1974. Behavioral thermoregulation in lizards: importance of associated costs. *Science*, 184:1001-1003.
- Huey, R.B., 1991b. Physiological consequences of habitat selection. *Am Nat*:91-115.
- Huey, R.B. and Bennett, A.F., 1987. Phylogenetic studies of coadaptation: preferred temperatures versus optimal performance temperatures of lizards. *Evolution*, 41:1098-1091 1115.

- Huey, R.B., Peterson, C.R., Arnold, S.J. and Porter, W.P., 1989. Hot rocks and not-so-hot rocks: retreat-site selection by garter snakes and its thermal consequences. *Ecology*, 70:931-944.
- Huey, R.B. and Slatkin, M., 1976. Costs and benefits of lizard thermoregulation. *The Quarterly Review Of Biology*, 51:363-384.
- Irschick, D.J., Carlisle, E., Elstrott, J., Ramos, M., Buckley, C., Vanhooydonck, B., Meyers, J.A.Y. and Herrel, A., 2005. A comparison of habitat use, morphology, clinging performance and escape behaviour among two divergent green anole lizard (*Anolis carolinensis*) populations. *Biological Journal of the Linnean Society*, 85:223-234.
- Iverson, L.R., Prasad, A. and Schwartz, M.W., 1999. Modeling potential future individual tree-species distributions in the eastern United States under a climate change scenario: a case study with *Pinus virginiana*. *Ecol Model*, 115:77-93.
- Jobbágy, E.G. and Jackson, R.B., 2000. The vertical distribution of soil organic carbon and its relation to climate and vegetation. *Ecological Applications*, 10:423-436.
- Kawashima, S., Ishida, T., Minomura, M. and Miwa, T., 2000. Relations between surface temperature and air temperature on a local scale during winter nights. *Journal of Applied Meteorology*, 39:1570-1579.
- Kearney, M. and Porter, W., 2009. Mechanistic niche modelling: combining physiological and spatial data to predict species' ranges. *Ecology Letters*, 12:334-350.
- Kearney, M. and Porter, W.P., 2004. Mapping the fundamental niche: Physiology, climate, and the distribution of a nocturnal lizard. *Ecology*, 85:3119-3131.
- Kearney, M.R., Wintle, B.A. and Porter, W.P., 2010. Correlative and mechanistic models of species distribution provide congruent forecasts under climate change. *Conservation Letters*, 3:203-213.
- Keiner, L.E. and Yan, X.H., 1998. A neural network model for estimating sea surface chlorophyll and sediments from thematic mapper imagery. *Remote Sensing of Environment*, 66:153-165.
- Kelly, R.E., McConnell, P.R.H. and Mildemberger, S.J., 1977. The gestalt photomapping system. *Photogrammetric Engineering and Remote Sensing*, 43:1407 - 1417.
- Kerr, G.D., Bottema, M.J. and Bull, C.M., 2008. Lizards with rhythm? Multi-day patterns in total daily movement. *J Zool*, 275:79-88.

- Kerr, G.D., Bull, C.M. and Burzacott, D., 2003. Refuge sites used by the scincid lizard *Tiliqua rugosa*. *Austral Ecology*, 28:152-160.
- Kerr, Y.H., Lagouarde, J.P. and Imbernon, J., 2010. Accurate land surface temperature retrieval from AVHRR data with use of an improved split window algorithm. *Remote Sensing of Environment*, 41:197-209.
- Kobler, A., Pfeifer, N., Ogrinc, P., Todorovski, L., Ostir, K. and Dzeroski, S., 2007. Repetitive interpolation: A robust algorithm for DTM generation from Aerial Laser Scanner Data in forested terrain. *Remote Sensing of Environment*, 108:9-23.
- Krebs, C.J., 1978. *Ecology : the experimental analysis of distribution and abundance*. Harper & Row, New York etc., 678 p.
- Kreith, F. and Kreider, J.F., 1978. *Principles of solar engineering*. Hemisphere Publishing Corporation, Washington, DC.
- Kumar, L., Skidmore, A.K. and Knowles, E., 1997. Modelling topographic variation in solar radiation in a GIS environment. *International Journal of Geographical Information Science*, 11:475 - 497.
- Kunwar, A., John, A., Nishinari, K., Schadschneider, A. and Chowdhury, D., 2004. Collective traffic-like movement of ants on a trail: Dynamical phases and phase transitions. *Journal of the Physical Society of Japan*, 73:2979-2985.
- Ladyman, M. and Bradshaw, D., 2003. The influence of dehydration on the thermal preferences of the Western tiger snake, *Notechis scutatus*. *Journal of Comparative Physiology B: Biochemical, Systemic, and Environmental Physiology*, 173:239-246.
- Lakshmi, V., Susskind, J. and Choudhury, B.J., 1998. Determination of land surface skin temperatures and surface air temperature and humidity from TOVS HIRS2/MSU data. *Advances in Space Research*, 22:629-636.
- Lee, J.C., 1980. Comparative thermal ecology of two lizards. *Oecologia*, 44:171-176.
- Lehmann, A., Overton, J.M.C. and Leathwick, J.R., 2002. GRASP: generalized regression analysis and spatial prediction. *Ecol Model*, 157:189-207.
- Levins, R., 1966. The strategy of model building in population biology. *American Scientist*, 54:421-431.
- Levins, R., 1968. Evolution in changing environments: Some theoretical exploration. *Niche: Theory and Application*:241-258.
- Leyequien, E., Verrelst, J., Slot, M., Schaepman-Strub, G., Heitkönig, I.M.A. and Skidmore, A.K., 2007. Capturing the fugitive: Applying remote

- sensing to terrestrial animal distribution and diversity. *International Journal of Applied Earth Observation and Geoinformation*, 9:1-20.
- Liu, H. and Zhou, L., 2007. Modeling dispersal of the plateau pika (*Ochotona curzoniae*) using a cellular automata model. *Ecological Modelling*, 202:487-492.
- Loomis, R.S., Rabbinge, R. and Ng, E., 1979. Explanatory models in crop physiology. *Annual Review of Plant Physiology*, 30:339-367.
- Luiselli, L. and Akani, G.C., 2002. Is thermoregulation really unimportant for tropical reptiles? Comparative study of four sympatric snake species from Africa. *Acta Oecologica*, 23:59-68.
- Lutterschmidt, W.I. and Reinert, H.K., 2012. Modeling body temperature and thermal inertia of large-bodied reptiles: Support for water-filled biophysical models in radiotelemetric studies. *Journal of Thermal Biology*, 37:282-285.
- Lutz, T., 1997. Modelling individual movements in heterogeneous landscapes: potentials of a new approach. *Ecological Modelling*, 103:33-42.
- Machamer, P., Darden, L. and Craver, C.F., 2000. Thinking about Mechanisms. *Philosophy of Science*, 67:1 - 25.
- Mao, K., Qin, Z., Shi, J. and Gong, P., 2005. A practical split-window algorithm for retrieving land-surface temperature from MODIS data. *International Journal of Remote Sensing*, 26:3181 - 3204.
- Marsili-Libelli, S., Guerrizio, S. and Checchi, N., 2003. Confidence regions of estimated parameters for ecological systems. *Ecological Modelling*, 165:127-146.
- Mateo, J.A. (Editor) 2004. *Timon lepidus*. En: Enciclopedia Virtual de los Vertebrados Españoles, Madrid, Spain.
- Mateo, J.A., 2006. Enciclopedia virtual de los vertebrados españoles. In: L.M. Carrascal, Salvador, A. (Editor). Museo Nacional de Ciencias Naturales.
- Medina, M., Gutierrez, J., Scolaro, A. and Ibargüengoytía, N., 2009. Thermal responses to environmental constraints in two populations of the oviparous lizard *Liolaemus bibronii* in Patagonia, Argentina. *Journal of Thermal Biology*, 34:32-40.
- Meiri, S., 2010. Length-weight allometries in lizards. *Journal of Zoology*, 281:218-226.
- Mitchell, S., Beven, K. and Freer, J., 2009. Multiple sources of predictive uncertainty in modeled estimates of net ecosystem CO<sub>2</sub> exchange. *Ecological Modelling*, 220:3259-3270.

- Mittermeier, R.A., Carr, J.L. and Swingland, I.R., 1992. Conservation of amphibians and reptiles. *Global biodiversity*, 60:70.
- Moore, A.D. and Noble, I.R., 1993. Automatic model simplification: The generation of replacement sequences and their use in vegetative modelling. *Ecological Modelling*, 70:137-157.
- Moore, I.D., Grayson, R.B. and Ladson, A.R., 1991. Digital terrain modelling: A review of hydrological, geomorphological, and biological applications. *Hydrological Processes*, 5:3-30.
- Moré, J.J., 1977. The Levenberg-Marquardt algorithm: implementation and theory. *Numerical analysis*. Springer Berlin, Heidelberg, pp. 105-116.
- Mueller, T.G. and Pierce, F.J., 2003. Soil carbon maps: Enhancing spatial estimates with simple terrain attributes at multiple scales. *Soil Science Society of America Journal*, 67:258-267.
- Mutanga, O. and Skidmore, A.K., 2004. Integrating imaging spectroscopy and neural networks to map grass quality in the Kruger National Park, South Africa. *Remote Sensing of Environment*, 90:104-115.
- Mynett, A. and Chen, Q., 2004. Cellular automata in ecological and ecohydraulics modelling. *Cellular Automata*, pp. 502-512.
- Neilson, R.P., 1995. A model for predicting continental-scale vegetation distribution and water balance. *Ecological Applications*, 5:362-385.
- Nicholson, K.L., Torrence, S.M., Ghioca, D.M., Bhattacharjee, J., Andrei, A.E., Owen, J., Radke, N.J.A. and Perry, G., 2005. The influence of temperature and humidity on activity patterns of the lizards *Anolis stratulus* and *Ameiva exsul* in the British Virgin Islands. *Caribbean Journal of Science*, 41:870-873.
- Nikolakopoulos, K.G., Kamaratakis, E.K. and Chrysoulakis, N., 2006. SRTM vs ASTER elevation products. Comparison for two regions in Crete, Greece. *International Journal of Remote Sensing*, 27:4819 - 4838.
- Norris, K., 1965. Color adaptation in desert reptiles and its thermal relationships. *Lizard ecology*. Univ. of Missouri Press, MO., p. 162.
- O'Connor, M.P., 1999. Physiological and ecological implications of a simple model of heating and cooling in reptiles. *J Therm Biol*, 24:113-136.
- O'Connor, M.P. and Spotila, J.R., 1992. Consider a spherical lizard: animals, models, and approximations. *American Zoologist*, 32:179-193.
- Papakostas, G., Karakasis, E. and Koulouriotis, D., 2010. Novel moment invariants for improved classification performance in computer vision applications. *Pattern recognition*, 43:58-68.

- Parmesan, C. and Yohe, G., 2003. A globally coherent fingerprint of climate change impacts across natural systems. *Nature*, 421:37-42.
- Pearson, R., Dawson, T., Berry, P. and Harrison, P., 2002. SPECIES: a spatial evaluation of climate impact on the envelope of species. *Ecological Modelling*, 154:289-300.
- Pearson, R.G. and Dawson, T.P., 2003. Predicting the impacts of climate change on the distribution of species: are bioclimate envelope models useful? *Global Ecology and Biogeography*, 12:361-371.
- Pei, T., Qin, C.-Z., Zhu, A.X., Yang, L., Luo, M., Li, B. and Zhou, C., 2010. Mapping soil organic matter using the topographic wetness index: A comparative study based on different flow-direction algorithms and kriging methods. *Ecological Indicators*, 10:610-619.
- Phillips, S.J., Anderson, R.P. and Schapire, R.E., 2006. Maximum entropy modeling of species geographic distributions. *Ecol Model*, 190:231-259.
- Phillips, S.J. and Dudík, M., 2008. Modeling of species distributions with Maxent: new extensions and a comprehensive evaluation. *Ecography*, 31:161-175.
- Pierce, D.W., Barnett, T.P., Santer, B.D. and Gleckler, P.J., 2009. Selecting global climate models for regional climate change studies. *Proceedings of the National Academy of Sciences*, 106:8441-8446.
- Pleguezuelos, J.M., Sá-Sousa, P., Pérez-Mellado, V., Marquez, R., Cheylan, M., Corti, C. and Martínez-Solano, I., 2008. *Timon lepidus*. in: IUCN Red List of Threatened Species, IUCN, [www.iucnredlist.org](http://www.iucnredlist.org).
- Poole, K.G. and Heard, D.C., 2003. Seasonal habitat use and movements of Mountain Goats, *Oreamnos americanus*, in East-central British Columbia. *Canadian Field-Naturalist*, 117:565-576.
- Porter, W.P., 1967. Solar radiation through the living body walls of vertebrates with emphasis on desert reptiles. *Ecological Monographs*, 37:274-296.
- Porter, W.P., 1989. New animal models and experiments for calculating growth potential at different elevations. *Physiological Zoology*, 62:286-313.
- Porter, W.P. and Gates, D.M., 1969. Thermodynamic equilibria of animals with environment. *Ecological Monographs*, 39:227-244.
- Porter, W.P. and James, F.C., 1979. Behavioral implications of mechanistic ecology ii: the African rainbow lizard, *Agama agama*. *Copeia*, 1979:594-619.
- Porter, W.P., Mitchell, J.W., Beckman, W.A. and DeWitt, C.B., 1973. Behavioral implications of mechanistic ecology. *Thermal and*

- behavioral modeling of desert ectotherms and their microenvironment. *Oecologia*, 13:1-54.
- Porter, W.P. and Tracy, C., 1983. Biophysical analyses of energetics, time-space utilization, and distributional limits. Harvard University Press, London, 55 - 83 pp.
- Price, C., Michaelides, S., Pashiardis, S. and Alpert, P., 1999. Long term changes in diurnal temperature range in Cyprus. *Atmospheric Research*, 51:85-98.
- Qin, Z., Karnieli, A. and Berliner, P., 2001. A mono-window algorithm for retrieving land surface temperature from Landsat TM data and its application to the Israel-Egypt border region. *International Journal of Remote Sensing*, 22:3719-3746.
- Raymond, B.H. and Montgomery, S., 1976. Cost and benefits of lizard thermoregulation. *Ecology*, 51:363-384.
- Rosenzweig, M.L., 1981. A theory of habitat selection. *Ecology*, 62:327-335.
- Rouag, R., Berrahma, I. and Luiselli, L., 2006. Food habits and daily activity patterns of the North African ocellated lizard *Timon pater* from northeastern Algeria. *Journal of Natural History*, 40:1369-1379.
- Row, J.R. and Blouin-Demers, G., 2006. Thermal quality influences habitat selection at multiple spatial scales in milksnakes. *Ecoscience*, 13:443-450.
- Roy, A., Tripathi, S.K. and Basu, S.K., 2004. Formulating diversity vector for ecosystem comparison. *Ecological Modelling*, 179:499-513.
- Sabo, J.L., 2003. Hot rocks or no hot rocks: overnight retreat availability and selection by a diurnal lizard. *Oecologia*, 136:329-335.
- Salvador, A., 1998. Reptiles. Museo nacional de ciencias naturales. CSIC, Madrid, 705 p.
- Schlesinger, C.A. and Shine, R., 1994. Choosing a rock: perspectives of a bush-rock collector and a saxicolous lizard. *Biological Conservation*, 67:49-56.
- Schofield, G., Bishop, C.M., Katselidis, K.A., Dimopoulos, P., Pantis, J.D. and Hays, G.C., 2009. Microhabitat selection by sea turtles in a dynamic thermal marine environment. *J. Animal Ecology*, 78:14-21.
- Sears, M.W., 2005. Geographic variation in the life history of the sagebrush lizard: the role of thermal constraints on activity. *Oecologia*, 143:25-36.
- Sears, M.W. and Angilletta, M.J., 2011. Introduction to the symposium: responses of organisms to climate change: a synthetic approach to the

- role of thermal adaptation. *Integrative and Comparative Biology*, 51:662-665.
- Sears, M.W., Raskin, E. and Angilletta Jr, M.J., 2011. The world is not flat: defining relevant thermal landscapes in the context of climate change. *Integrative and Comparative Biology*, 51:666-675.
- Seburn, D., Seburn, C., Amphibian, C. and Network, R.C., 2000. Conservation priorities for the amphibians and reptiles of Canada. World Wildlife Fund Canada.
- Seo, C., Thorne, J.H., Hannah, L. and Thuiller, W., 2009. Scale effects in species distribution models: implications for conservation planning under climate change. *Biology Letters*, 5:39-43.
- Sharma, A., Tiwari, K. and Bhadoria, P., 2011. Determining the optimum cell size of digital elevation model for hydrologic application. *Journal of Earth System Science*, 120:573-582.
- Shine, R. and Kearney, M., 2001. Field studies of reptile thermoregulation: how well do physical models predict operative temperatures? *Functional Ecology*, 15:282-288.
- Sinclair, B.J., Vernon, P., Jaco Klok, C. and Chown, S.L., 2003. Insects at low temperatures: an ecological perspective. 18:257-262.
- Sinclair, S.J., White, M.D. and Newell, G.R., 2010. How useful are species distribution models for managing biodiversity under future climates? *Ecology and Society*, 15:8.
- Skidmore, A.K., 2002. Environmental modelling with GIS and remote sensing. Taylor & Francis, London.
- Skidmore, A.K., Franklin, J., Dawson, T.P. and Pilesjö, P., 2011. Geospatial tools address emerging issues in spatial ecology: a review and commentary on the Special Issue. *International Journal of Geographical Information Science*, 25:337-365.
- Skidmore, A.K., Gauld, A. and Walker, P., 1996. Classification of kangaroo habitat distribution using three GIS models. *International Journal of Geographical Information Systems*, 10:441-454.
- Sobrino, J.A., Jiménez-Muñoz, J.C. and Paolini, L., 2004. Land surface temperature retrieval from LANDSAT TM 5. *Remote Sensing of Environment*, 90:434-440.
- Spellerberg, I.F., 1972. Temperature tolerances of Southeast Australian reptiles examined in relation to reptile thermoregulatory behaviour and distribution. *Oecologia*, 9:23-46.

- SPOT-IMAGE-Co., 2005. SPOT DEM product description (version 1.2), <http://tinyurl.com/yby9p2z> (official download).
- Stephen, C.A. and Porter, W.P., 1993. Temperature, activity, and lizard life histories. *The American Naturalist*, 42:273-293.
- Stockwell, D., 1999. The GARP modelling system: problems and solutions to automated spatial prediction. *International Journal of Geographical Information Science*, 13:143-158.
- Su, Z., 2002. The Surface Energy Balance System (SEBS) for estimation of turbulent heat fluxes. *Hydrology and Earth System Sciences*, 6:85-100.
- Templeton, J., 1970. Lizard. In: G. Whittow (Editor), *Comparative physiology of thermoregulation*. Academic Press, New York.
- Thomas, J.A., Rose, R.J., Clarke, R.T., Thomas, C.D. and Webb, N.R., 1999. Intraspecific variation in habitat availability among ectothermic animals near their climatic limits and their centres of range. *Functional Ecology*, 13:55-64.
- Thuiller, W., 2003. BIOMOD—optimizing predictions of species distributions and projecting potential future shifts under global change. *Global Change Biology*, 9:1353-1362.
- Toutin, T., 2002. DEM from stereo Landsat 7 ETM + data over high relief areas. *International Journal of Remote Sensing*, 23:2133 - 2139.
- Tracy, C.R., 1976. A model of the dynamic exchanges of water and energy between a terrestrial amphibian and its environment. *Ecological Monographs*, 46:293-326.
- Tracy, C.R., 1982. Biophysical modeling in reptilian physiology and ecology. *Biology of the Reptilia*, 12:275-321.
- Tracy, C.R., Christian, K.A. and Tracy, C.R., 2010. Not just small, wet, and cold: effects of body size and skin resistance on thermoregulation and arboreality of frogs. *Ecology*, 91:1477-1484.
- Turner, J.S. and Tracy, C.R., 1986. Body size, homeothermy and the control of heat exchange in mammal-like reptiles. In: P.D. Maclean, J.J. Roth and E.C. Roth (Editor), *The Ecology and Biology of Mammal-like Reptiles*. Smithsonian Institution Press, Washington, pp. 185-194.
- Turner, W., Spector, S., Gardiner, N., Fladeland, M., Sterling, E. and Steininger, M., 2003. Remote sensing for biodiversity science and conservation. *Trends in Ecology and Evolution*, 18:306-314.
- Urban, D.L., Bonan, G.B., Smith, T.M. and Shugart, H.H., 1991. Spatial applications of gap models. *Forest Ecology and Management*, 42:95-110.

- Vincent, P.J. and Haworth, J.M., 1983. Poisson regression models of species abundance. *Journal of Biogeography*, 10:153-160.
- Vitt, L.J., Zani, P.A. and Avila-Pires, T.C.S., 1997. Ecology of the arboreal tropidurid lizard *Tropidurus* (= *Plica*) *umbra* in the Amazon region. *Canadian Journal of Zoology*, 75:1876-1882.
- Vogel, S., 1981. *Life in moving fluids: the physical biology of flow*. Princeton University Press, Princeton, New Jersey.
- Vogel, S. and Märker, M., 2010. Reconstructing the Roman topography and environmental features of the Sarno River Plain (Italy) before the AD 79 eruption of Somma-Vesuvius. *Geomorphology*, 115:67-77.
- Wahba, G., 1981. Spline interpolation and smoothing on the sphere. *SIAM Journal on Scientific and Statistical Computing*, 2:5-16.
- Waldschmidt, S. and Tracy, C.R., 1983. Interactions between a lizard and its thermal environment: implications for sprint performance and space utilization in the lizard *Uta stansburiana* ( Colorado, Texas). *Ecology*, 64:476-484.
- Walther, G.R., Post, E., Convey, P., Menzel, A., Parmesan, C., Beebee, T.J.C., Fromentin, J.M., Hoegh-Guldberg, O. and Bairlein, F., 2002. Ecological responses to recent climate change. *Nature*, 416:389-395.
- Wan, Z., Zhang, Y., Zhang, Q. and Li, Z.-L., 2004. Quality assessment and validation of the MODIS global land surface temperature. *International Journal of Remote Sensing*, 25:261 - 274.
- Wang, T., Skidmore, A.K., Zend, Z., Beck, P.S.A., Si Y., Song, Y., Liu, X. and Prins, H.H.T., 2010. Migration patterns of two endangered sympatric species from a remote sensing perspective. *Photogrammetric Engineering and Remote Sensing*, 76:1343-1352.
- Wang, T., Zaar, M., Arvedsen, S., Vedel-Smith, C. and Overgaard, J., 2002. Effects of temperature on the metabolic response to feeding in *Python molurus*. *Comparative Biochemistry and Physiology - Part A: Molecular & Integrative Physiology*, 133:519-527.
- Wicker, K.M., Johnston, J.B. and Young, M.W., 1980. Mississippi Deltaic Plain Region ecological characterization: a habitat mapping study: a user's guide to habitat maps. U.S. Department of the Interior, Washington, 45 p.
- Wiens, J.A., Stralberg, D., Jongsomjit, D., Howell, C.A. and Snyder, M.A., 2009. Niches, models, and climate change: Assessing the assumptions and uncertainties. *Proceedings of the National Academy of Sciences*, 106:19729-19736.

- Williams, G.A. and Morritt, D., 1995. Habitat partitioning and thermal tolerance in a tropical limpet, *Cellana grata*. *Marine ecology progress series*, Oldendorf, 124:89-103.
- Wolfram, S., 1984. Cellular automata as models of complexity. *Nature*, 311:419-424.
- Woodward, F.I. and Cramer, W., 1996. Plant functional types and climatic change : [based on contributions presented at the GCTE workshop held at the Potsdam Institute for Climatic Impact Research, 26-30 October, 1994]. *Opulus*, Uppsala, 126 p.
- Yamazaki, D., Baugh, C.A., Bates, P.D., Kanae, S., Alsdorf, D.E. and Oki, T., 2012. Adjustment of a spaceborne DEM for use in floodplain hydrodynamic modeling. *Journal of Hydrology*, 436-437:81-91.
- Yi, Q., Huang, J., Wang, F., Wang, X. and Liu, Z., 2007. Monitoring rice nitrogen status using hyperspectral reflectance and artificial neural network. *Environmental Science & Technology*, 41:6770-6775.
- Zeng, Z.G., Beck, P.S.A., Wang, T.J., Skidmore, A.K., Song, Y.L., Gong, H.S. and Prins, H.H.T., 2010. Effects of plant phenology and solar radiation on seasonal movement of golden takin in the Qinling mountains, China. *Journal of Mammalogy*, 91:92-100.
- Zhang, K., Chen, S.C., Whitman, D., Shyu, M.L., Yan, J. and Zhang, C., 2003. A progressive morphological filter for removing nonground measurements from airborne LIDAR data. *Geoscience and Remote Sensing, IEEE Transactions on*, 41:872-882.

## AUTHOR'S BIOGRAPHY



Teng Fei was born on 2<sup>nd</sup> August, 1981 in Shanghai, China. In 2003 he obtained his bachelor degree in the school of Remote Sensing and Information Engineering, Wuhan University after four years of study. Then he joined a student exchange program between Wuhan University and the International Institute for Geo-information Science and Earth Observation (ITC) in Enschede, the Netherlands from 2004 to 2006 and obtained an MSc degree with distinction from ITC. In the same year, he was awarded a doctoral scholarship from ITC, with partial financial support from Wuhan University. In 2007, he moved to the Netherlands again to start his PhD research at ITC, University of Twente. Meanwhile, he served as a lecturer in school of resource and environmental science of Wuhan University, China. His major research interests include ecological modelling, hyperspectral remote sensing and GIS.



## SUMMARY

Wildlife conservation and management requires reliable information on the abundance and spatial distribution of species as well as their habitats. The climate change debate has generated widespread interest in the response of organisms to the thermal environment. We know that the thermal environment is of particular importance to reptiles since their body temperature is in equilibrium with their environment. But we know relatively little about how the effects of thermal landscape on individual performance translate into spatial utilization of its habitat.

In this study, a spatially explicit dynamic model was developed to simulate the change of thermal landscape and the response of lizards, in order to map and understand the microhabitat use of reptiles. To do so, a physically based model was built to predict the transient body temperature of lizards in a thermally heterogeneous environment. A Monte Carlo simulation was employed to calibrate the bio-physical parameters of the target animal. Animal experiments were conducted to evaluate the calibrated body temperature model and the spatially explicit dynamic model in a terrarium under a controlled thermal environment. The results showed that the body temperature dynamics of lizards may be accurately modelled through monitoring the dynamics of the thermal environment. To reduce the computational load of the individual based dynamic model, a thermal roughness index was proposed to represent the thermal heterogeneity as well as the thermal contrast of the local habitat of lizards. The results revealed a consistent pattern between the “thermal roughness” of a local habitat and the spatial occupancy of a lizard within the habitat. In addition, this study has also solved some difficulties encountered in similar field studies by offering flexible and economical methods for building accurate digital elevation models at fine scales, as well as for modelling the local surface temperature from in-site meteorological data.

In short, this study has demonstrated that the response of lizards to thermal landscape can be successfully modelled in laboratory conditions or in their natural habitat, and the thermal landscape can be used to explain a large portion of the habitat spatial utilization of reptiles, exemplified by *Timon lepidus*. The methods developed in this research are particularly useful for understanding the effects of climate change on the distribution of terrestrial ectotherms.



## **SAMENVATTING**

Het beheer van de natuur vereist betrouwbare informatie over de dichtheid en verspreiding van soorten alsmede hun leefomgeving. Voor reptielen is deze informatie van vitaal belang voor het begrijpen van hun ecologie en voor het voorzien van de instandhouding van deze diersoort op de lange termijn. Toch weten we relatief weinig over hoe de effecten van het thermische landschap op de individuele prestaties te vertalen zijn naar de ruimtelijke benutting van zijn leefomgeving.

In deze studie werd een innovatieve methode ontwikkeld om de microhabitat van reptielen te begrijpen en in kaart te brengen. De methode is gebaseerd op een ruimtelijk expliciet dynamisch model, dat de verandering van thermische landschappen en de respons van reptielen simuleert. Met behulp van dit model kan de beweging van een reptiel worden gesimuleerd, dat uiteindelijk leidt tot een kaart van de ruimtelijke bezetting van hun microhabitat. De simulatie werd daarnaast vergeleken met geobserveerde data en uit de resultaten blijkt dat de bezetting van de microhabitat van een hagedis in een terrarium kan worden verklaard met behulp van een cellulaire automaat algoritme in een mechanisch thermisch oogpunt.

Om ondersteuning te bieden aan een dergelijke dynamisch model, werd een fysiek gebaseerd thermodynamisch model gebouwd om de dynamiek in lichaamstemperatuur van hagedissen met een thermische omgeving te simuleren. Een nieuwe Monte Carlo simulatie werd ontwikkeld om de biofysische parameters van een hagedis, gebaseerd op fysiologische literatuur, in te kunnen schatten. Dierproeven werden uitgevoerd om het model van de lichaamstemperatuur in een terrarium te kunnen testen onder een beheerste temperatuur. De resultaten toonden dat de dynamische lichaamstemperatuur van hagedissen nauwkeurig kan worden gemodelleerd door het monitoren van de thermische omgeving.

Om de problemen van individuele dynamische modellen zoals de intensieve berekeningen (rekenlast) te overwinnen, wordt voorgesteld om een nieuwe index van "thermische ruwheid" op te zetten om de thermische contrast van de microhabitat van ectotherms te kunnen vertegenwoordigen. Door deze index,

## *Samenvatting*

---

wordt de microhabitat bezetting van een hagedis met succes voorspeld en met minder intensieve berekeningen.

Dit onderzoek heeft ook geprobeerd om een aantal hindernissen weg te nemen, wanneer dit laboratorium onderzoek wordt gebaseerd op onderzoek binnen een natuurlijke omgeving. De temperatuur van het aardoppervlak en de topografische informatie van de microhabitat van het dier werden gemodelleerd door nieuwe en praktische methoden die ontwikkeld zijn in dit proefschrift. De resultaten van de modellen zijn naar tevredenheid gedaan: voor wat betreft het natuurlijke terrain is de verticale fout kleiner dan 0,2 m, van de land oppervlakte-temperatuur, is de nauwkeurigheid van de voorspelling minder dan 1,5 K in termen van “ root mean square error”. Deze methoden kunnen van groot nut zijn voor een aantal ecologische onderzoeken op een gedetailleerde schaal.

De belangrijkste bijdrage van dit onderzoek is de vaststelling dat de reactie van hagedissen in een thermisch landschap met succes kan worden gemodelleerd, in laboratoria of in hun natuurlijke leefomgeving. De thermische landschap methode kan worden gebruikt om een groot deel van het gebruik aan ruimte in de leefomgeving van ectotherms te verklaren, bijvoorbeeld in geval van de *Timon Lepidus* soort.

## **ITC DISSERTATION LIST**

[http://www.itc.nl/Pub/research\\_programme/Graduate-programme/Graduate-programme-Phd\\_Graduates.html](http://www.itc.nl/Pub/research_programme/Graduate-programme/Graduate-programme-Phd_Graduates.html)